DNA-TR-88-72

UPDATED EXCITATION AND IONIZATION CROSS SECTIONS FOR ELECTRON IMPACT ON ATOMIC OXYGEN

R. R. Laher
F. R. Gilmore
R & D Associates
P.O. Box 9695
Marina del Rey, CA 90295

29 February 1988

Technical Report

CONTRACT No. DNA 001-85-C-0022

THIS WORK WAS SPONSORED BY THE DEFENSE NUCLEAR AGENCY
UNDER RDT&E RMC CODE B4632D RD RC 00001 25904D.

Prepared for
Director
Defense Nuclear Agency
Washington, DC 20305-1000

Destroy this report when it is no longer needed. Do not return to sender.

PLEASE NOTIFY THE DEFENSE NUCLEAR AGENCY, ATTN: CSTI, WASHINGTON, DC 20305-1000, IF YOUR ADDRESS IS INCORRECT, IF YOU WISH IT DELETED FROM THE DISTRIBUTION LIST, OR IF THE ADDRESSEE IS NO LONGER EMPLOYED BY YOUR ORGANIZATION.

DISTRIBUTION LIST UPDATE

This mailer is provided to enable DNA to maintain current distribution lists for reports. We would appreciate your providing the requested information.

☐ Add the individual listed to your distribution list.

☐ Delete the cited organization/individual.

☐ Change of address.

NAME: _____

ORGANIZATION: _____

OLD ADDRESS	CURRENT ADDRESS
_____	_____
_____	_____
_____	_____

TELEPHONE NUMBER: (___) _____

SUBJECT AREA(s) OF INTEREST:

_____	_____
_____	_____
_____	_____

DNA OR OTHER GOVERNMENT CONTRACT NUMBER: _____

CERTIFICATION OF NEED-TO-KNOW BY GOVERNMENT SPONSOR (if other than DNA):

SPONSORING ORGANIZATION: _____

CONTRACTING OFFICER OR REPRESENTATIVE: _____

SIGNATURE: _____

CUT HERE AND RETURN

Director
Defense Nuclear Agency
ATTN: TITL
Washington, DC 20305-1000

Director
Defense Nuclear Agency
ATTN: TITL
Washington, DC 20305-1000

UNCLASSIFIED
SECURITY CLASSIFICATION OF THIS PAGE

REPORT DOCUMENTATION PAGE

1a REPORT SECURITY CLASSIFICATION UNCLASSIFIED	1b RESTRICTIVE MARKINGS
2a SECURITY CLASSIFICATION AUTHORITY N/A since Unclassified	3 DISTRIBUTION/AVAILABILITY OF REPORT Approved for public release; distribution is unlimited.
2b DECLASSIFICATION/DOWNGRADING SCHEDULE N/A since Unclassified	
4 PERFORMING ORGANIZATION REPORT NUMBER(S) RDA-TR-135603-009	5 MONITORING ORGANIZATION REPORT NUMBER(S) DNA-TR-88-72
6a NAME OF PERFORMING ORGANIZATION R & D Associates 6b OFFICE SYMBOL (If applicable)	7a NAME OF MONITORING ORGANIZATION Director Defense Nuclear Agency
6c ADDRESS (City, State, and ZIP Code) P.O. Box 9695 Marina del Rey, CA 90295	7b ADDRESS (City, State, and ZIP Code) Washington, DC 20305-1000
8a NAME OF FUNDING/SPONSORING ORGANIZATION 8b OFFICE SYMBOL (If applicable) DFPR/Bachkosky	9 PROCUREMENT INSTRUMENT IDENTIFICATION NUMBER DNA 001-85-C-0022
8c ADDRESS (City, State, and ZIP Code)	10 SOURCE OF FUNDING NUMBERS PROGRAM ELEMENT NO: 62715H; PROJECT NO: RD; TASK NO: RC; WORK UNIT ACCESSION NO: DH008670

11 TITLE (Include Security Classification)
UPDATED EXCITATION AND IONIZATION CROSS SECTIONS FOR ELECTRON IMPACT ON ATOMIC OXYGEN

12 PERSONAL AUTHOR(S)
Laher, Russ R.; Gilmore, Forrest R.

13a TYPE OF REPORT	13b TIME COVERED	14 DATE OF REPORT (Year, Month, Day)	15 PAGE COUNT
Technical	FROM 871001 TO 880229	880229	98

16 SUPPLEMENTARY NOTATION
This work was sponsored by the Defense Nuclear Agency under RDT&E RMC Code B4632D RD RC 00001 25904D.

17 COSATI CODES		
FIELD	GROUP	SUB-GROUP
18	1	
7	2	

18 SUBJECT TERMS (Continue on reverse if necessary and identify by block number)
Electron Impact Excitation; Atomic Oxygen; Electron Impact Ionization; Electron Energy Deposition; Cross Sections

19 ABSTRACT (Continue on reverse if necessary and identify by block number)

Cross sections for the excitation and ionization of atomic oxygen by electron impact are presented as the result of a critical review of experimental and theoretical work on this subject. An effort has been made to compile the most accurate and complete set of cross sections available. More than 60 profiles of excitation cross sections versus electron-impact energy are presented. These include transitions to the forbidden metastable $O(^1D)$ and $O(^1S)$ states, the allowed autoionizing $O(2s^2 2p^3\ ^3P^o)$ state, nine allowed Rydberg series, and twenty-nine forbidden Rydberg series. Recommended ionization cross sections for transitions to the outer-electron ionization states $O^+(^4S^o)$, $O^+(^2D^o)$, and $O^+(^2P^o)$, to the inner-electron ionization state $O^+(^4P)$, and to the O^{2+} state are also given. Many of these excitation and ionization cross sections are based on recently published laboratory measurements, and differ from previously accepted values by factors of ~2-3, and in a few cases by up to a factor of 10. The data presented in this report will be useful in calculations of aeronomical and artificially-induced electron impact on atomic oxygen, an

20 DISTRIBUTION/AVAILABILITY OF ABSTRACT ☐ UNCLASSIFIED/UNLIMITED ☒ SAME AS RPT ☐ DTIC USERS	21 ABSTRACT SECURITY CLASSIFICATION UNCLASSIFIED
22a NAME OF RESPONSIBLE INDIVIDUAL Bennie E. Maddox	22b TELEPHONE (Include Area Code) (202) 325-1078
22c OFFICE SYMBOL DNA/CSTI	

DD Form 1473, JUN 86 — Previous editions are obsolete — SECURITY CLASSIFICATION OF THIS PAGE UNCLASSIFIED

19. ABSTRACT (Continued)

important component of the upper atmosphere.

SUMMARY

Cross sections for the excitation and ionization of atomic oxygen by electron impact are presented as the result of a critical review of experimental and theoretical work on this subject. An effort has been made to compile the most accurate and complete set of cross sections available. More than 60 profiles of excitation cross section versus electron-impact energy are presented. These include transitions to the forbidden metastable $O(2p^4\ ^1D)$ and $O(2p^4\ ^1S)$ states, the allowed autoionizing $O(2p^5\ ^3P^o)$ state, nine allowed Rydberg series, and twenty-nine forbidden Rydberg series. Recommended ionization cross sections for transitions to the outer-electron ionization states $O^+(^4S^o)$, $O^+(^2D^o)$, and $O^+(^2P^o)$, to the inner-electron ionization state $O^+(^4P)$, and to the O^{2+} state are also given. Many of these excitation and ionization cross sections are based on recently published laboratory measurements, and differ from previously accepted values by factors of $\sim$ 2-3, and in a few cases by up to a factor of 10. The data presented in this report will be useful in calculations of aeronomical and artificially-induced electron impact on atomic oxygen, an important component of the upper atmosphere.

PREFACE

The authors thank Prof. J. P. Doering who kindly provided preprints of several of the papers used as reference material in this review.

CONVERSION TABLE

Conversion factors for U.S. customary to metric (SI) units of measurement

(Symbols of SI units given in parentheses in middle column)

To convert from	To	Multiply by
angstrom (Å)	meters (m)	$1.000\ 000 \times 10^{-10}$
atmosphere (normal)	kilo pascal (kPa)	$1.013\ 25 \times 10^{2}$
bar	kilo pascal (kPa)	$1.000\ 000 \times 10^{2}$
barn	meters (m^2)	$1.000\ 000 \times 10^{-28}$
British thermal unit (thermochemical)	joule (J)	$1.054\ 350 \times 10^{3}$
calorie (thermochemical)	joule (J)	4.184 000
cal (thermochemical)/cm^2	mega joule/m^2 (MJ/m^2)	$4.184\ 000 \times 10^{-2}$
curie	giga Becquerel (GBq)*	$3.700\ 000 \times 10^{1}$
degree (angle)	radian (rad)	$1.745\ 329 \times 10^{-2}$
degree Fahrenheit (°F)	degree kelvin (K)	$T_K = (T_{°F} + 459.67)/1.8$
electron volt	joule (J)	$1.602\ 19 \times 10^{-19}$
erg	joule (J)	$1.000\ 000 \times 10^{-7}$
erg/second	watt (W)	$1.000\ 000 \times 10^{-7}$
foot	meter (m)	$3.048\ 000 \times 10^{-1}$
foot-pound-force	joule (J)	1.355 818
gallon (U.S. liquid)	meter^3 (m^3)	$3.785\ 412 \times 10^{-3}$
inch	meter (m)	$2.540\ 000 \times 10^{-2}$
jerk	joule (J)	$1.000\ 000 \times 10^{9}$
joule/kilogram (J/kg) (radiation dose absorbed)	Gray (Gy)**	1.000 000
kilotons	tera joules	4.183
kip (1000 lbf)	newton (N)	$4.448\ 222 \times 10^{3}$
kip/inch^2 (ksi)	kilo pascal (kPa)	$6.894\ 757 \times 10^{3}$
ktap	newton-second/m^2 (N-s/m^2)	$1.000\ 000 \times 10^{2}$
micron	meter (m)	$1.000\ 000 \times 10^{-6}$
mil	meter (m)	$2.540\ 000 \times 10^{-5}$
mile (international)	meter (m)	$1.609\ 344 \times 10^{3}$
ounce	kilogram (kg)	$2.834\ 952 \times 10^{-2}$
pound-force (lbf avoirdupois)	newton (N)	4.448 222
pound-force inch	newton-meter (N-m)	$1.129\ 848 \times 10^{-1}$
pound-force/inch	newton/meter (N/m)	$1.751\ 268 \times 10^{2}$
pound-force/foot^2	kilo pascal (kPa)	$4.788\ 026 \times 10^{-2}$
pound-force/inch^2 (psi)	kilo pascal (kPa)	6.894 757
pound-mass (lbm avoirdupois)	kilogram (kg)	$4.535\ 924 \times 10^{-1}$
pound-mass-foot^2 (moment of inertia)	kilogram-meter^2 (kg-m^2)	$4.214\ 011 \times 10^{-2}$
pound-mass/foot^3	kilogram/meter^3 (kg/m^3)	$1.601\ 846 \times 10^{1}$
rad (radiation dose absorbed)	Gray (Gy)**	$1.000\ 000 \times 10^{-2}$
roentgen	coulomb/kilogram (C/kg)	$2.579\ 760 \times 10^{-4}$
shake	second (s)	$1.000\ 000 \times 10^{-8}$
slug	kilogram (kg)	$1.459\ 390 \times 10^{1}$
torr (mm Hg, 0° C)	kilo pascal (kPa)	$1.333\ 22 \times 10^{-1}$

* The Becquerel (Bq) is the SI unit of radioactivity; 1 Bq = 1 event/s.

** The Gray (Gy) is the SI unit of absorbed radiation.

TABLE OF CONTENTS

TABLE OF CONTENTS (continued)

LIST OF ILLUSTRATIONS

LIST OF ILLUSTRATIONS (continued)

LIST OF TABLES

LIST OF TABLES (continued)

SECTION 1

INTRODUCTION

Electron-impact cross sections of atmospheric gases are needed as input data for calculations of the chemical and radiative properties of the atmosphere when bombarded by electrons from various natural and artificial sources. These sources include auroral electrons from the sun, fast electrons (beta rays) from the fission products of nuclear bursts, and photoelectrons produced by the ultraviolet and X-rays from the sun or from nuclear bursts.

At altitudes above about 90 km atomic oxygen is a major atmospheric constituent. Until recently the available measurements of the cross sections for exciting this gas to its various electronic and ionic states were quite limited, due to the experimental difficulties in working with this very reactive species. However, over the last three years there has been renewed activity in this subject, and several pertinent experimental papers have been published. This new information has prompted the present review and compilation, which combines the new data with the older measurements and theoretical results to derive a reasonably complete and accurate set of cross sections, although some cross sections are still uncertain by a factor of two or so.

Before discussing in sequence the cross sections for exciting specific electronic states, it is useful to note some general characteristics of the theoretical calculations and measurements. Existing theoretical calculations generally have uncertainties of a factor of 2 or greater, except at electron energies above about 200 eV. However, theory is very useful for extrapolating measurements to high energies, and for obtaining approximate cross sections where accurate measurements have not been made.

Measurements of the total ionization cross section of a gas by electrical means are relatively simple and direct. However, measurements of the cross section for exciting a given electronic state of an atom or ion are more difficult. In atomic oxygen, two methods have been used. In the optical method, radiation from the excited state is detected and measured. The biggest problem with this method is

that the bombarding electrons generally excite many higher states, some of which may radiatively cascade down to the state of interest, giving an apparent cross section which is larger than the true direct cross section. In some cases the cascade contribution is known to be small; in others it can be determined by measuring the intensity of the cascade radiation, although this may lie in an inconvenient spectral region. Other important limitations of this method are that it cannot measure cross sections for exciting metastable (nonradiating) states, and, for high-lying radiating states that also autoionize, it measures only the fraction that does not autoionize. In addition, until recently absolute calibrations of optical measurements in some spectral regions have had uncertainties of a factor of 2 or more.

A more direct method of measuring an excitation cross section is to measure the fraction of the incident electrons that have lost an amount of energy equal to the excitation energy of the state under consideration. This method, however, is experimentally more difficult, and only with improved techniques in the last few years has it given accurate results.

Table 1 gives the final states of atomic oxygen transitions considered in this report, along with the corresponding threshold energies (Moore, 1976). These final states and threshold energies are also shown in the energy level diagrams given in Figures 1 and 2. The threshold energies for Rydberg excitations, where not available from measurements, are computed using the well-known formula

$$W_n = W_I - \frac{R}{(n-\delta)^2}, \tag{1}$$

where the subscript n denotes n^{th} state in the series, W_I is the ionization energy (series limit), R is the Rydberg energy, and δ is the quantum defect for the series. Values of W_I are listed in Table 1, and values of δ for the Rydberg series considered in this report, obtained from Jackman *et al.* (1977), are given in Table 2. In all cases the initial state prior to the inelastic electron-scattering is the $2s^2 2p^4\ ^3P$ ground state of atomic oxygen. Only transitions to states with angular momentum orbitals s, s', s'', p, p', p'', d, d', and d'' (where the unprimed, primed, and double-primed orbital symbols refer to the $^4S^o$, $^2D^o$, and $^2P^o$ ion cores of the excited states

of atomic oxygen, respectively) are considered. Electron-impact cross sections for higher angular momentum states are not available, but theoretical considerations indicate that they are generally small. For certain sets of high states with similar electron configurations and energy thresholds, such as the O($4d'\ ^3F^o$) and O($4d'\ ^3G^o$) states, we present only the sum of the cross sections, and use the notation O($4d'\ ^3FG^o$) to refer to this sum. The cross sections as a function of electron-impact energy are presented in both graphical and tabular form, with inclusion of formulas in the tables for extrapolating these values to higher energies.

In an earlier report Slinker and Ali (1986), in connection with a calculation of excitation and electron energy loss in bombarded atomic oxygen, tabulated a number of electron-impact cross sections for this species. However, this tabulation was based on older data, much of which has since been superseded. For allowed transitions many of the new values differ by factors of $\sim$ 2-3 from the older cross sections. For low-lying metastable excitations the new measurements show that the cross section falls off more gradually with increasing energy in the 10-30 eV range than the E^{-3} fall off assumed by Slinker and Ali. New cross sections for higher forbidden transitions that are now available, from both energy-loss and optical measurements, allow better determination of cascade contributions, leading to cross sections that differ from the older values by up to a factor of 10. In addition, the earlier tabulation did not include some cross sections now known to be significant, such as the $2p^5\ ^3P^o$ excitation. Finally, no information was given on autoionization, which has a cross section that is $\sim$ 20% of the total inelastic cross section, and has a significant effect on the relative production of different O^+ states and on the energy distribution of the secondary electrons created in the ionization process. Application of the updated cross sections presented in this report to electron/oxygen-atom scattering calculations will provide more accurate values for excitation and ionization efficiencies, the secondary electron distribution, and the average electron energy lost per ion pair created.

SECTION 2

ELECTRON-IMPACT EXCITATION CROSS SECTIONS

2.1 TRANSITIONS TO NON-RYDBERG STATES.

2.1.1 $O(^3P \longrightarrow 2p^4\ ^1D)$.

Shyn and Sharp (1986) have made measurements of the excitation cross section of the $O(^3P \longrightarrow 2p^4\ ^1D)$ transition by electron impact at 7, 10, 15, 20, and 30 eV, using the electron energy-loss technique. These values, with an assigned 50% uncertainty, are within 20% of the theoretical results of Henry *et al.* (1969) and Vo Ky Lan *et al.* (1972). The theoretical results of Thomas and Nesbet (1975), which are available for electron-impact energies up to 10 eV, are also within 20% of the measurements at 7 and 10 eV. We fit the experimental data to a generalization of the semi-empirical formula of Jackman *et al.* (1977):

$$\sigma(E) = \frac{qF}{W^2(1+\gamma E^2/W^2)}\left[1-\left(\frac{W}{E}\right)^{\alpha}\right]^{\beta}\left(\frac{W}{E}\right)^{\Omega}, \qquad (2)$$

where $\sigma(E)$ is the cross section in units of cm^2, E is the electron-impact energy in units of eV, $q = 4\pi a_o^2 R^2 = 6.513 \times 10^{-14}$ cm^2-eV^2 (a_o is the Bohr radius and R is the Rydberg energy), W is the threshold energy of the excitation in eV, and F, α, β, Ω and γ are adjustable parameters for use in fitting the formula to the experimental data. We have added the γ-term to the Jackman *et al.* formula so that (with $\Omega = 1$) the cross section for this transition has an E^{-3} asymptotic behavior at high energies ($E > 200$ eV) as required for spin-forbidden transitions (Henry *et al.*, 1969). Using $W = 1.96$ eV, and the parameters $F = 0.012$, $\alpha = 1$, $\beta = 2$, and $\Omega = 1$ from Jackman *et al.* (1977), and $\gamma = 0.002$, formula (2) yields values for the $O(^3P \longrightarrow 2p^4\ ^1D)$ cross section that agree well with the theoretical results for energies lower than 7 eV, and fit the measurements of Shyn and Sharp (1986) within 30%. The cross sections computed using formula (2) are shown in Figure 3, and are tabulated in Table 3.

2.1.2 $O(^3P \longrightarrow 2p^4\ ^1S)$.

Shyn *et al.* (1986) have measured the cross section of the $O(^3P \longrightarrow 2p^4\ ^1S)$ excitation at 10, 15, 20, and 30 eV. In these measurements the direct method of electron energy-loss was used. While the experimental profile shape in the 10 to 30 eV range closely resembles the theoretical cross-section curves of Henry *et al.* (1969) and Vo Ky Lan *et al.* (1972), the experimental data are greater in magnitude by a factor of two. Note, however, that the data have a 54% uncertainty. To fit the excitation cross sections for this transition as a function of electron-impact energy, we use formula (2) with $W = 4.18$ eV, $F = 0.006$, $\alpha = 0.5$, $\beta = 1$, $\Omega = 1$, and $\gamma = 0.0004$, where the values for α, β, and Ω are from Jackman *et al.* (1977). Given the large error bars on the experimental data and the large differences between the experimental and theoretical cross sections, we have chosen the parameter F such that $\sigma(E)$ peaks at a value intermediate to the recent measurement and the theoretical result at 10 eV. Figure 3 and Table 3 present the recommended cross sections for this transition.

2.1.3 $O(^3P \longrightarrow 2p^5\ ^3P^o)$.

The only experimental cross sections for the excitation of $O(2p^5\ ^3P^o)$ are those of Vaughan and Doering (1988), obtained from electron energy-loss measurements. The curve shown in Figure 3 is based on the experimental data at 30, 50, 100, 150, and 200 eV. We have reduced the measurement at 150 eV by 16% to smooth the cross section, given the large error bar on this particular datum.

For energies greater than $\sim$ 200 eV, the excitation cross section for an allowed transition can be approximated by the formula

$$\sigma(E) = \frac{A + (qF/W)\ \ln E}{E}, \qquad (3)$$

where A is a constant, q and W have been defined in Subsection 2.1.1, and F is the optical oscillator strength (Jackman *et al.*, 1977). For this transition, $F = 0.070$ (Doering *et al.*, 1985), and we choose $A = -9.14 \times 10^{-16}$ cm^2-eV to

give a smooth transition to the experimental data at lower energies. The cross sections are tabulated in Table 3.

2.2 SCALING OF CROSS SECTIONS FOR RYDBERG STATES.

No cross section measurements are available for many of the Rydberg states of atomic oxygen. For these cross sections we have used a procedure of scaling from the measured cross sections of related Rydberg states, which is a generalization of the method of Jackman *et al.* (1977). These writers used semi-empirical cross section formulas, and assumed that the shape-controlling parameters in the formulas are the same for all the states in a given Rydberg series. This is nearly equivalent to assuming that all of the cross sections have the same shape, but scaled by a factor. For optically allowed transitions this factor is F/W, where F is the optical oscillator strength and W is the threshold energy for a given state in the series (see equation (3)). For forbidden transitions, equation (2) with $\gamma = 0$ holds, and the F/W scaling holds (except near threshold) when $\Omega = 1$. For simplicity, the F/W scaling was also used for other values of Ω, since the relatively small variation in W among the states in a given Rydberg series makes this a reasonable approximation.

The known cross section for a Rydberg state of quantum number n can be used to calculate that of another state n' by using the relation

$$\sigma_{n'}(E) = \frac{W_n F_{n'}}{W_{n'} F_n} \sigma_n(E). \tag{4}$$

(This relation is not accurate very near the energy threshold, where the curve must be shifted slightly to give the proper threshold behavior.) In this equation the F_n values are given by

$$F_n = \frac{F^*}{(n-\delta)^3}, \tag{5}$$

where F^* is a constant for a given Rydberg series which can be calculated using the quantum defect (Table 2) and a known optical oscillator strength for allowed transitions, or the known $\sigma_n(E)$ and equation (2) for forbidden transitions.

The cross sections for the higher Rydberg states, $n \geq 5$, are conveniently summed by approximating the different thresholds W_n by a single, intermediate value $W_A = (W_5 + W_I)/2$, and the sum by an integral (accurate to within a few percent):

$$\sigma_{n\geq 5}(E) \equiv \sum_{n=5}^{\infty} \sigma_n(E) = \sum_{n=5}^{\infty} \frac{W_3}{W_n} \frac{(3-\delta)^3}{(n-\delta)^3} \sigma_3(E)$$
$$\approx \frac{W_3(3-\delta)^3}{2W_A(4.5-\delta)^2} \sigma_3(E). \qquad (6)$$

In writing equation (6) we have assumed that the $n = 3$ cross section is the only cross section available in a given Rydberg series. For some of the Rydberg series treated in Subsections 2.3, 2.4, and 2.5, however, the $n = 4$ cross section or optical oscillator strength is available. In these cases the $\Sigma n \geq 5$ cross section is scaled from the $n = 4$ cross section, rather than the $n = 3$ cross section as done in equation (6).

2.3 TRANSITIONS TO RYDBERG STATES WITH AN $O^+(2s^2 2p^3\ ^4S^o)$ CORE.

2.3.1 $O(^3P \longrightarrow 3s\ ^5S^o)$.

The only published measurements of these excitation cross sections are the optical data of Stone and Zipf (1974) which cover the electron-impact energy range of 11-70 eV. Above 25 eV, their data scatter by a factor of two or more about the mean. Later Zipf and Erdman (1985) determined that these measurements should be divided by a constant at least equal to 1.34, and possibly as large as 2.8, due to a re-evaluation of their measurement technique and a better measurement of their absolute calibration standard. If these data are divided by 2 they agree quite well with the theoretical calculations of Julienne and Davis (1976) for the excitation cross section, including cascade contribution. These calculations indicate that over half of the optical cross section is due to cascade contributions, so that the Stone and Zipf measurements cannot be used alone to determine this excitation cross section. Evidence for the accuracy of the Julienne and Davis calculations is provided by their

value for exciting the $3p\ ^5P$ state at 15 eV, which agrees well with the measurement (see Subsection 2.3.3). Accordingly, we conclude that these theoretical results give the best values currently available for the excitation cross section of $O(^3P \longrightarrow 3s\ ^5S^o)$.

The recommended values are given in Figure 4 and Table 4. For electron-impact energies $E > 50$ eV, the approximation

$$\sigma(E) = (3.88 \times 10^{-14}\ \text{cm}^2\ \text{eV}^3)E^{-3} \tag{7}$$

is used. Equation (7) is consistent with the well known high-energy behavior of spin-forbidden transitions.

2.3.2 $O(^3P \longrightarrow 3s\ ^3S^o)$.

The $O(^3P \longrightarrow 3s\ ^3S^o)$ excitation by electron impact is by far the most widely investigated of all atomic oxygen transitions. The latest measurements have been performed by Gulcicek and Doering (1988) and Vaughan and Doering (1986, 1987), who made electron energy-loss measurements in the 13.87-200 eV range. Previously Stone and Zipf (1971, 1974) employed optical measurement techniques and obtained larger values due to systematic errors and cascade contributions from higher states; however, the measurements were later lowered by 64% (Zipf and Erdman, 1985). According to Vaughan and Doering the revised optical cross sections of Zipf and Erdman, less reasonable cascade contributions, will yield values similar to theirs for impact energies greater than 30 eV; below 30 eV the agreement is not as good, the new measurements being roughly a factor of 1.2 larger than the optical data after cascade corrections are applied. The theoretical cross sections of Julienne and Davis (1976) and Rountree and Henry (1972) scaled upward by factors of 1.6 and 1.3, respectively, closely match the recent measurements. The theoretical results of Sawada and Ganas (1973) and Smith (1976) differ in variation with energy as well as magnitude from the recent measurements.

Thus the measurements of Gulcicek and Doering (1988) and Vaughan and Doering (1986, 1987) are in line with previous work. Assuming that technological

advances over the years have produced a better laboratory apparatus, the newest measurements are preferred. The curve shown in Figure 4 is a hand fit of the data; corresponding values are listed in Table 4. For impact energies greater than 200 eV, the cross sections are obtained from formula (3), where $F = 0.048$ (Doering *et al.*, 1985) and $A = -8.69 \times 10^{-16}$ cm^2-eV.

2.3.3 $O(^3P \longrightarrow 3p\ ^5P,\ 3p\ ^3P)$.

Gulcicek *et al.* (1988) and Gulcicek and Doering (1987) report for the first time direct measurements of the excitation cross section for the $O(^3P \longrightarrow 3p\ ^5P)$ transition in the 13.87-30 eV range. Their results are fairly close to the calculated values of Julienne and Davis (1976). The semi-empirical cross section of Dalgarno and Lejeune (1971), which has a peak value of 1.7×10^{-18} cm^2 at 15 eV, is approximately 25% smaller than the experimental value.

We have used the direct measurements as a basis for constructing a cross-section profile versus electron-impact energy for the $O(^3P \longrightarrow 3p\ ^5P)$ transition. This is shown in Figure 5; values are given in Table 5. For energies greater than 30 eV the following approximation is used:

$$\sigma(E) = (1.81 \times 10^{-14}\ \text{cm}^2\ \text{eV}^3)E^{-3}. \tag{8}$$

Gulcicek *et al.* (1988) and Gulcicek and Doering (1987) also report direct measurements of the $O(^3P \longrightarrow 3p\ ^3P)$ cross section in the 13.87-100 eV range. Gulcicek *et al.* write that optical data of E. C. Zipf, which include experimentally-determined corrections for cascading, support these measurements for electron-impact energies greater than 30 eV (from a private communication between Gulcicek *et al.* and E. C. Zipf). The theoretical cross section of Julienne and Davis (1976) at 20 eV is 26% less in magnitude than the latest measurement. The semi-empirical cross section of Dalgarno and Lejuene (1971) is about a factor of 10 lower than the new measurements.

Figure 5 and Table 5 give the recommended values for the $O(^3P \longrightarrow 3p\ ^3P)$ cross section, based on the experimental results. For $E > 100$ eV,

$$\sigma(E) = (1.10 \times 10^{-16} \text{cm}^2 \text{ eV}) E^{-1} \tag{9}$$

is a valid approximation for these electric quadrupole transitions.

2.3.4 $O(^3P \longrightarrow 3d\ ^5D^o,\ 3d\ ^3D^o)$.

No experimental data on the $O(^3P \longrightarrow 3d\ ^5D^o)$ cross section as a function of electron-impact energy are available, as is the case for many of the atomic oxygen Rydberg states. We therefore use equation (2), with $W = 12.07$ eV, $\alpha = 1$, $\beta = 2$, $\Omega = 3$, and $F = 0.2/(3 - 0.01)^3 = 0.007$ (Jackman *et al.*, 1977), and $\gamma = 0$. This cross section is plotted in Figure 5; corresponding values are given in Table 5.

Recent measurements of the $O(^3P \longrightarrow 3d\ ^3D^o)$ excitation cross section at electron-impact energies of 30, 50, and 100 eV, by the method of electron energy loss, are reported by Vaughan and Doering (1988). Their results agree with the optical cross sections of Zipf and Erdman (1985) within experimental error except at energies greater than $\sim$ 80 eV where Vaughan and Doering's data fall off more rapidly with increasing energy. Vaughan and Doering suggest that this is because cascade contributions in the optical measurements become progressively more important at higher energies: they do not, however, speculate on the identities of the cascade states. Zipf and Erdman, on the other hand, point out that their optical cross sections probably contain cascade contributions from $nf\ ^3F$ states which may be significant below 50 eV.

We have decided to adopt the measurements of Vaughan and Doering (1988) for the $O(^3P \longrightarrow 3d\ ^3D^o)$ cross section. The cross section is shown in Figure 5, and values are tabulated in Table 5. For electron-impact energies greater than 100 eV we approximate the cross section using formula (3) with $F = 0.019$ (Doering *et al.*, 1985) and $A = -2.98 \times 10^{-16}$ cm^2-eV.

2.3.5 Transitions to $O^+(^4S^o)$-Core Rydberg States with $n = 4$.

For excitation to the $4s\ ^5S^o$ Rydberg state the quantum defect method outlined in Subsection 2.2 is used. We find that this cross section is 20% of the $3s\ ^5S^o$ cross section. The $O(^3P \longrightarrow 4s\ ^5S^o)$ cross section is given in Figure 6 and Table 6.

We scale the $O(^3P \longrightarrow 3s\ ^3S^o)$ cross section by

$$\frac{W_3 F_4}{W_4 F_3} = \frac{(9.51\ \text{eV})(0.01)}{(11.92\ \text{eV})(0.048)} = 0.17 \tag{10}$$

in order to obtain the $O(^3P \longrightarrow 4s\ ^3S^o)$ cross section, where the optical oscillator strengths, F_3 and F_4, for the $n = 3$ and $n = 4$ states, respectively, have been measured by Doering *et al.* (1985). Note that if we had used equation (5) instead of the measured value for F_4, the required scale factor would be overestimated by 28%, thus indicating the limitations of the quantum defect method for this transition. Values for this cross section as a function of electron energy are given in Figure 6 and Table 6.

The excitation cross section for the $4p\ ^5P$ Rydberg state is calculated using equations (4) and (5). This cross section is 28% of the $3p\ ^5P$ cross section. The results are given in Figure 7 and Table 7.

Equations (4) and (5) are also used to obtain the cross sections for the $4p\ ^3P$ Rydberg state from the $n = 3$ cross section. Accordingly, the scale factor is 0.30. This cross section is shown in Figure 7 and listed in Table 7.

The $O(^3P \longrightarrow 4d\ ^5D^o)$ cross section is obtained using equation (2), with $W = 12.74$ eV, $\alpha = 1$, $\beta = 2$, $\Omega = 3$, and $F = 0.2/(4 - 0.01)^3 = 0.003$ (Jackman *et al.*, 1977), and $\gamma = 0$. This cross section is plotted in Figure 7; corresponding values are given in Table 7.

Excitation cross-section measurements of the $O(^3P \longrightarrow nd\ ^3D^o)$ Rydberg transitions for $n = 4$, 5, and 6 have been made at 30, 50, and 100 eV, and the cross section for the $O(^3P \longrightarrow 7d\ ^3D^o)$ transition has been measured at 100 eV (Vaughan and

Doering, 1988). The $n \geq 4$ profiles of cross section versus electron-impact energy are of similar shape, and are distinctly more sharply peaked than the $n = 3$ case (see Subsection 2.3.4). We therefore fit a curve to the $n = 4$ data (see Figure 7 and Table 7), and assume that its shape will be the same for all higher Rydberg transitions in this series. From the optical oscillator strength $F_4 = 0.016$ (Doering *et al.*, 1985), the corresponding energy threshold (given in Table 1), and the measurement at 100 eV, the $n = 4$ cross section for electron energies greater than 100 eV can be approximated using formula (3) with $A = -3.06 \times 10^{-16}$ cm^2-eV.

2.3.6 Transitions to $O^+(^4S^o)$-Core Rydberg States with $n \geq 5$.

For excitations to the $n \geq 5$ states of the $ns\ ^5S^o$ Rydberg series, equation (6) requires that the $\Sigma n \geq 5$ cross section is 18% of the $3s\ ^5S^o$ cross section. This cross section is given in Figure 8 and Table 8.

For the sum of the cross sections of the $n \geq 5$ states in the $ns\ ^3S^o$ Rydberg series, we scale the $O(^3P \longrightarrow 4s\ ^3S^o)$ cross section by

$$\frac{W_4(4-\delta)^3}{2W_A(4.5-\delta)^2} = \frac{(11.92\text{ eV})(4-1.16)^3}{2(13.15\text{ eV})(4.5-1.16)^2} = 0.93. \qquad (11)$$

Values for this cross section as a function of electron energy are given in Figure 8 and Table 8.

The sum of the cross sections for the $n \geq 5$ states of the $np\ ^5P$ Rydberg series is calculated using equation (6). It is found to be 31% of the $3p\ ^5P$ cross section. This cross section is graphed in Figure 9 and tabulated in Table 9.

From equation (6), we find that the composite cross section for the $n \geq 5$ states of the $np\ ^3P$ Rydberg series is 35% of the $3p\ ^3P$ cross section. The $\Sigma n \geq 5$ cross section for this series is given in Figure 9 and Table 9.

We obtain the $O(^3P \longrightarrow \Sigma(n \geq 5)nd\ ^5D^o)$ cross section using equation (2), with $W = 13.33$ eV from Table 1, $\alpha = 1$, $\beta = 2$, $\Omega = 3$, and $F = 0.2/(2(4.5 - 0.01)^2) = 0.005$ (Jackman *et al.*, 1977), and $\gamma = 0$. The expression for F is consistent with the

quantum defect method discussed in Subsection 2.2. This cross section is plotted in Figure 9; corresponding values are given in Table 9.

For $\sigma_{n\geq 5}(E)$ of the $nd\ ^3D^o$ Rydberg series, we scale the $4d\ ^3D^o$ data using an equation similar to equation (6):

$$\sigma_{n\geq 5}(E) = \sum_{n=5}^{\infty} \sigma_n(E) = \frac{W_4(4-\delta)^3}{2W_A(4.5-\delta)^2}\sigma_4(E)$$
$$= \frac{(12.75\text{ eV})(4-0.01)^3}{2(13.33\text{ eV})(4.5-0.01)^2}\sigma_4(E) \approx (1.5)\sigma_4(E). \qquad (12)$$

The data show that this method of approximation gives cross sections within experimental error up to $n = 7$ in the series. Figure 9 and Table 9 give the recommended values for the this cross section.

2.4 TRANSITIONS TO RYDBERG STATES WITH AN $O^+(2s^2 2p^3\ ^2D^o)$ CORE.

2.4.1 $O(^3P \longrightarrow 3s'\ ^3D^o,\ 3s'\ ^1D^o,\ 3p'\ ^3PDF,\ 3p'\ ^1PDF)$.

Electron energy-loss measurements of the $O(^3P \longrightarrow 3s'\ ^3D^o)$ excitation cross section have been made by Vaughan and Doering (1987) and Gulcicek and Doering (1988) in the 20-200 eV range. In the latter work a new value for the electron-impact cross section at 20 eV, measured following improvements to the experimental apparatus for near-threshold energies, is reported which replaces the 20 and 25 eV values of the former work. These data are a factor of three lower than the optical cross sections reported by Zipf and Erdman (1985); however, the profile shapes are similar. Vaughan and Doering write that, based on the assumption that cascade contributions to the optical cross sections of Zipf and Erdman are 25% or less, a reduction in the Zipf and Erdman values by a factor of two would be needed to make the values consistent with their own measurements. As a result of their analysis of mid-latitude dayglow data obtained from rocket measurements, Gladstone *et al.* (1987) came to the similar conclusion that the Zipf and Erdman values should be reduced by a factor of $\sim$ 2-3 in order to explain their observations using the

1173-Å/989-Å branching ratio measured by Morrison (1985) and Erdman and Zipf (1986). In addition Gladstone *et al.* (1987) also cite other airglow studies, over a wide range of aeronomical conditions, that also require a reduction in the Zipf and Erdman cross sections to bring the models into agreement with the observations. Note that Meier (1982) required a cross section of 8.4×10^{-18} cm^2 at 25 eV in order to explain rocket observations of the 989 Å dayglow under optically thick conditions, but this was based on a model value of the 7990-Å/989-Å branching ratio shown later by Erdman and Zipf (1983) to be too large by more than an order of magnitude.

We therefore recommend that the new measurements be used. A hand interpolation of the data from threshold to 200 eV is shown in Figure 10, and numerical values are tabulated in Table 10. For $E > 200$ eV the cross section is approximated by formula (3) with $F = 0.061$ (Doering *et al.*, 1985) and $A = -1.145 \times 10^{-15}$ cm^2-eV.

No measured cross sections for transitions to the $3s'\ ^1D^o$, $3p'\ ^3PDF$, and $3p'\ ^1PDF$ states (where the P, D, and F cross sections for a given spin have been added due to their similar thresholds and theoretical high-energy behaviors, resulting in a composite PDF cross section) are available. However, Jackman *et al.* (1977) have estimated values for these excitations which can be calculated using equation (2) (with $\gamma = 0$). For $3s'\ ^1D^o$, $W = 12.72$ eV, $\alpha = 1$, $\beta = 2$, $\Omega = 3$, and $F = 0.2/(3 - 1.18)^3 = 0.033$. For $3p'\ ^3PDF$, $W = 14.06$ eV, $\alpha = 2$, $\beta = 1$, $\Omega = 1$, and $F = 0.1/(3 - 0.84)^3 = 0.01$. And for $3p'\ ^1PDF$, $W = 14.20$ eV, $\alpha = 1$, $\beta = 1$, $\Omega = 3$, and $F = 0.04/(3 - 0.83)^3 = 0.004$. These cross sections are plotted in Figure 10 and listed in Table 10.

2.4.2 $O(^3P \longrightarrow 3d'\ ^3S^o, 3d'\ ^3P^o, 3d'\ ^3D^o, 3d'\ ^3FG^o, 3d'\ ^1SPDFG^o)$.

There are currently no measured cross sections available for excitation to the $3d'\ ^3S^o$, $3d'\ ^3P^o$, and $3d'\ ^3D^o$ states; however, Vaughan and Doering (1988) have measured the $O(^3P \longrightarrow 4d'\ ^3P^o)$ cross section using the electron energy-loss method. We make the assumption that the $O(^3P \longrightarrow 3d'\ ^3P^o)$ cross section is related to the $O(^3P \longrightarrow 4d'\ ^3P^o)$ cross section by a scale factor. Then using the quantum defect method (as explained in Subsection 2.2) and the quantum defect $\delta = 0.04$ given by

Jackman *et al.* (1977) for this Rydberg series, the scale factor is given by

$$\frac{W_4(4-\delta)^3}{W_3(3-\delta)^3} = \frac{(16.08\text{ eV})(4-0.04)^3}{(15.36\text{ eV})(3-0.04)^3} = 2.51, \tag{13}$$

where W_3 and W_4 are the threshold energies for the $n = 3$ and $n = 4$ states, respectively, given in Table 1. The $O(^3P \longrightarrow 3d'\ ^3P^o)$ cross section is presented in Figure 11 and in Table 11 as a function of electron-impact energy. For $E > 200$ eV the $O(^3P \longrightarrow 3d'\ ^3P^o)$ cross section is approximated by letting $F = 0.0077$ (Jackman *et al.*, 1977) and $A = 2.71 \times 10^{-16}$ cm^2-eV in formula (3). We furthermore make the assumption that $^3S^o$ and $^3D^o$ cross sections are related to the $^3P^o$ cross section by scale factors, and use the optical oscillator strengths 0.0065 and 0.0052 for the $^3S^o$ and $^3D^o$ states, respectively (Jackman *et al.*, 1977), as relative weights. The resulting $^3S^o$ and $^3D^o$ cross sections are also plotted in Figure 11, with corresponding values presented in Table 11.

No measured cross sections have been reported for transitions to the $3d'\ ^3FG^o$ and $3d'\ ^1SPDFG^o$ states. The estimates of Jackman *et al.* (1977) are therefore used, namely, equation (2) (with $\gamma = 0$) and the following parameters: for $3d'\ ^3FG^o$, $W = 15.39$ eV, $\alpha = 2$, $\beta = 1$, $\Omega = 1$, and $F = 0.1/(3-0.04)^3 = 0.004$; for $3d'\ ^1SPDFG^o$, $W = 15.40$ eV, $\alpha = 1$, $\beta = 2$, $\Omega = 3$, and $F = 0.2/(3-0.04)^3 = 0.008$. These cross sections are plotted in Figure 11 and listed in Table 11.

2.4.3 Transitions to $O^+(^2D^o)$-Core Rydberg States with $n = 4$.

The $O(^3P \longrightarrow 4s'\ ^3D^o)$ cross section is obtained using equations (4) and (5), and data from Tables 1 and 2; it is found to be 22% of the $O(^3P \longrightarrow 3s'\ ^3D^o)$ cross section. The results are presented in Figure 12 and Table 12.

The cross sections for transitions to the $4s'\ ^1D^o$, $4p'\ ^3PDF$, and $4p'\ ^1PDF$ states are obtained from the estimates of Jackman *et al.* (1977). We therefore use equation (2) (with $\gamma = 0$) and the following: for $4s'\ ^1D^o$, $W = 15.22$ eV, $\alpha = 1$, $\beta = 2$, $\Omega = 3$, and $F = 0.2/(4-1.18)^3 = 0.009$; for $4p'\ ^3PDF$, $W = 15.59$ eV, $\alpha = 2$, $\beta = 1$, $\Omega = 1$, and $F = 0.1/(4-0.84)^3 = 0.003$; and for $3p'\ ^1PDF$, $W = 15.58$ eV, $\alpha = 1$,

$\beta = 1$, $\Omega = 3$, and $F = 0.04/(4 - 0.83)^3 = 0.0013$. These cross sections are plotted in Figure 12 and listed in Table 12.

Vaughan and Doering (1988) have measured the O($^3P \longrightarrow 4d'\ ^3P^o$) cross section at 30, 50, 100, 150, and 200 eV, using the electron energy-loss method. As done in Subsection 2.4.2 the relative optical oscillator strengths for the $nd'\ ^3S^o$, $nd'\ ^3P^o$, and $nd'\ ^3D^o$ states given by Jackman *et al.* (1977) are used to determine the magnitudes of the O($^3P \longrightarrow 4d'\ ^3S^o$) and O($^3P \longrightarrow 4d'\ ^3D^o$) cross sections, under the assumption that the variation of the cross section with electron energy is the same for all three series. In Figure 13 and Table 13 values for the summed O($^3P \longrightarrow 4d'\ ^3SPD^o$) cross section are presented. For $E > 200$ eV this total cross section is given by formula (3) with $F = 0.008$ (Jackman *et al.*, 1977) and $A = 2.72 \times 10^{-16}$ cm^2-eV.

Using equation (2) (with $\gamma = 0$), the $4d'\ ^3FG^o$ cross section is obtained with $W = 16.07$ eV, $\alpha = 2$, $\beta = 1$, $\Omega = 1$, and $F = 0.1/(4 - 0.04)^3 = 0.0016$, and the $4d'\ ^3SPDFG^o$ cross section is obtained with $W = 16.07$ eV, $\alpha = 1$, $\beta = 2$, $\Omega = 3$, and $F = 0.2/(4 - 0.04)^3 = 0.0032$ (Jackman *et al.*, 1977). These cross sections are plotted in Figure 13 and listed in Table 13.

2.4.4 Transitions to $O^+(^2D^o)$-Core Rydberg States with $n \geq 5$.

The O($^3P \longrightarrow \Sigma(n \geq 5)ns'\ ^3D^o$) cross section is 20% of the corresponding $n = 3$ cross section, according to equation (6). This cross section is given in Figure 14 and Table 14.

The $\Sigma(n \geq 5)\ ns'\ ^1D^o$, $\Sigma(n \geq 5)\ np'\ ^3PDF$, and $\Sigma(n \geq 5)\ np'\ ^1PDF$ cross sections are computed using equation (2) (with $\gamma = 0$) and the following: for $ns'\ ^1D^o$, $W = 16.47$ eV, $\alpha = 1$, $\beta = 2$, $\Omega = 3$, and $F = 0.2/(2(4.5 - 1.18)^2) = 0.009$; for $np'\ ^3PDF$, $W = 16.54$ eV, $\alpha = 2$, $\beta = 1$, $\Omega = 1$, and $F = 0.1/(2(4.5 - 0.84)^2) = 0.0037$; and for $np'\ ^1PDF$, $W = 16.54$ eV, $\alpha = 1$, $\beta = 1$, $\Omega = 3$, and $F = 0.04/(2(4.5 - 0.83)^2) = 0.0015$ (Jackman *et al.*, 1977). These cross sections are presented in Figure 14 and Table 14.

The $O(^3P \longrightarrow \Sigma(n \geq 5)nd'\ ^3SPD^o)$ cross section is obtained by multiplying the $O(^3P \longrightarrow 4d'\ ^3SPD^o)$ cross section by the scale factor

$$\frac{W_4(4-\delta)^3}{2W_A(4.5-\delta)^2} = \frac{(16.08\text{ eV})(4-0.04)^3}{2(16.65\text{ eV})(4.5-0.04)^2} = 1.5; \qquad (14)$$

values for this cross section are given in Figure 15 and Table 15.

Using equation (2) (with $\gamma = 0$), the $\Sigma(n \geq 5)\ nd'\ ^3FG^o$ cross section is obtained with $W = 16.65$ eV, $\alpha = 2$, $\beta = 1$, $\Omega = 1$, and $F = 0.1/(2(4.5-0.04)^2) = 0.0025$, and the $\Sigma(n \geq 5)\ nd'\ ^1SPDFG^o$ cross section is obtained with $W = 16.66$ eV, $\alpha = 1$, $\beta = 2$, $\Omega = 3$, and $F = 0.2/(2(4.5-0.04)^2) = 0.005$ (Jackman *et al.*, 1977). These cross sections are plotted in Figure 15 and listed in Table 15.

2.5 TRANSITIONS TO RYDBERG STATES WITH AN $O^+(2s^22p^3\ ^2P^o)$ CORE.

2.5.1 $O(^3P \longrightarrow 3s''\ ^3P^o,\ 3s''\ ^1P^o,\ 3p''\ ^3SPD,\ 3p''\ ^1SPD)$.

Excitation cross sections for the $O(^3P \longrightarrow 3s''\ ^3P^o)$ transition, measured by Vaughan and Doering (1988) using the electron energy-loss technique, are available in the 30-200 eV range. Upon comparison of these data with the optical cross sections of Zipf and Kao (1986) we find that the optical measurements overestimate the direct results, by a factor of ~ 2 at the peak of the cross section at 50 eV, and that the optical measurements fall off more slowly with increasing energy compared to the direct measurements. Vaughan and Doering conclude that these differences are due to cascading and perhaps other experimental difficulties as well. A reduction in the emission/autoionization branching ratio by 15%, as allowed by the uncertainties of the branching ratio measurement (Dehmer *et al.*, 1977), coupled with a reasonable estimate of the cascade contribution (e.g., 25% of the optical measurement), is still not enough to account for the discrepancies between the direct and optical cross sections.

The recent measurements, which are recommended, have been fit to a curve by hand. The resulting profile for this transition is shown in Figure 16; Table 16 gives

the recommended values. For $E > 200$ eV the cross sections are given by formula (3) with $F = 0.086$ (Doering *et al.*, 1985) and $A = -1.17 \times 10^{-15}$ cm^2-eV.

The $3s''\ ^1P^o$, $3p''\ ^3SPD$, and $3p''\ ^1SPD$ cross sections are computed using equation (2) (with $\gamma = 0$) and the following: for $3s''\ ^1P^o$, $W = 14.36$ eV, $\alpha = 1$, $\beta = 2$, $\Omega = 3$, and $F = 0.2/(3 - 1.19)^3 = 0.034$; for $3p''\ ^3SPD$, $W = 15.77$ eV, $\alpha = 2$, $\beta = 1$, $\Omega = 1$, and $F = 0.1/(3 - 0.86)^3 = 0.01$; and for $3p''\ ^1SPD$, $W = 15.99$ eV, $\alpha = 1$, $\beta = 1$, $\Omega = 3$, and $F = 0.04/(3 - 0.85)^3 = 0.004$ (Jackman *et al.*, 1977). The $3s''\ ^1P^o$ cross section is given in Figure 16 and Table 16; the other two cross sections are presented in Figure 17 and Table 17.

2.5.2 $O(^3P \longrightarrow 3d''\ ^3P^o, 3d''\ ^3D^o, 3d''\ ^3F^o, 3d''\ ^1PDF^o)$.

No measurements of the $O(^3P \longrightarrow 3d''\ ^3P^o, ^3D^o)$ cross sections are available to our knowledge; therefore, we use the semi-empirical cross section formula for optically-allowed transitions of Jackman *et al.* (1977), given by

$$\sigma(E) = \frac{qF}{WE}\left[1 - \left(\frac{W}{E}\right)^{\alpha}\right]^{\beta} \ln\left(\frac{4EC}{W} + e\right), \tag{15}$$

where σ, E, q, W, α, and β have been defined in Subsection 2.1.1; e is the base of the natural logarithm; F is the optical oscillator strength; and C is an empirical parameter. For these excitations $W = 17.09$ eV, $\alpha = 1.26$, $\beta = 0.490$, and $C = 0.610$; for the $^3P^o$ state, $F = 0.008$, and for the $^3D^o$ state, $F = 0.006$ (Jackman *et al.*, 1977). The $^3P^o$ and $^3D^o$ cross sections are plotted as a function of electron-impact energy in Figure 18; corresponding values are given in Table 18.

We might mention here that an attempt was made to fit by this formula the cross sections of the other allowed transitions for which good experimental data are available. For the $O(^3P \longrightarrow 3s''\ ^3P^o)$ cross section the fit is fairly good, using $F = 0.086$ (Doering *et al.*, 1985) and the other parameters from Jackman *et al.* (1977), but for all other cross sections considered, no good fit could be obtained.

The $3d''\ ^3F^o$ and $3d''\ ^1PDF^o$ cross sections are obtained using equation (2) (with $\gamma = 0$) and the following: for $3d''\ ^3F^o$, $W = 17.09$ eV, $\alpha = 2$, $\beta = 1$, $\Omega = 1$, and

$F = 0.1/(3-0.05)^3 = 0.0039$; and for $3d''\ ^1PDF^o$, $W = 17.09$ eV, $\alpha = 1$, $\beta = 2$, $\Omega = 3$, and $F = 0.2/(3-0.05)^3 = 0.008$ (Jackman *et al.*, 1977). These cross sections are given in Figure 18 and Table 18.

2.5.3 Transitions to $O^+(^2P^o)$-Core Rydberg States with $n = 4$.

The $O(^3P \longrightarrow 4s''\ ^3P^o)$ cross section is obtained by scaling the corresponding $n = 3$ profile using equations (4) and (5), and data from Tables 1 and 2. The scale factor for the $n = 4$ cross section is 0.22. The resulting cross section is given in Figure 19 and Table 19.

The $4s''\ ^1P^o$, $4p''\ ^3SPD$, and $4p''\ ^1SPD$ cross sections are computed using equation (2) (with $\gamma = 0$) and the following: for $4s''\ ^1P^o$, $W = 16.90$ eV, $\alpha = 1$, $\beta = 2$, $\Omega = 3$, and $F = 0.2/(4-1.19)^3 = 0.009$; for $4p''\ ^3SPD$, $W = 17.24$ eV, $\alpha = 2$, $\beta = 1$, $\Omega = 1$, and $F = 0.1/(4-0.86)^3 = 0.003$; and for $4p''\ ^1SPD$, $W = 17.25$ eV, $\alpha = 1$, $\beta = 1$, $\Omega = 3$, and $F = 0.04/(4-0.85)^3 = 0.0013$ (Jackman *et al.*, 1977). These cross sections are plotted in Figure 19; values are tabulated in Table 19.

For the $O(^3P \longrightarrow 4d''\ ^3PD^o)$ cross section, we use the semi-empirical formula of Jackman *et al.* (1977), together with equation (5) for the F value. The result becomes

$$\sigma_4(E) = \frac{qF^*}{W_4 E(4-\delta)^3}\left[1-\left(\frac{W_4}{E}\right)^{\alpha}\right]^{\beta} \ln\left(\frac{4EC}{W_4}+e\right). \qquad (16)$$

In formula (16): $F^* = 0.360$ (Jackman *et al.*, 1977); α, β, and C are the same as for the $n = 3$ cross section; W_4 is given in Table 1; and δ is given in Table 2. This cross section is plotted in Figure 20 and tabulated in Table 20.

The $4d''\ ^3F^o$ and $4d''\ ^1PDF^o$ cross sections are obtained using equation (2) (with $\gamma = 0$) and the following: for $4d''\ ^3F^o$, $W = 17.77$ eV, $\alpha = 2$, $\beta = 1$, $\Omega = 1$, and $F = 0.1/(4-0.05)^3 = 0.0016$; and for $4d''\ ^1PDF^o$, $W = 17.77$ eV, $\alpha = 1$, $\beta = 2$, $\Omega = 3$, and $F = 0.2/(4-0.05)^3 = 0.0032$ (Jackman *et al.*, 1977). These cross sections are given in Figure 20 and Table 20.

2.5.4 Transitions to $O^+(^2P^o)$-Core Rydberg States with $n \geq 5$.

The $O(^3P \longrightarrow \Sigma(n \geq 5)ns''\ ^3P^o)$ cross section is obtained by scaling the $n = 3$ profile using equation (6), and data from Tables 1 and 2. The scale factor that results is 0.20 for this set of states. This cross section is presented in Figure 21 and Table 21.

The $\Sigma(n \geq 5)\ ns''\ ^1P^o$, $\Sigma(n \geq 5)\ np''\ ^3SPD$, and $\Sigma(n \geq 5)\ np''\ ^1SPD$ cross sections are computed using equation (2) (with $\gamma = 0$) and the following: for $ns''\ ^1P^o$, $W = 18.16$ eV, $\alpha = 1$, $\beta = 2$, $\Omega = 3$, and $F = 0.2/(2(4.5 - 1.19)^2) = 0.009$; for $np''\ ^3SPD$, $W = 18.22$ eV, $\alpha = 2$, $\beta = 1$, $\Omega = 1$, and $F = 0.1/(2(4.5 - 0.86)^2) = 0.0038$; and for $np''\ ^1SPD$, $W = 18.22$ eV, $\alpha = 1$, $\beta = 1$, $\Omega = 3$, and $F = 0.04/(2(4.5 - 0.85)^2) = 0.0015$ (Jackman *et al.*, 1977). These cross sections are given in Figure 21 and Table 21.

For the $O(^3P \longrightarrow \Sigma(n \geq 5)nd''\ ^3PD^o)$ cross section, we use the following semi-empirical formula of Jackman *et al.* (1977):

$$\sigma_{n\geq 5}(E) = \frac{qF^*}{2W_A E(4.5-\delta)^2}\left[1 - \left(\frac{W_A}{E}\right)^{\alpha}\right]^{\beta} \ln\left(\frac{4EC}{W_A} + e\right), \qquad (17)$$

where F^*, α, β, and C are the same as given in the previous subsection, W_A is given in Table 1, and δ is given in Table 2. This cross section is shown in Figure 22 and tabulated in Table 22.

The $\Sigma(n \geq 5)\ nd''\ ^3F^o$ and $\Sigma(n \geq 5)\ nd''\ ^1PDF^o$ cross sections are computed using equation (2) (with $\gamma = 0$) and the following: for $nd''\ ^3F^o$, $W = 18.35$ eV, $\alpha = 2$, $\beta = 1$, $\Omega = 1$, and $F = 0.1/(2(4.5 - 0.05)^2) = 0.0025$; and for $nd''\ ^1PDF^o$, $W = 18.35$ eV, $\alpha = 1$, $\beta = 2$, $\Omega = 3$, and $F = 0.2/(2(4.5-0.05)^2) = 0.005$ (Jackman *et al.*, 1977). These cross sections are given in Figure 22 and Table 22.

SECTION 3

ELECTRON-IMPACT IONIZATION CROSS SECTIONS

3.1 SINGLE IONIZATION.

For the single-ionization cross section of atomic oxygen, we use the measurements of Zipf (1985) and Brook *et al.* (1978). The data of Zipf, which cover the 40-300 eV impact energy range, are in very good agreement with the values of Brook *et al.*, which extend from threshold to 1000 eV. Moreover, according to Zipf, the absolute magnitudes of these data have an accuracy in the ±5-10% range. The Brook *et al.* cross sections are recommended by Bell *et al.* (1983).

We allow branching to four different ion states: the usual outer-electron ionization states $^4S^o$, $^2D^o$ and $^2P^o$, and the inner-electron ionization state $2s2p^4\ ^4P$. For the ^4P state, we use the optical cross-section measurements of Zipf *et al.* (1985a; 1985b), which are in good agreement with the theoretical cross sections of Peach (1970). The branching ratios for direct ionization to the remaining three states of O^+ were calculated from theoretical ionization cross sections given by Peach (1968; 1971), and these were used to scale the experimental ionization cross section (after subtracting the ^4P and autoionization [see Section 4] contributions) to give the corresponding partial ionization cross sections. To these we must add the autoionization contribution, which we have assumed goes entirely into the $O^+(^4S^o)$ cross section, since most of the autoionizing states do not have large enough energies to excite the higher O^+ states.

The results are shown in Figure 23 and tabulated in Table 23. Note that for impact energy $E > 1000$ eV we approximate the single-ionization cross section with the formula

$$\sigma(E) = \frac{A + B\ \ln E}{E}. \tag{18}$$

The parameters $A = -4.31 \times 10^{-14}$ cm^2-eV and $B = 1.32 \times 10^{-14}$ cm^2-eV give

a reasonable high-energy fit. The branching ratios to the $^4S^o$, $^2D^o$, $^2P^o$, and ^4P states for $E > 1000$ eV are 0.36, 0.30, 0.17, and 0.18, respectively.

3.2 DOUBLE IONIZATION.

The cross section for doubly-ionizing atomic oxygen is only about 1 percent of the single-ionization cross section at 75 eV and about 4 percent at energies above 150 eV (Zipf, 1985). However, in some problems it still needs to be considered. We recommend use of the cross section measurements of Zipf (1985), which extend up to 300 eV. These measurements, with an accuracy of ±5-10%, are consistent with the data of Ziegler *et al.* (1982).

For $E > 300$ eV, the double-ionization cross section is approximated by formula (18) with $A = 6.60 \times 10^{-16}$ cm^2-eV and $B = 1.06 \times 10^{-16}$ cm^2-eV. The recommended values are shown in Figure 24 and tabulated in Table 24.

SECTION 4

DISCUSSION

We have compiled a set of updated electron-bombardment cross sections for essentially all of the atomic oxygen excitation and ionization processes of practical interest.

In electron-impact calculations involving excitation and ionization, it is often important that autoionization be taken into account. The ionization cross sections given in Figure 23 already include autoionization contributions and therefore these must be removed from the excitation cross sections in order to avoid overestimating the total inelastic cross section. The total excitation cross sections, both with and without autoionization contributions, and the ionization cross sections recommended in this report are plotted in Figure 25 and tabulated in Table 25. The autoionizing excited-states of atomic oxygen and associated autoionization factors (i.e., branching ratios for ionization) are listed in Table 26. The autoionization factors given for the $2p^5\ ^3P^o$, $3d'\ ^3P^o$, and $3s''\ ^3P^o$ states were computed by taking a statistically-weighted mean of the autoionization factors given for each $^3P^o_J$ fine-structure level by Dehmer *et al.* (1977). The errors for these data are at least $\pm 15\%$, and possibly larger. The autoionization factors for the remaining autoionizing states were obtained from Jackman *et al.* (1977); although the uncertainties associated with these numbers were not given, we surmise that they are larger than $\pm 15\%$.

In Figure 25 the values used in the report by Slinker and Ali (1986) are also plotted for a quick overall comparison. The two sets of total ionization cross sections agree very well, since the recent measurements have differed only slightly from the older measurements. The differences between the total excitation cross sections are greater, but still within a factor of 2. These differences between the total excitation cross sections are considerably smaller than the differences between many of the individual cross sections because some of the the latter have been corrected upward and some downward. However, in most applications it is not just the total

excitation and ionization cross sections that matter, but also the branching ratios. The revised branching ratios presented in this report will have important effects on the relative production of different excited states and on the secondary electron distribution obtained in electron/oxygen scattering calculations.

SECTION 5

LIST OF REFERENCES

Bell, K. L., H. B. Gilbody, J. G. Hughes, A. E. Kingston, and F. J. Smith (1983), Recommended data on the electron impact ionization of light atoms and ions, *J. Phys. Chem. Ref. Data* **12**, 891.

Brook, E., M. F. A. Harrison, and A. C. H. Smith (1978), Measurements of the electron impact ionisation cross sections of He, C, O and N atoms, *J. Phys. B* **11**, 3115.

Dalgarno, A. and G. Lejeune (1971), The absorption of electrons in atomic oxygen, *Planet. Space Sci.* **19**, 1653.

Dehmer, P. M., W. L. Luken, and W. A. Chupka (1977), Competition between autoionization and radiative emission in the decay of excited states of the oxygen atom, *J. Chem. Phys.* **67**, 195.

Doering, J. P., E. E. Gulcicek, and S. O. Vaughan (1985), Electron impact measurement of oscillator strengths for dipole-allowed transitions of atomic oxygen, *J. Geophys. Res.* **90**, 5279.

Erdman, P. W. and E. C. Zipf (1983), Electron impact excitation of the λ7990-Å multiplet, *J. Geophys. Res.* **88**, 7245.

Erdman, P. W. and E. C. Zipf (1986), Electron impact excitation of the O I λ1172.6 Å multiplet, *Planet. Space Sci.* **34**, 1155.

Gladstone, G. R., R. Link, S. Chakrabarti, and J. C. McConnel (1987), Modeling of the O I 989-Å to 1173-Å ratio in the terrestrial dayglow, *J. Geophys. Res.* **92**, 12445.

Gulcicek, E. E. and J. P. Doering (1987), Absolute differential and integral electron excitation cross sections of the atomic oxygen ^3P and ^5P states at 30 eV, *J. Geophys. Res.* **92**, 3445.

List of References (continued)

Gulcicek, E. E. and J. P. Doering (1988), Absolute differential and integral electron excitation cross sections for atomic oxygen 5. revised values for the $^3P \longrightarrow {}^3S^o$ (1304 Å) and $^3P \longrightarrow {}^3D^o$ (989 Å) transitions below 30 eV, *J. Geophys. Res.* **93**, 5879.

Gulcicek, E. E., J. P. Doering, and S. O. Vaughan (1988), Absolute differential and integral electron excitation cross sections for atomic oxygen 6. the $^3P \longrightarrow {}^3P$ and $^3P \longrightarrow {}^5P$ transitions from 13.87 eV to 100 eV, *J. Geophys. Res.* **93**, 5885.

Henry, R. J. W., P. G. Burke, and A.-L. Sinfailam (1969), Scattering of electrons by C, N, O, N^+, O^+, and O^{++}, *Phys. Rev.* **178**, 218.

Jackman, C. H., R. H. Garvey, and A. E. S. Green (1977), Electron impact on atmospheric gases I. updated cross sections, *J. Geophys. Res.* **82**, 5081.

Julienne, P. S. and J. Davis (1976), Cascade and radiation trapping effects on atmospheric atomic oxygen emission excited by electron impact, *J. Geophys. Res.* **81**, 1397.

Meier, R. R. (1982), Spectroscopy of the OI 989- and 7990-Å multiplets in the dayglow and aurora, *J. Geophys. Res.* **87**, 6307.

Moore, C. E. (1976), Selected tables of atomic spectra, *NSRDS-NBS* **3**.

Morrison, M. D. (1985), Laboratory measurements of the OI 1173/989 Å branching ratio, *Planet. Space Sci.* **33**, 135.

Peach, G. (1968), Ionization of neutral atoms with outer $2p$ and $3p$ electrons by electron and proton impact, *J. Phys. B* **1**, 1088.

Peach, G. (1970), Ionization of neutral atoms with outer $2p$, $3s$ and $3p$ electrons by electron and proton impact, *J. Phys. B* **3**, 328.

Peach, G. (1971), Ionization of atoms and positive ions by electron and proton impact, *J. Phys. B* **4**, 1670.

List of References (continued)

Rountree, S. P. and R. J. W. Henry (1972), Electron-impact excitation cross sections for atomic oxygen: $^3P - 3s\ ^3S^o$, *Phys. Rev. A* **6**, 2106.

Sawada, T. and P. S. Ganas (1973), Distorted-wave calculation of electron-impact excitation of atomic oxygen, *Phys. Rev. A* **7**, 617.

Shyn, T. W. and W. E. Sharp (1986), Differential excitation cross section of atomic oxygen by electron impact: (^3P–^1D transition), *J. Geophys. Res.* **91**, 1691.

Shyn, T. W., S. Y. Cho, and W. E. Sharp (1986), Differential excitation cross section of atomic oxygen by electron impact: (^3P—^1S transition), *J. Geophys. Res.* **91**, 13751.

Slinker, S. and A. W. Ali (1986), Electron energy deposition in atomic oxygen, *NRL Memorandum Report 5909.*

Smith, E. R. (1976), Electron-impact excitation of atomic oxygen, *Phys. Rev. A* **13**, 65.

Stone, E. J. and E. C. Zipf (1971), Excitation of the OI(^3S) and NI(^4P) resonance states by electron impact on O and N, *Phys. Rev. A* **4**, 610.

Stone, E. J. and E. C. Zipf (1974), Electron-impact excitation of the $^3S^o$ and $^5S^o$ states of atomic oxygen, *J. Chem. Phys.* **60**, 4237.

Thomas, L. D. and R. K. Nesbet (1975), Low-energy electron scattering by atomic oxygen, *Phys. Rev. A* **11**, 170.

Vaughan, S. O. and J. P. Doering (1986), Absolute experimental differential and integral electron excitation cross sections for atomic oxygen 2. the ($^3P \longrightarrow {}^3S^o$) transition (1304 Å) from 16.5 to 200 eV with comparison to atomic hydrogen, *J. Geophys. Res.* **91**, 13755.

Vaughan, S. O. and J. P. Doering (1987), Absolute experimental differential and integral electron excitation cross sections for atomic oxygen 3. the ($^3P \longrightarrow {}^3D^o$) transition (989 Å) from 20 to 200 eV with improved values for the ($^3P \longrightarrow {}^3S^o$) transition (1304 Å), *J. Geophys. Res.* **92**, 7749.

List of References (continued)

Vaughan, S. O. and J. P. Doering (1988), Absolute experimental differential and integral electron excitation cross sections for atomic oxygen 4. the ($^3P \longrightarrow 3s''\ ^3P^o$), ($^3P \longrightarrow 2s2p^5\ ^3P^o$), ($^3P \longrightarrow 4d'\ ^3P^o$) autoionizing transitions (878 Å, 792 Å, and 770 Å) and five members of the ($^3P \longrightarrow nd\ ^3D^o$) Rydberg series (1027 Å), *J. Geophys. Res.* **93**, 289.

Vo Ky Lan, N. Feautrier, M. Le Dourneuf, and H. Van Regemorter (1972), Cross sections calculations for electron-oxygen scattering using the polarized orbital close coupling theory, *J. Phys. B* **5**, 1506.

Ziegler, D. L., H. H. Newman, K. Smith, and R. F. Stebbings (1982), Double ionization of atomic oxygen by electron impact, *Planet. Space Sci.* **30**, 451.

Zipf, E. C. (1985), The ionization of atomic oxygen by electron impact, *Planet. Space Sci.* **33**, 1303.

Zipf, E. C. and P. W. Erdman (1985), Electron impact excitation of atomic oxygen: revised cross sections, *J. Geophys. Res.* **90**, 11087.

Zipf, E. C., W. W. Kao, and R. W. McLaughlin (1985a), The excitation of the OII($2s2p^4\ ^4P \longrightarrow 2s^22p^3\ ^4S$; λ834 Å) transition by electron impact on atomic and molecular oxygen, *Chem. Phys. Lett.* **118**, 591.

Zipf, E. C., W. W. Kao, and P. W. Erdman (1985b), On the simultaneous ionization-excitation of the OII(λ834 Å) resonance transition by electron impact on atomic oxygen, *Planet. Space Sci.* **33**, 1309.

Zipf, E. C. and W. W. Kao (1986), Electron-impact excitation of the $3s''\ ^3P^o$ and $2s2p^5\ ^3P^o$ autoionizing states of atomic oxygen. *Chem. Phys. Lett.* **125**, 394.

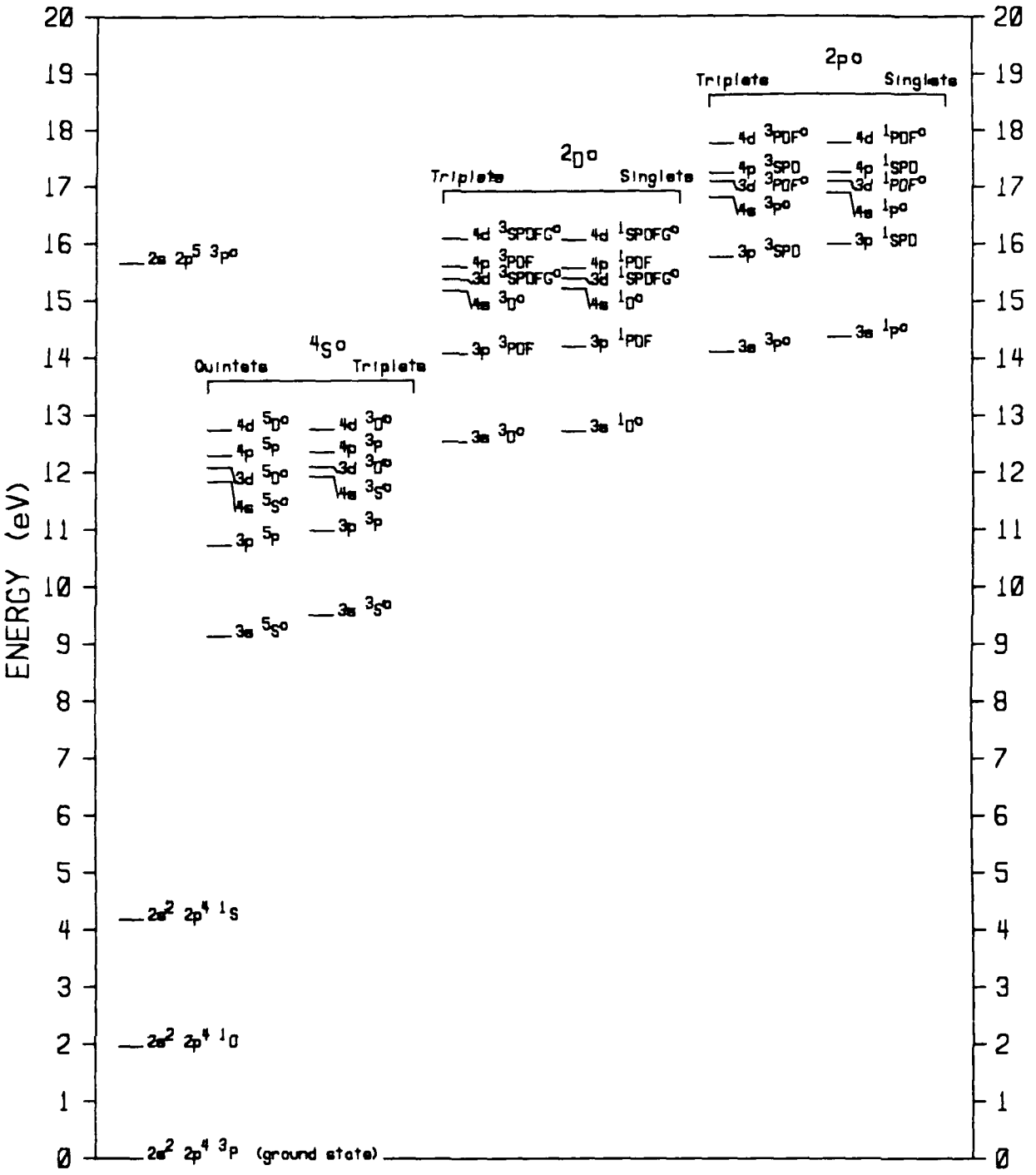

Figure 1. Atomic oxygen threshold energies for electronic excitation to lower excited states.

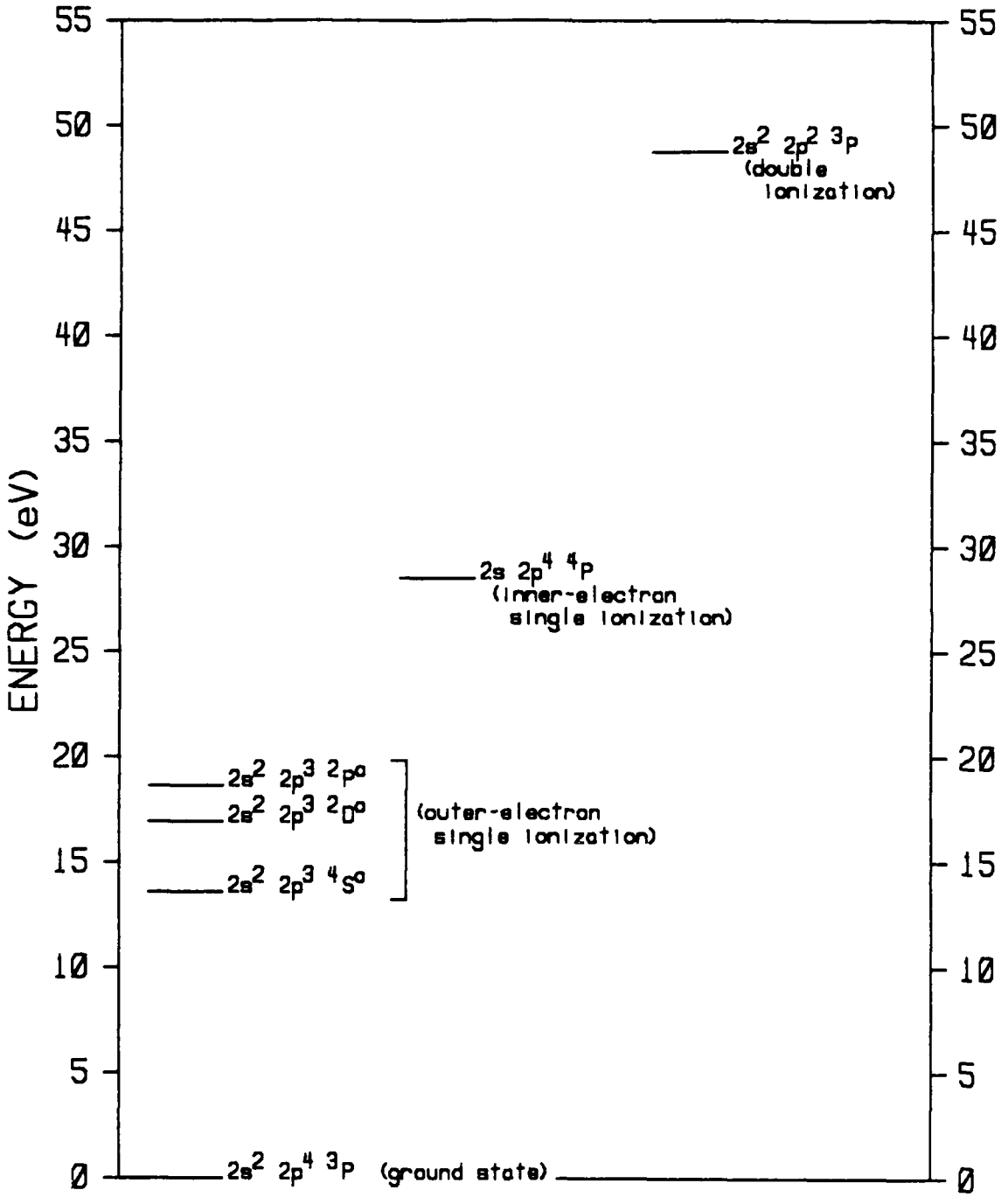

Figure 2. Atomic oxygen threshold energies for ionization to single and double ion states.

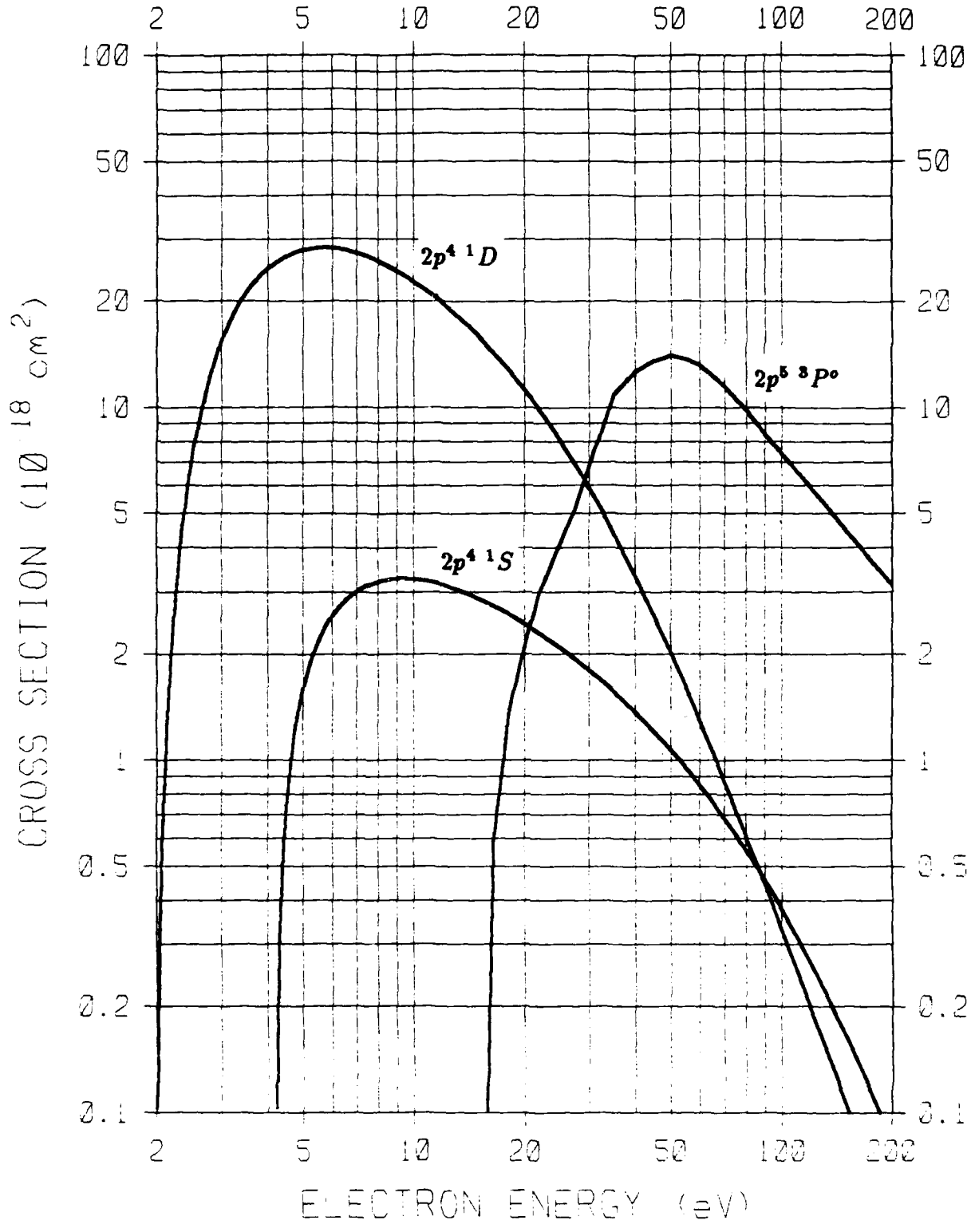

Figure 3. $O(^3P \longrightarrow 2p^4\ ^1D,\ 2p^4\ ^1S,\ 2p^5\ ^3P^o)$ **excitation cross sections.**

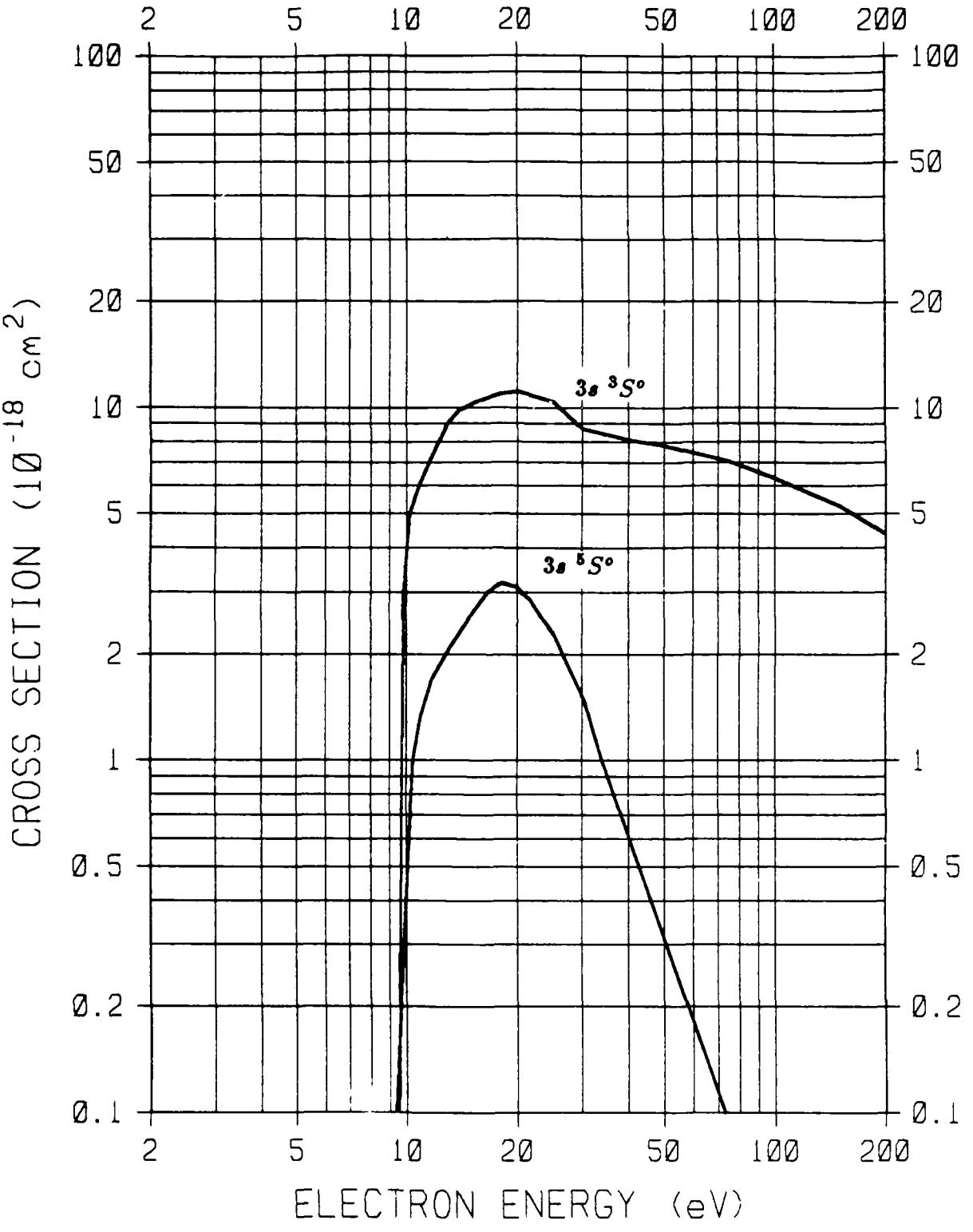

Figure 4. O($^3P \longrightarrow 3s\ ^5S^o$, $3s\ ^3S^o$) excitation cross sections.

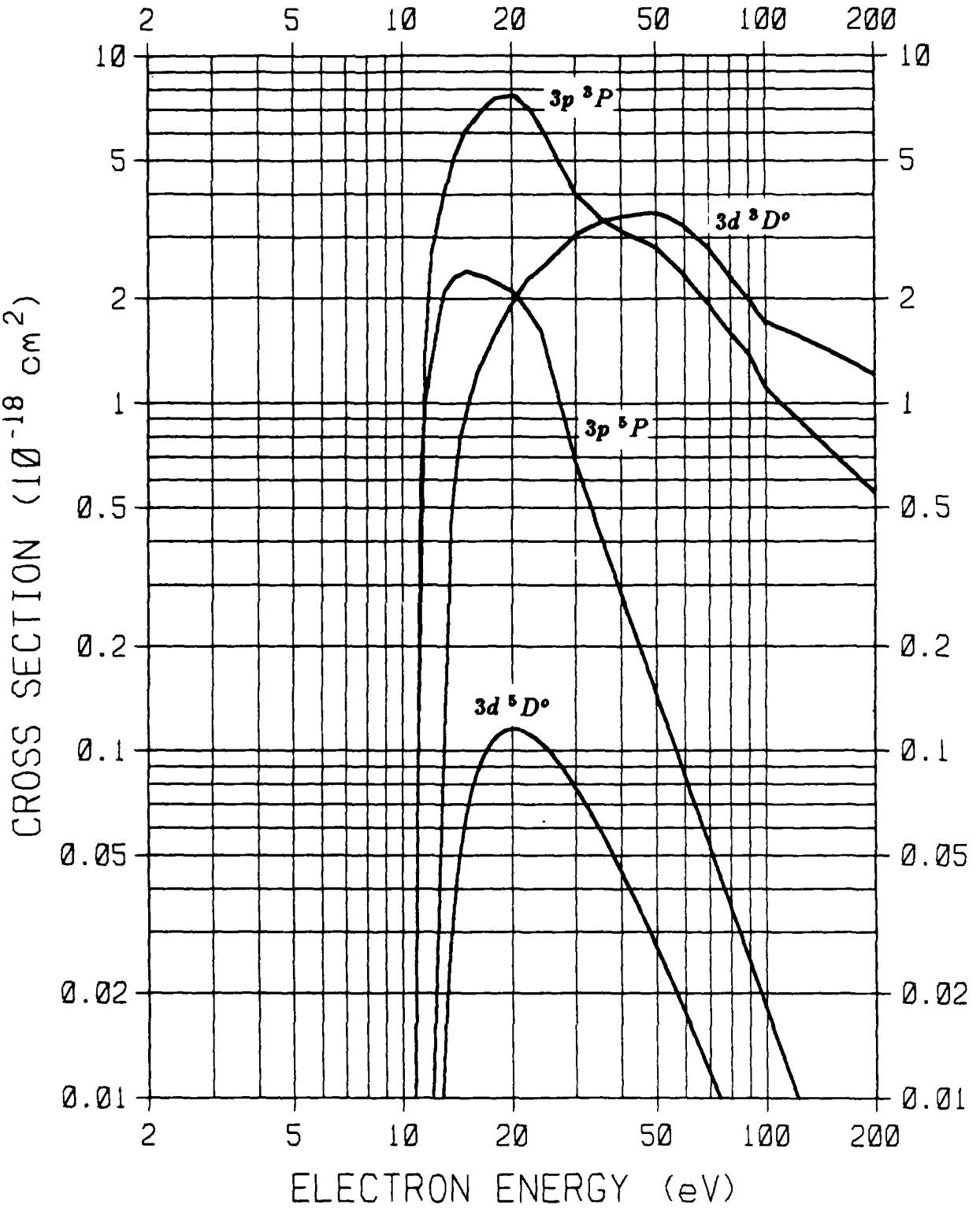

Figure 5. O($^3P \longrightarrow 3p\ ^5P$, $3p\ ^3P$, $3d\ ^5D^o$, $3d\ ^3D^o$) excitation cross sections.

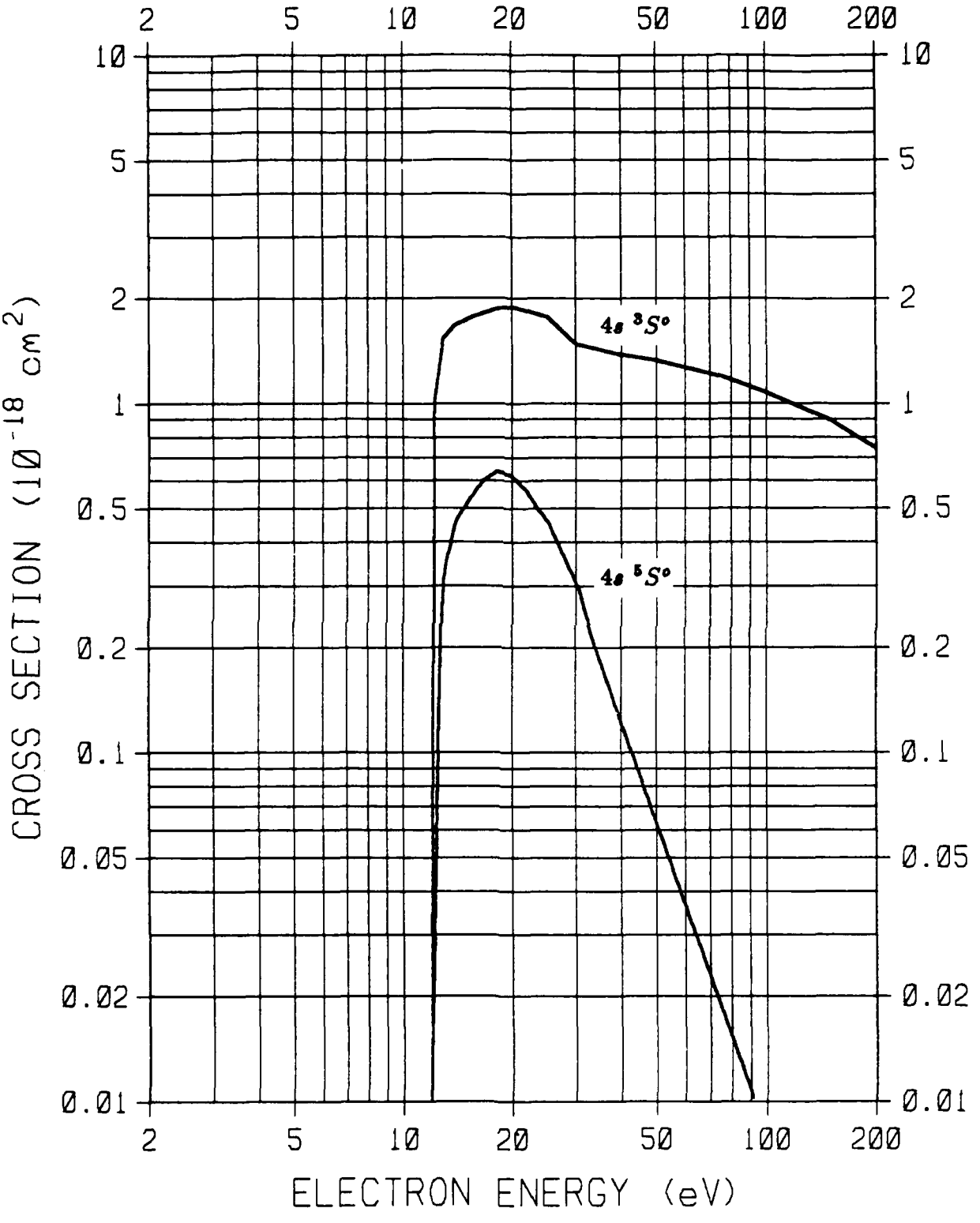

Figure 6. O($^3P \longrightarrow 4s\ ^5S^o$, $4s\ ^3S^o$) excitation cross sections.

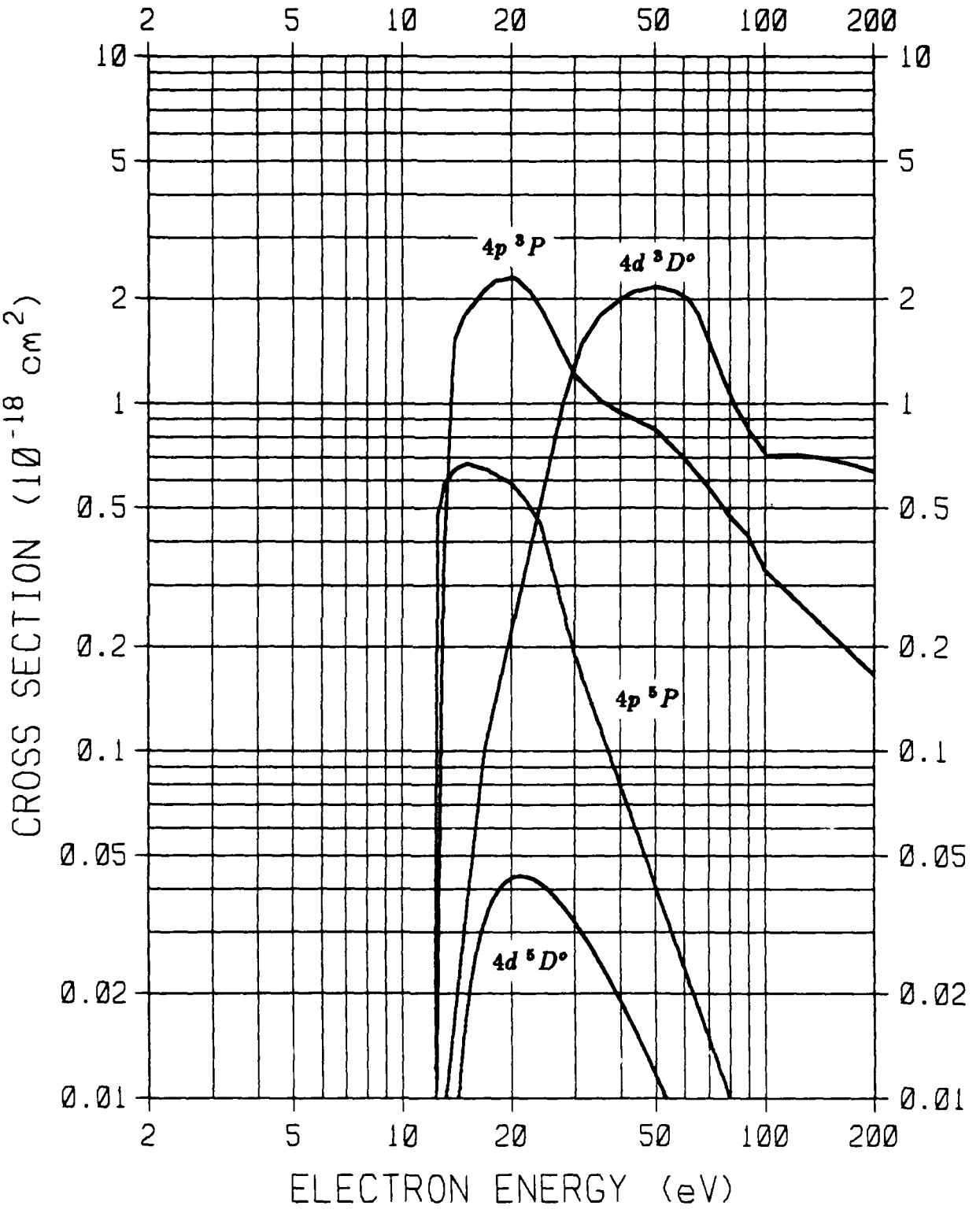

Figure 7. $O(^3P \longrightarrow 4p\ ^5P,\ 4p\ ^3P,\ 4d\ ^5D^o,\ 4d\ ^3D^o)$ **excitation cross sections.**

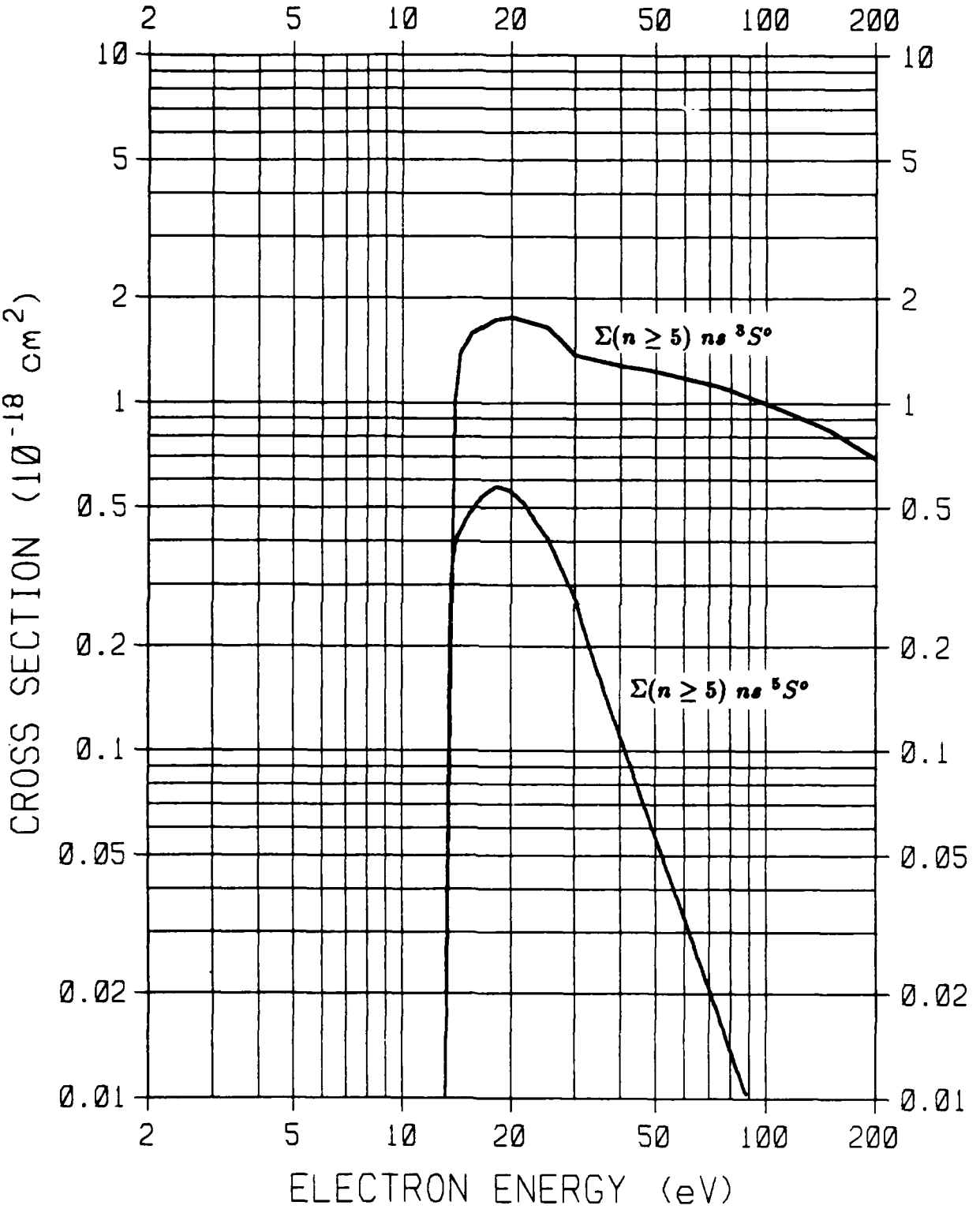

Figure 8. $O(^3P \longrightarrow \Sigma(n \geq 5)\ ns\ ^5S^o, \Sigma(n \geq 5)\ ns\ ^3S^o)$ **excitation cross sections.**

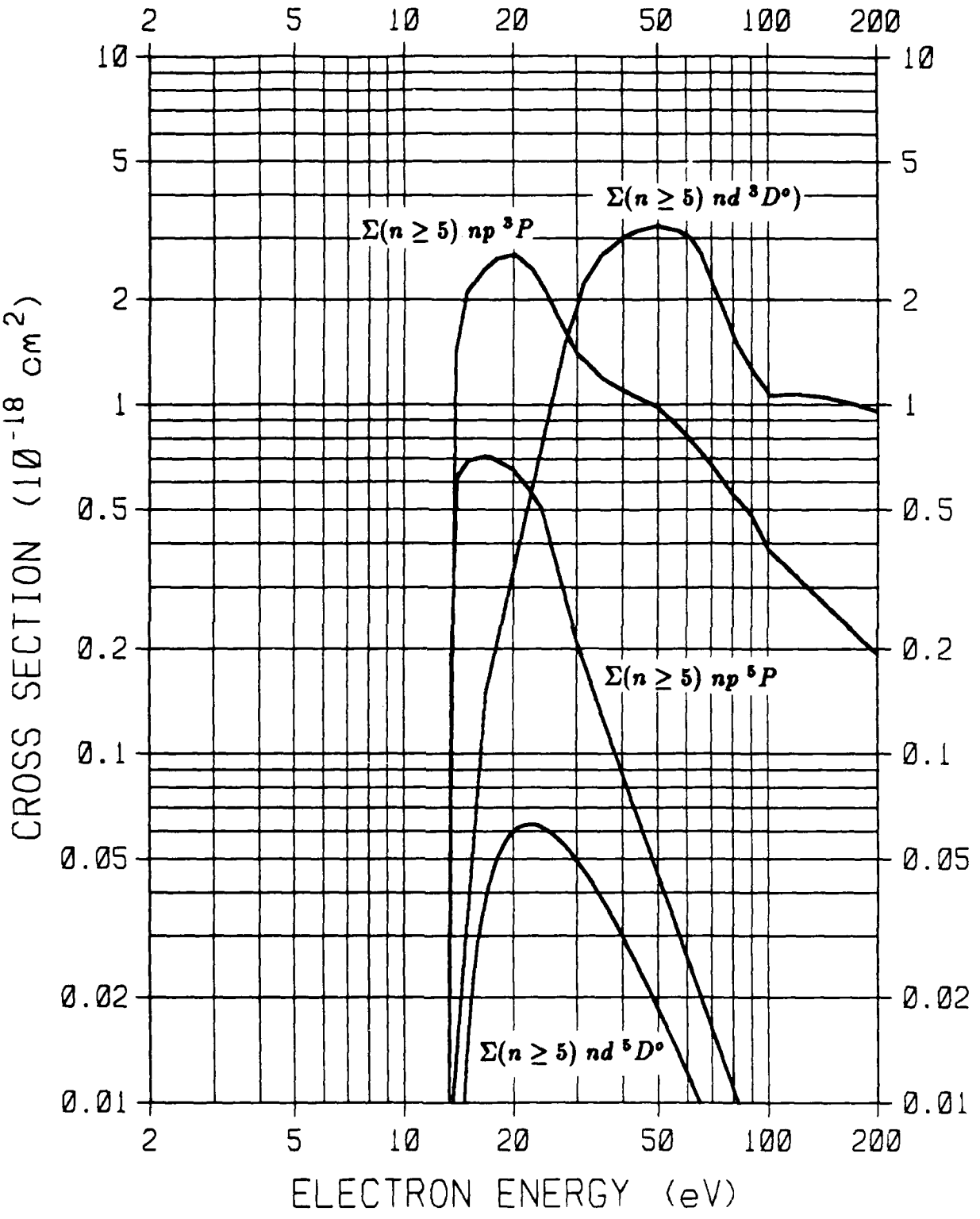

Figure 9. $O(^3P \longrightarrow \Sigma(n \geq 5)\ np\ ^5P, \Sigma(n \geq 5)\ np\ ^3P, \Sigma(n \geq 5)\ nd\ ^5D^o, \Sigma(n \geq 5)\ nd\ ^3D^o)$ **excitation cross sections.**

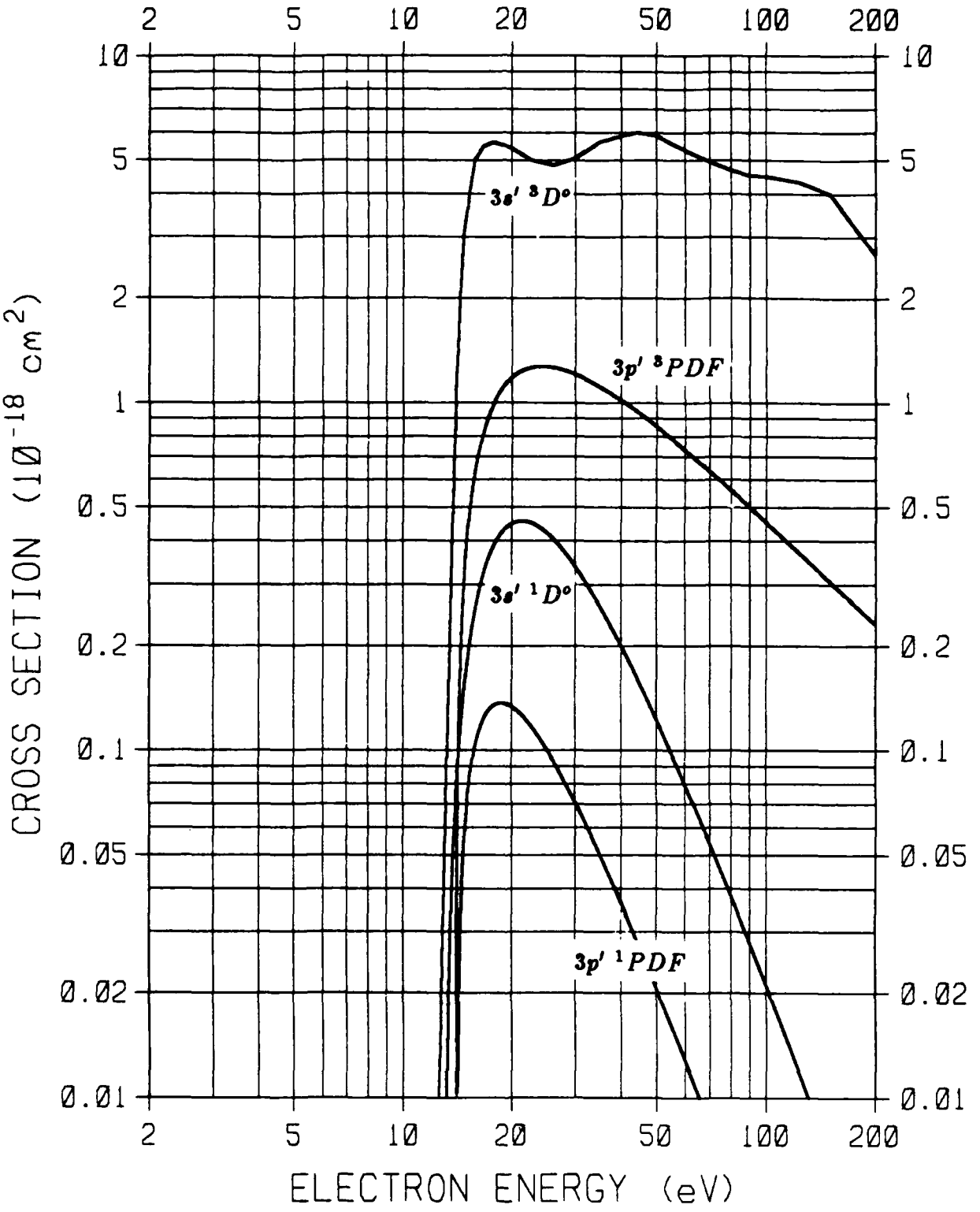

Figure 10. O($^3P \longrightarrow 3s'\ ^3D^o$, $3s'\ ^1D^o$, $3p'\ ^3PDF$, $3p'\ ^1PDF$) excitation cross sections.

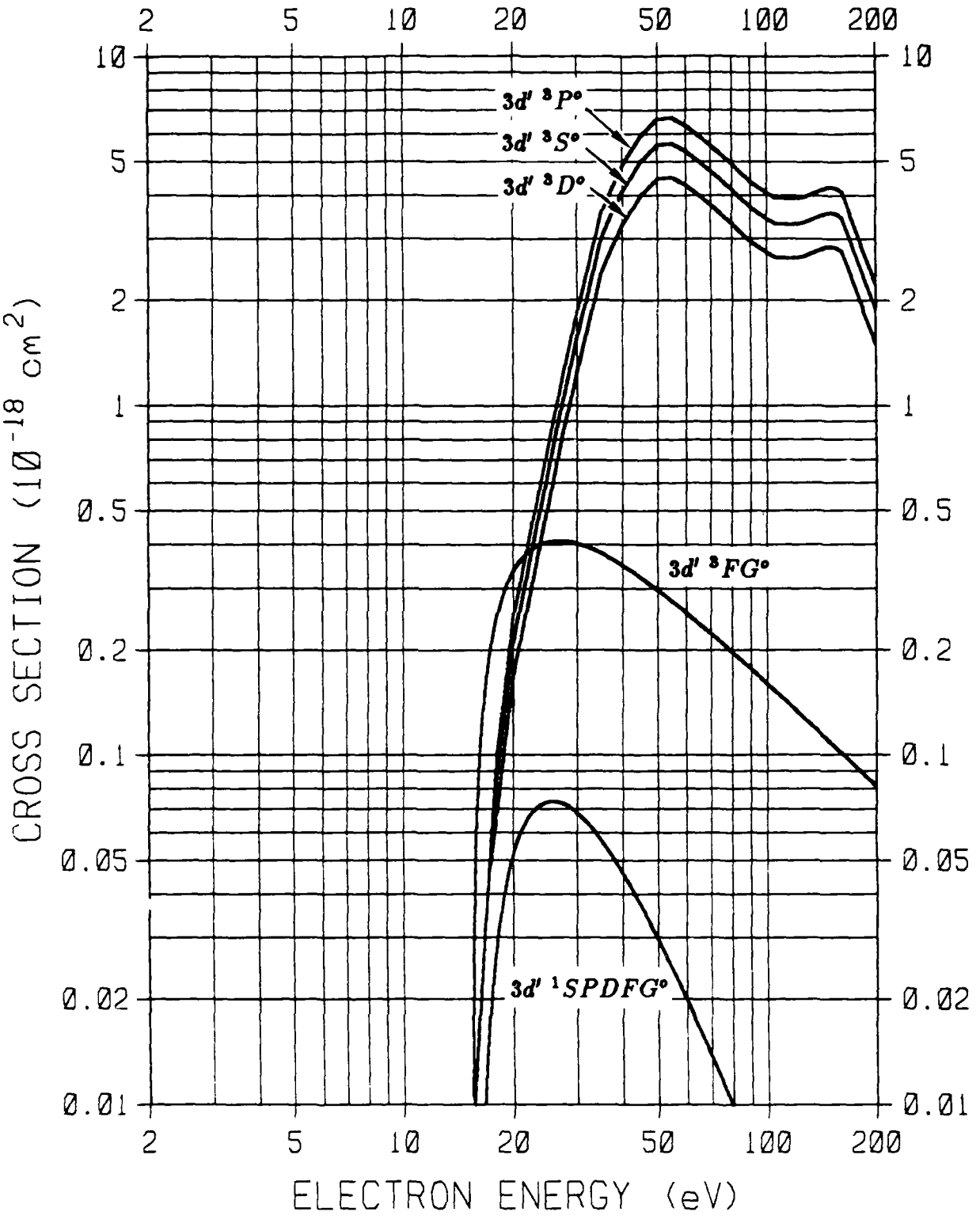

Figure 11. O($^3P \longrightarrow 3d'\ ^3S^o$, $3d'\ ^3P^o$, $3d'\ ^3D^o$, $3d'\ ^3FG^o$, $3d'\ ^1SPDFG^o$) excitation cross sections.

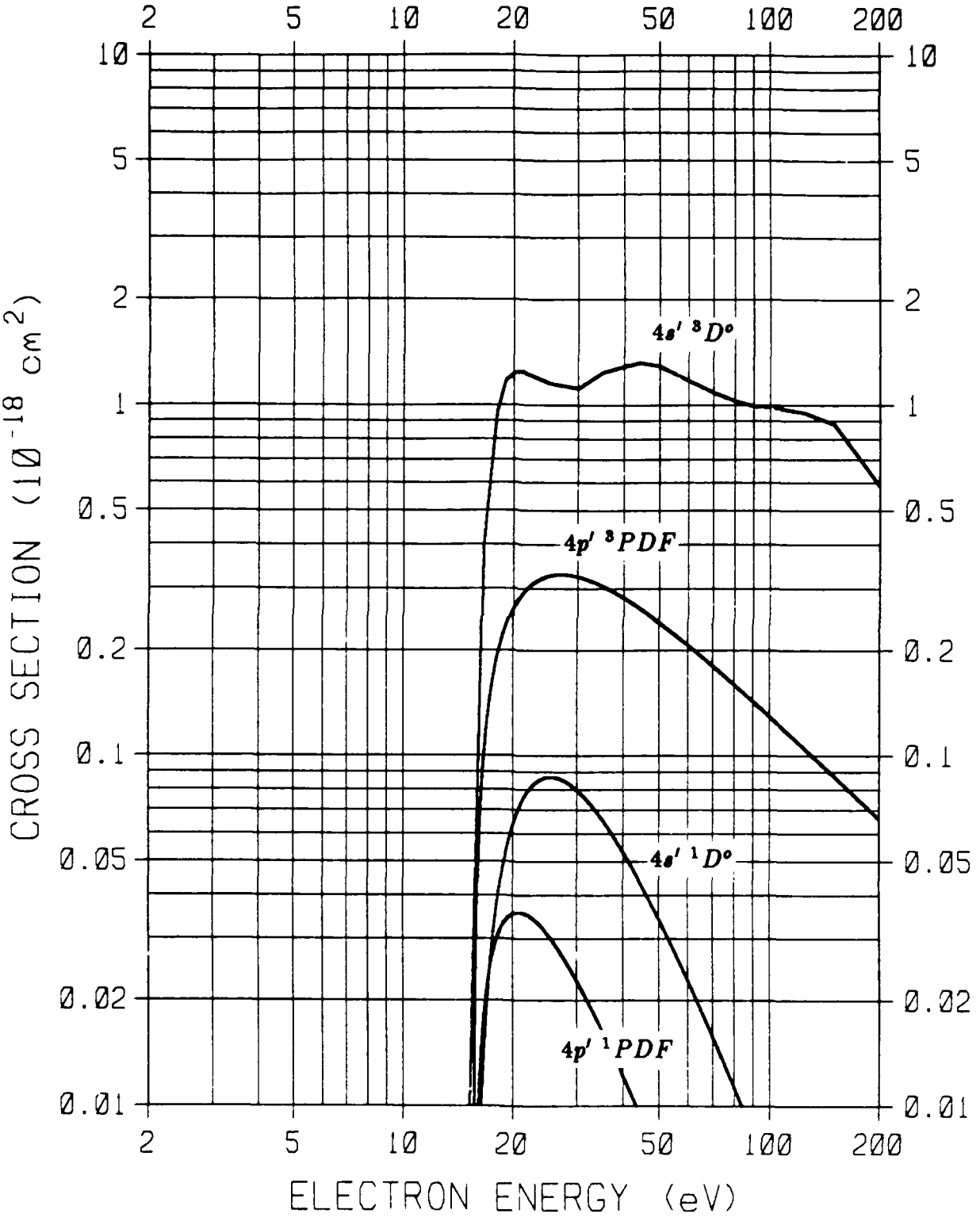

Figure 12. O($^3P \longrightarrow 4s'\ ^3D^o$, $4s'\ ^1D^o$, $4p'\ ^3PDF$, $4p'\ ^1PDF$) excitation cross sections.

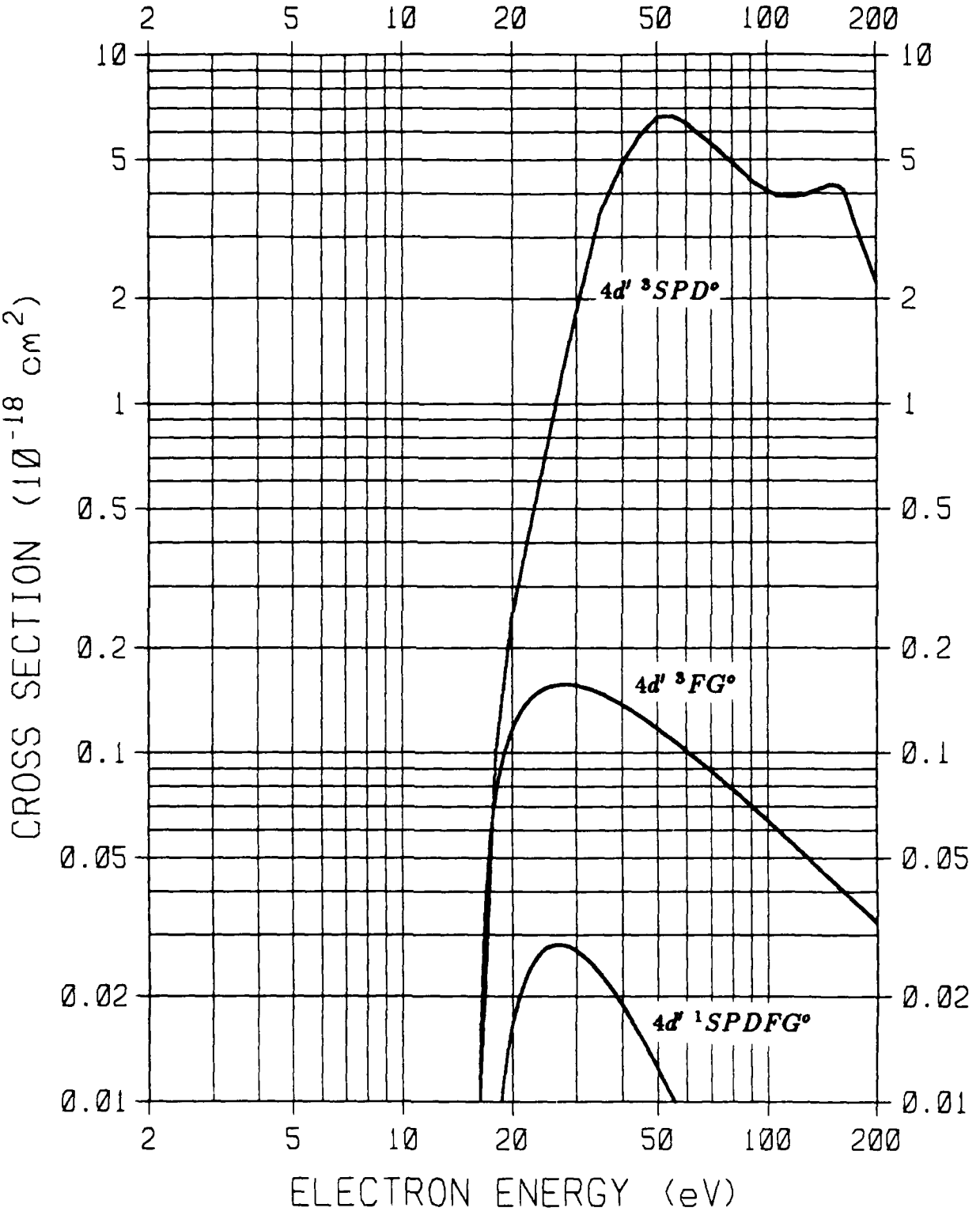

Figure 13. O($^3P \longrightarrow 4d'\ ^3SPD^o$, $4d'\ ^3FG^o$, $4d'\ ^1SPDFG^o$) excitation cross sections.

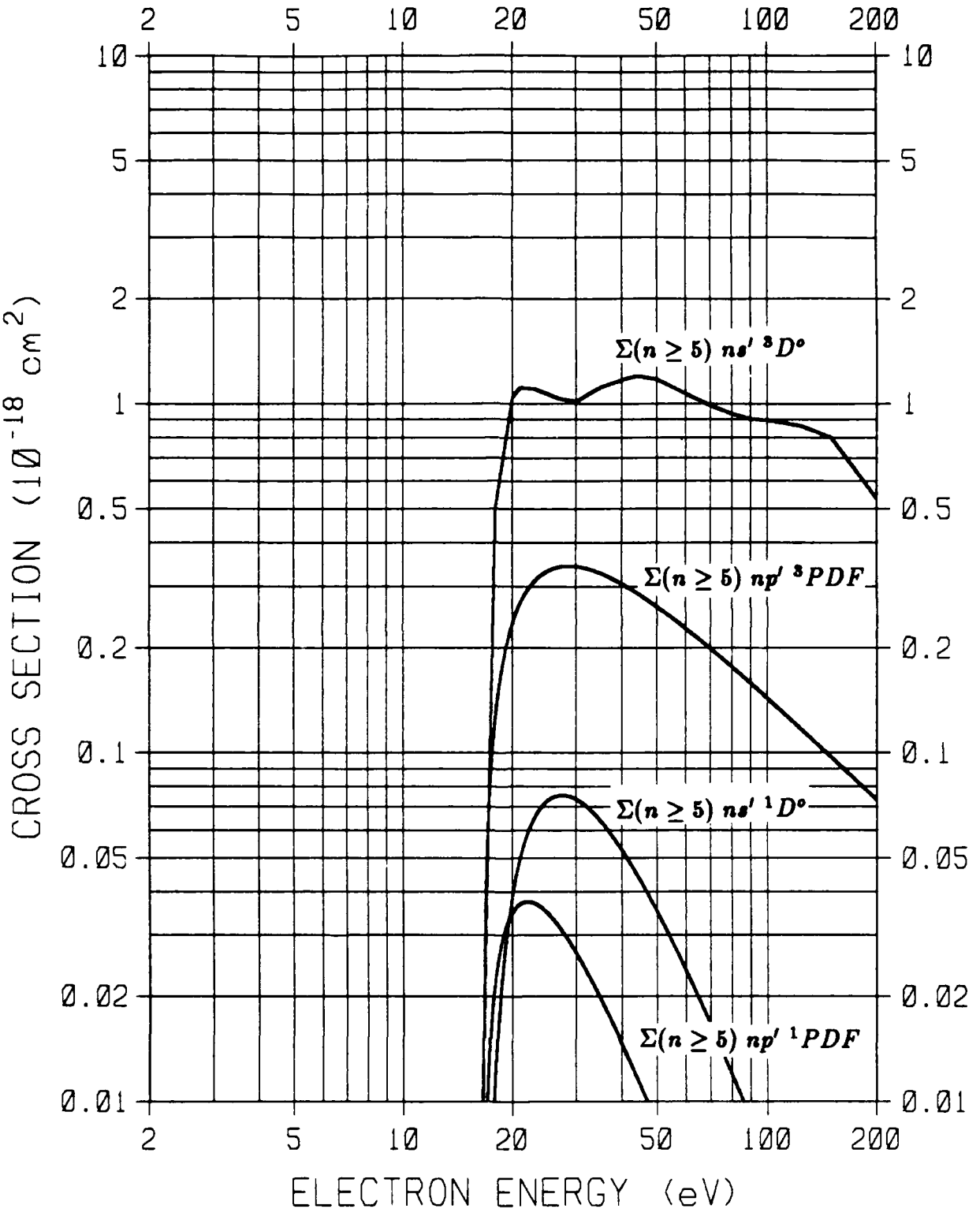

Figure 14. $O(^3P \longrightarrow \Sigma(n \geq 5)\ ns'\ ^3D^o$, $\Sigma(n \geq 5)\ ns'\ ^1D^o$, $\Sigma(n \geq 5)\ np'\ ^3PDF$, $\Sigma(n \geq 5)\ np'\ ^1PDF)$ **excitation cross sections.**

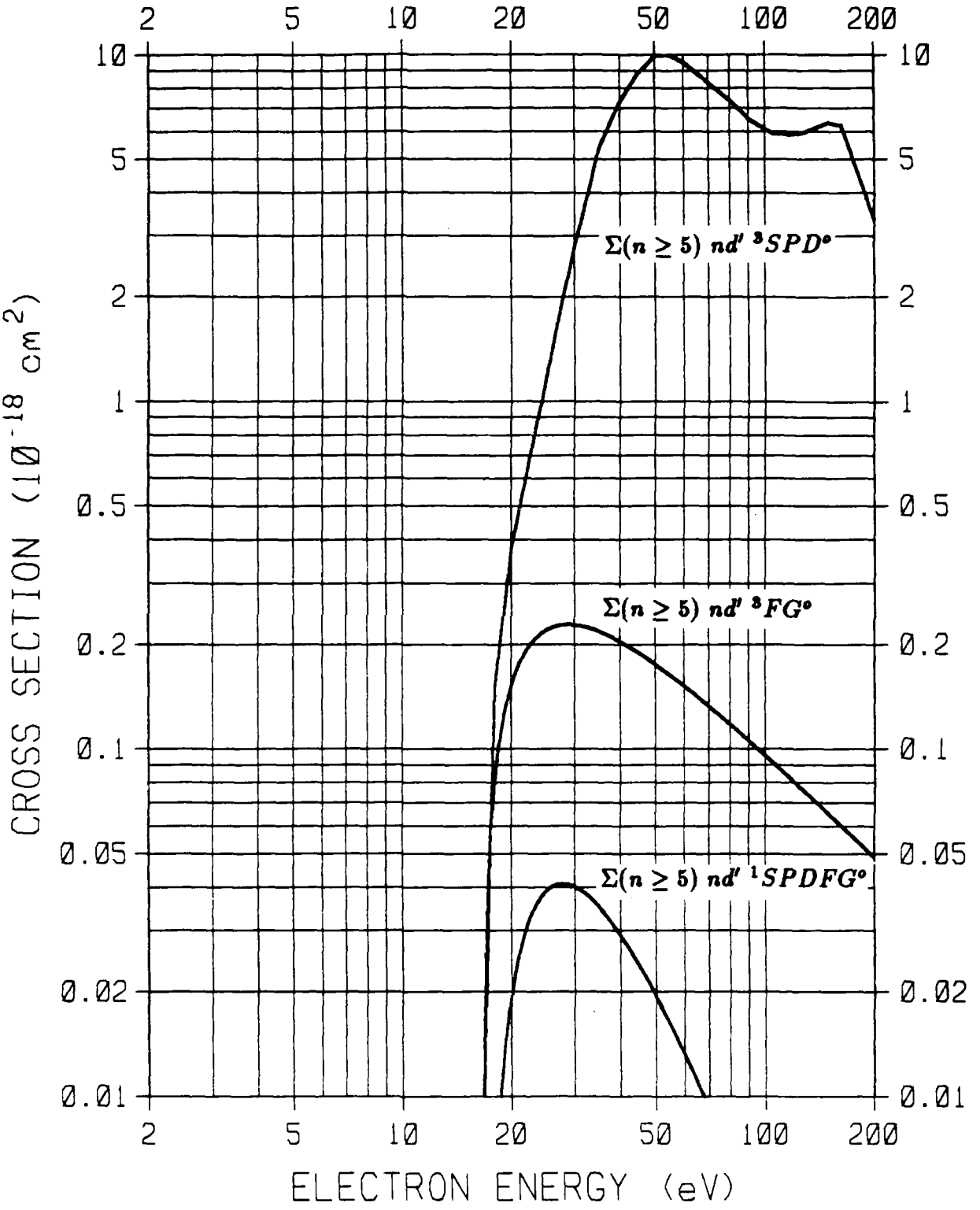

Figure 15. $O(^3P \longrightarrow \Sigma(n \geq 5)\ nd'\ ^3SPD^o, \Sigma(n \geq 5)\ nd'\ ^3FG^o, \Sigma(n \geq 5)\ nd'\ ^1SPDFG^o)$ excitation cross sections.

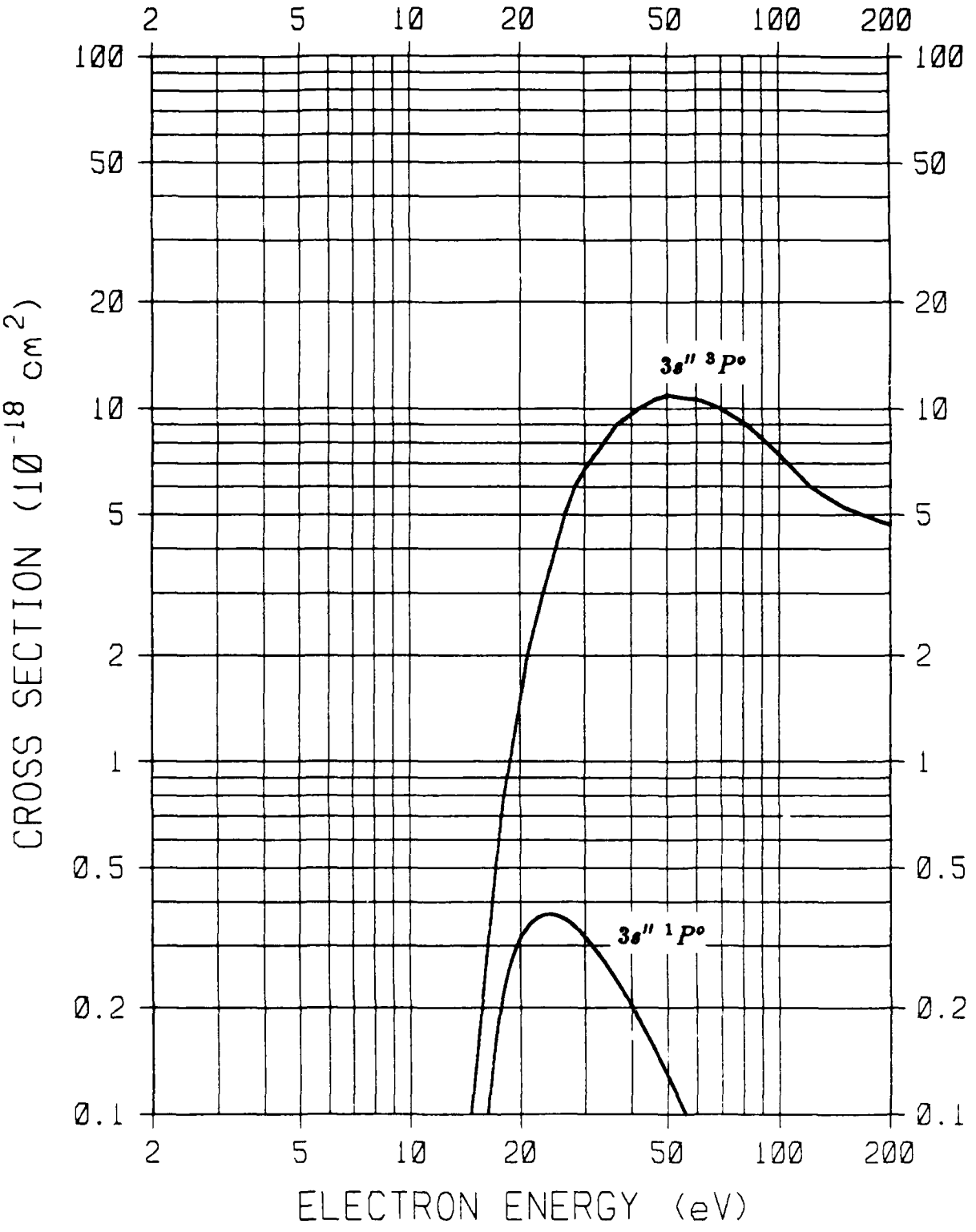

Figure 16. $O(^3P \longrightarrow 3s''\ ^3P^o, 3s''\ ^1P^o)$ excitation cross sections.

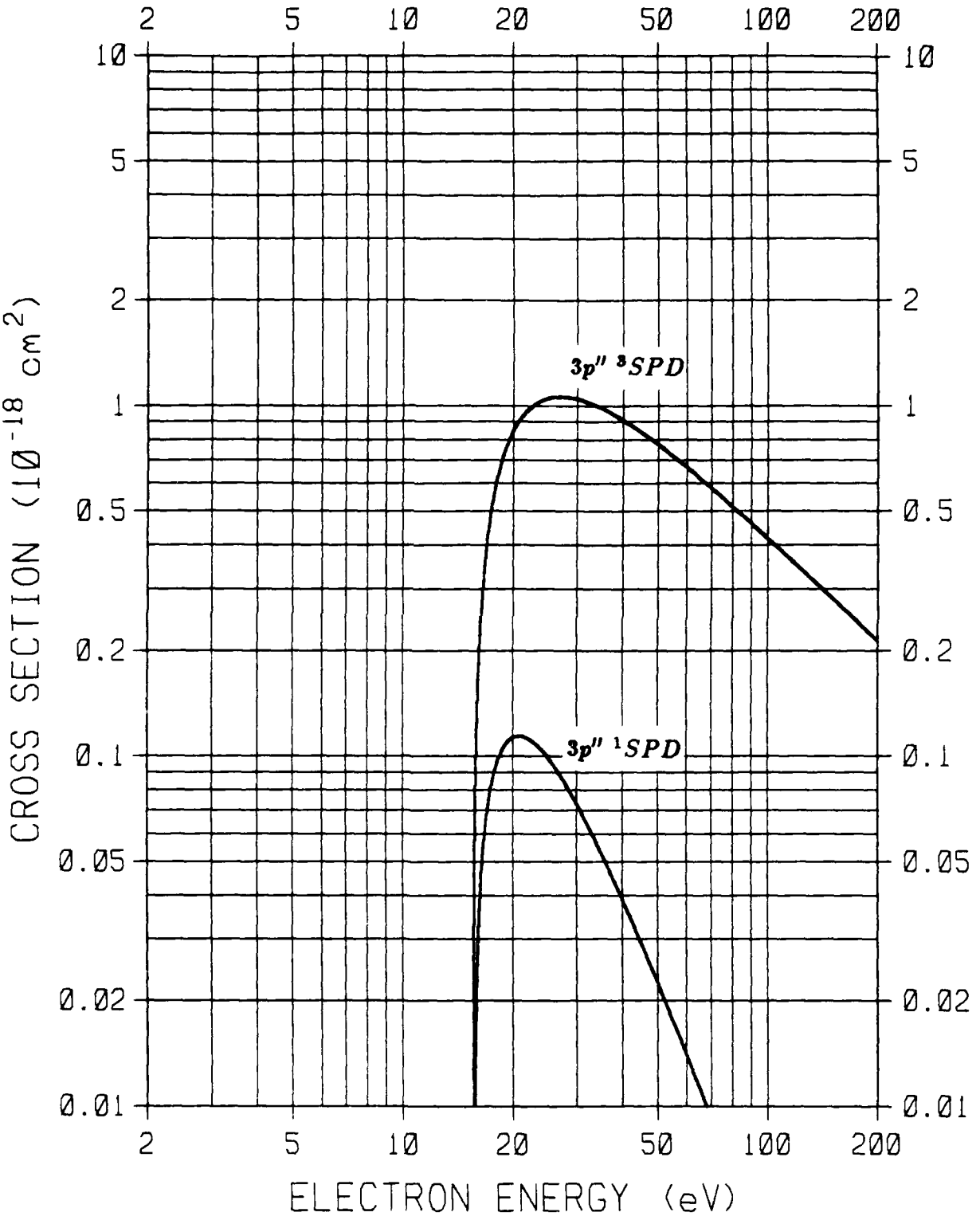

Figure 17. $O(^3P \longrightarrow 3p''\ ^3SPD,\ 3p''\ ^1SPD)$ **excitation cross sections.**

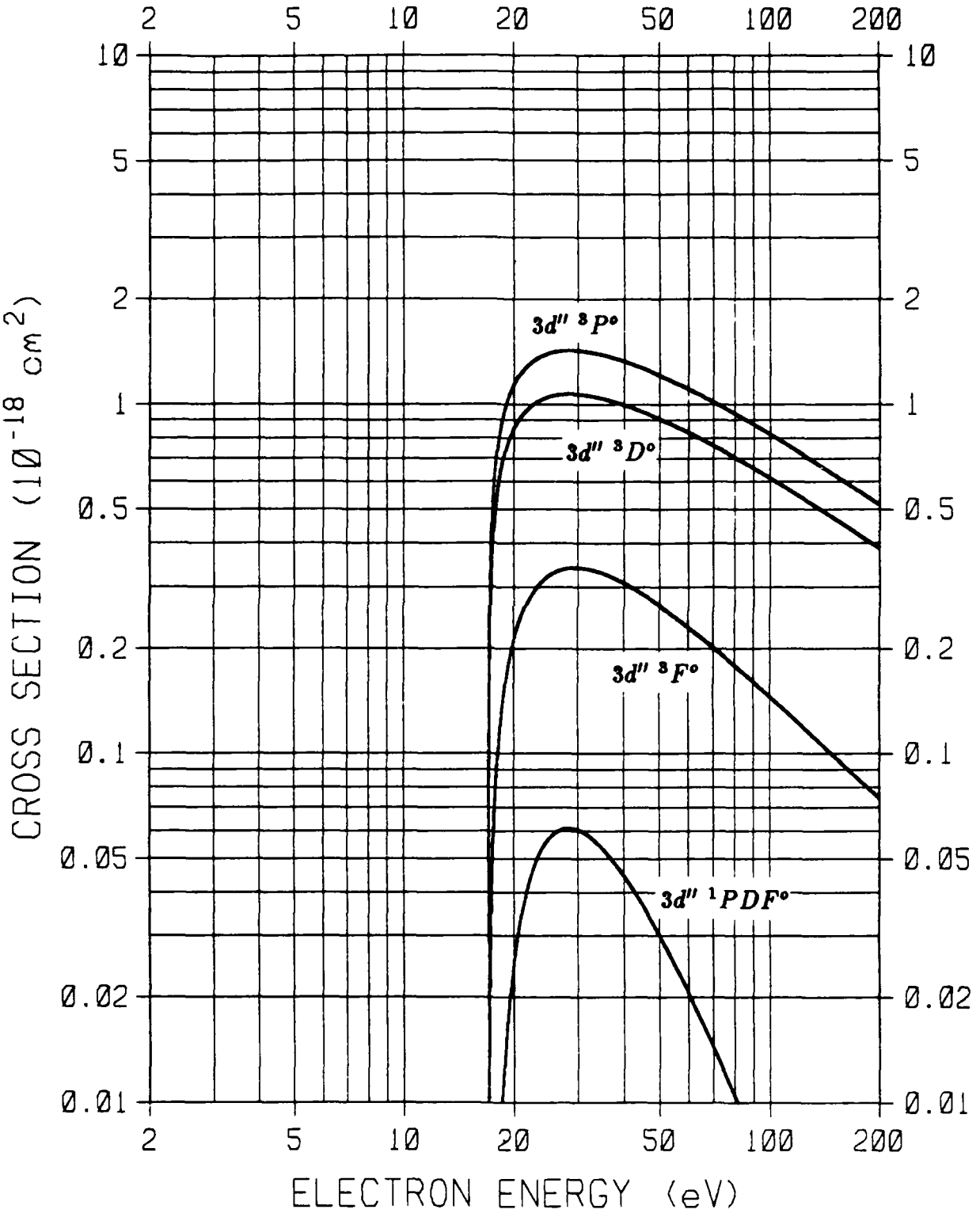

Figure 18. $O(^3P \longrightarrow 3d''\ ^3P^o,\ 3d''\ ^3D^o,\ 3d''\ ^3F^o,\ 3d''\ ^1PDF^o)$ **excitation cross sections.**

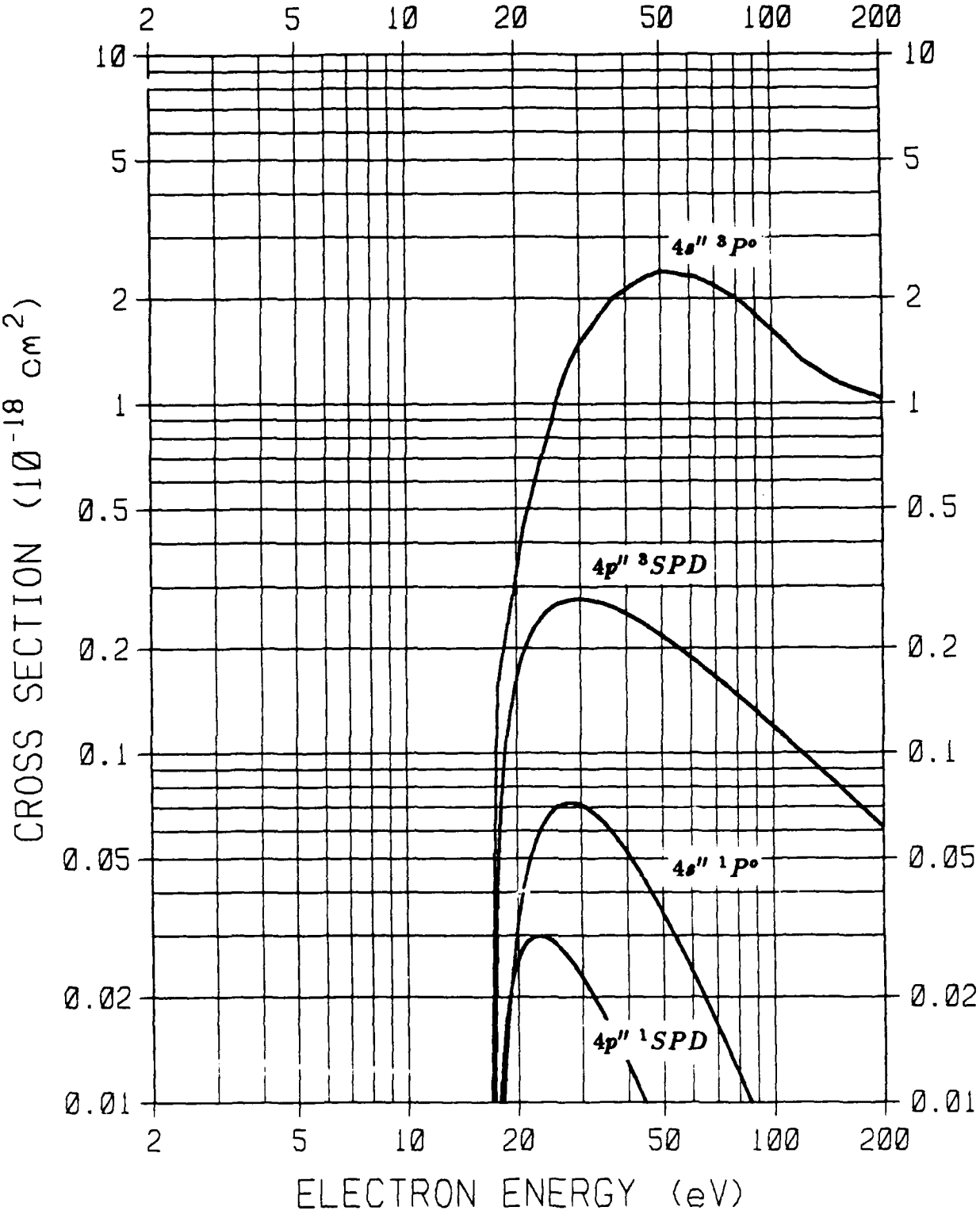

Figure 19. O($^3P \longrightarrow 4s''\ ^3P^o$, $4s''\ ^1P^o$, $4p''\ ^3SPD$, $4p''\ ^1SPD$) **excitation cross sections.**

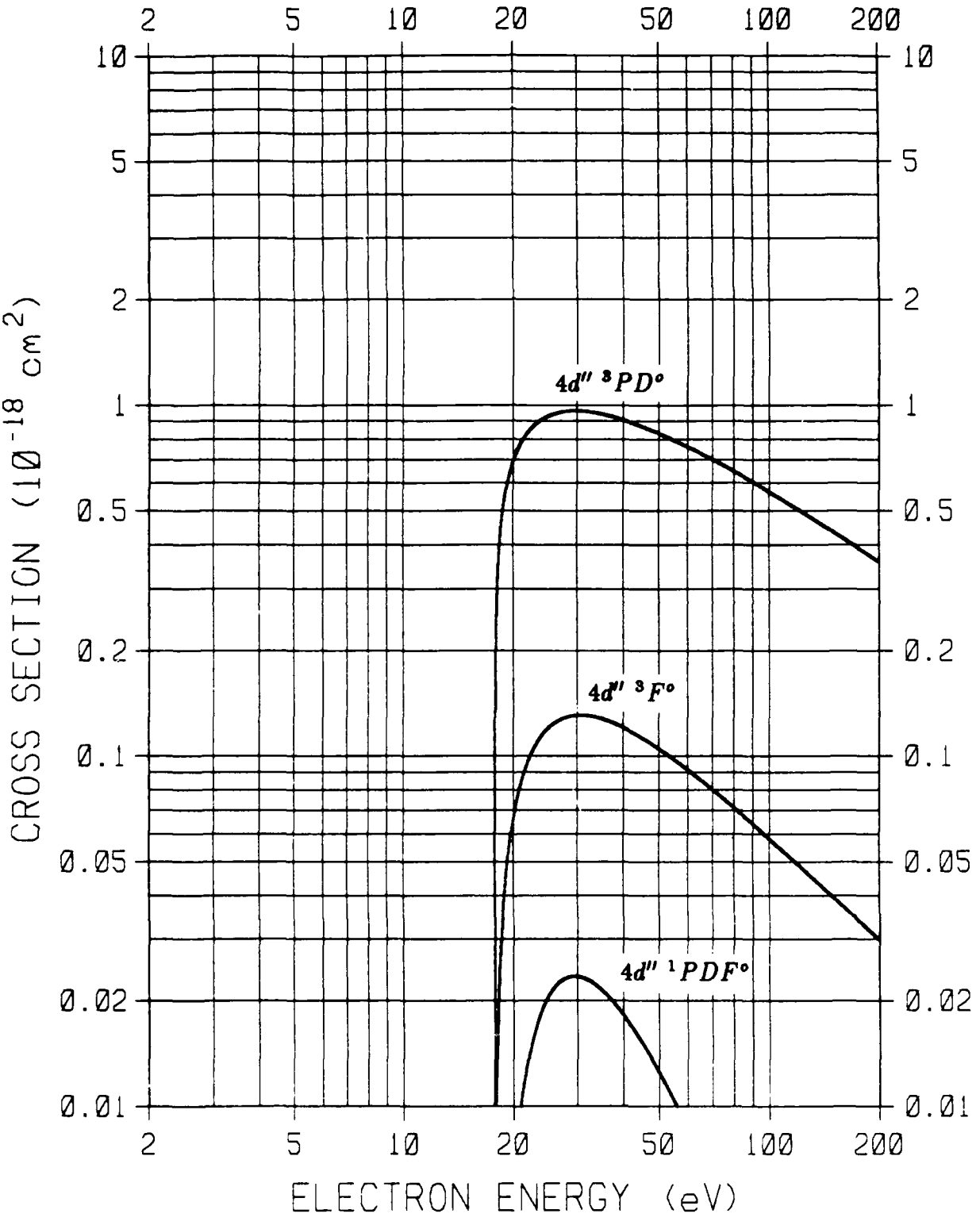

Figure 20. $O(^3P \longrightarrow 4d''\ ^3PD^\circ, 4d''\ ^3F^\circ, 4d''\ ^1PDF^\circ)$ **excitation cross sections.**

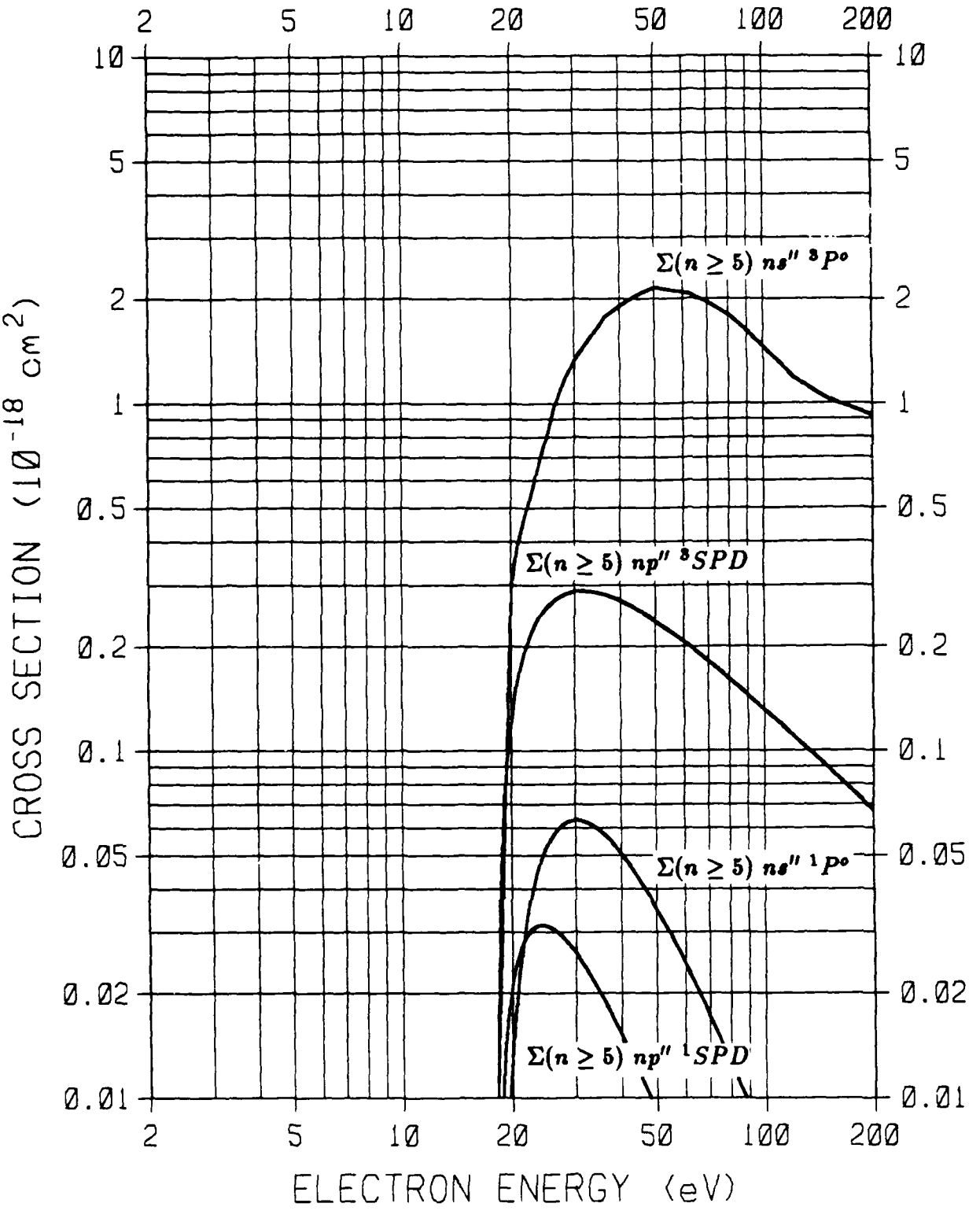

Figure 21. $O(^3P \longrightarrow \Sigma(n \geq 5)\ ns''\ ^3P^o, \Sigma(n \geq 5)\ ns''\ ^1P^o, \Sigma(n \geq 5)\ np''\ ^3SPD, \Sigma(n \geq 5)\ np''\ ^1SPD)$ excitation cross sections.

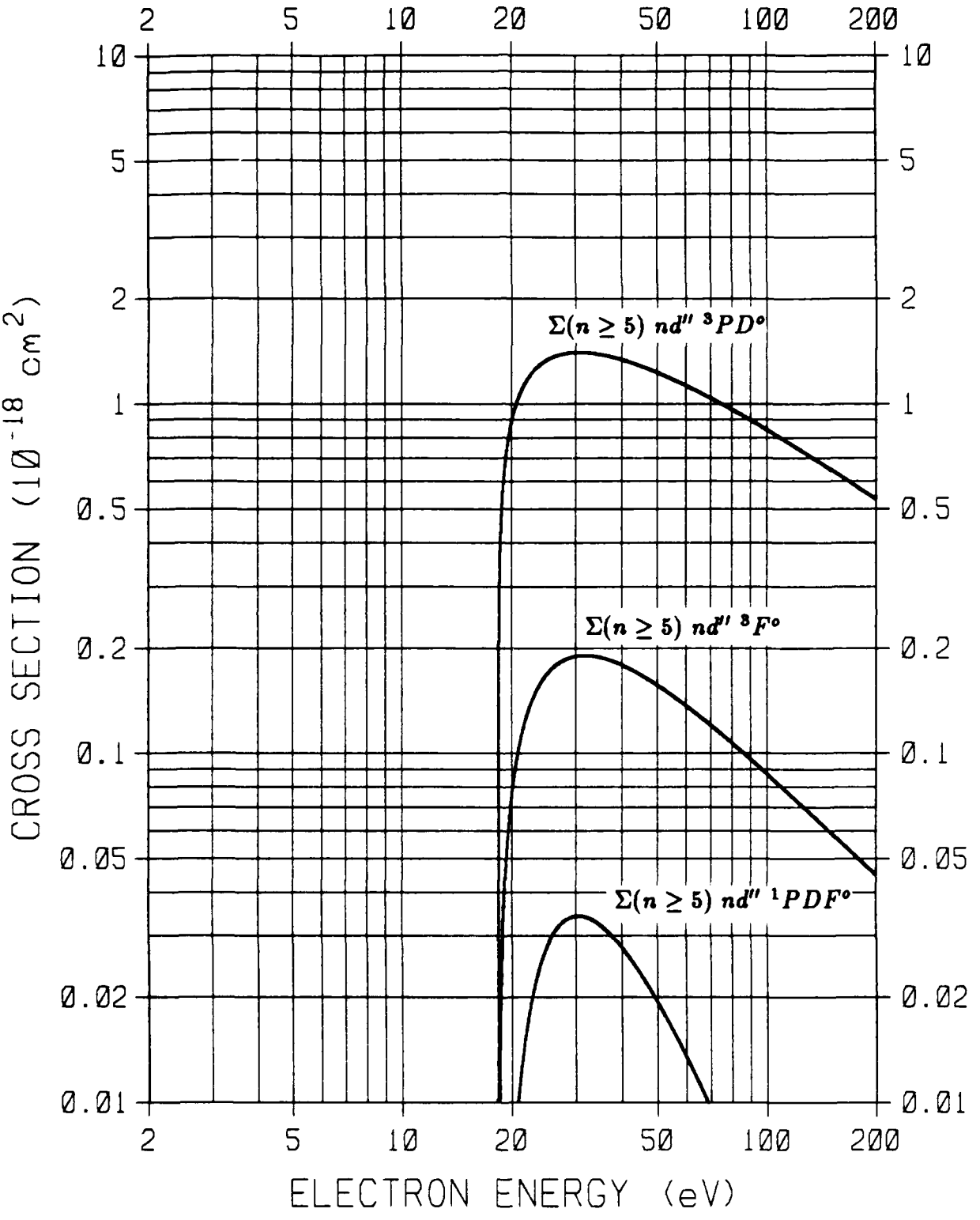

Figure 22. $O(^3P \longrightarrow \Sigma(n \geq 5)\ nd''\ ^3PD^o, \Sigma(n \geq 5)\ nd''\ ^3F^o, \Sigma(n \geq 5)\ nd''\ ^1PDF^o)$ **excitation cross sections.**

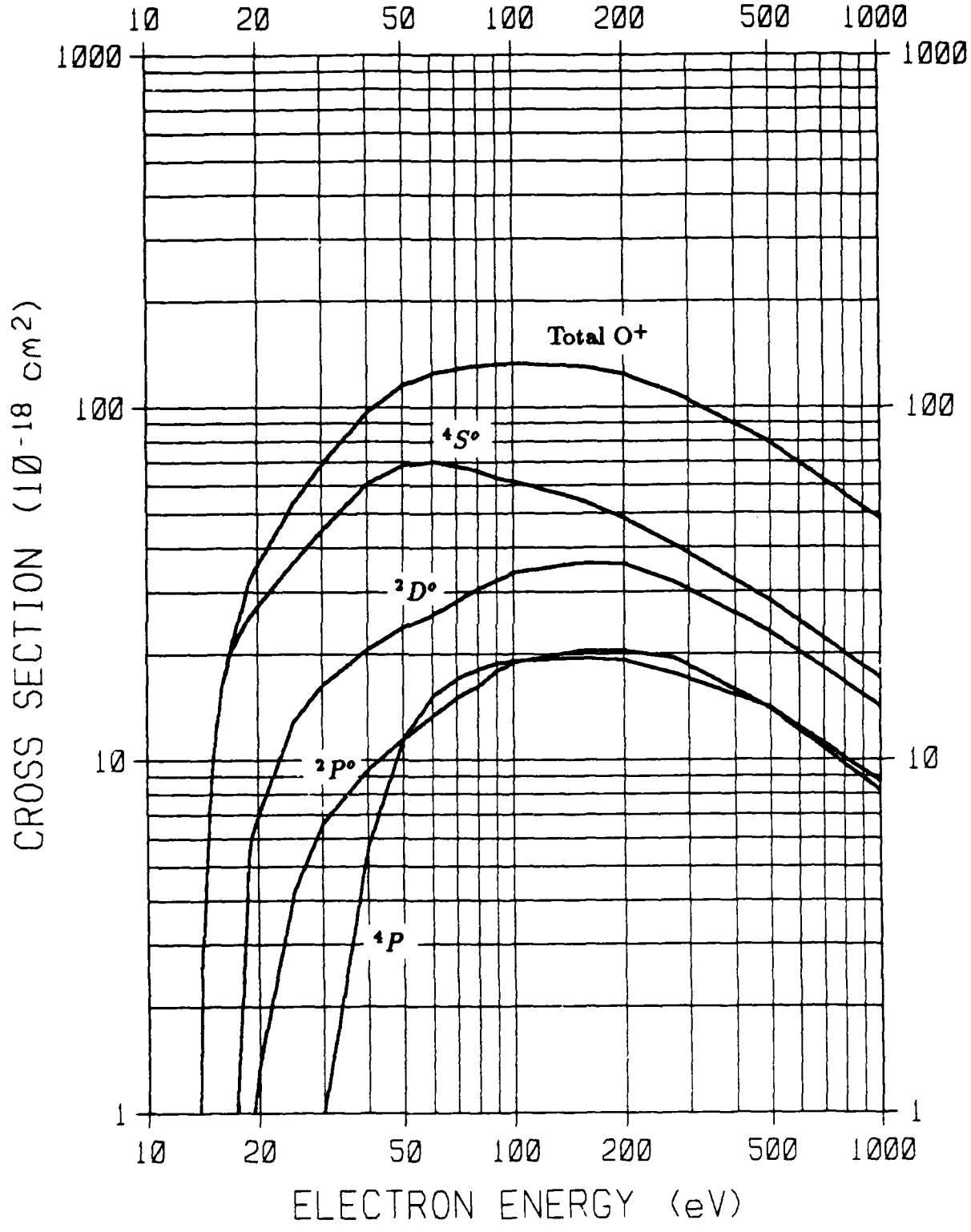

Figure 23. $O(^3P) \longrightarrow O^+(^4S^o, ^2D^o, ^2P^o, ^4P)$ **ionization cross sections.**

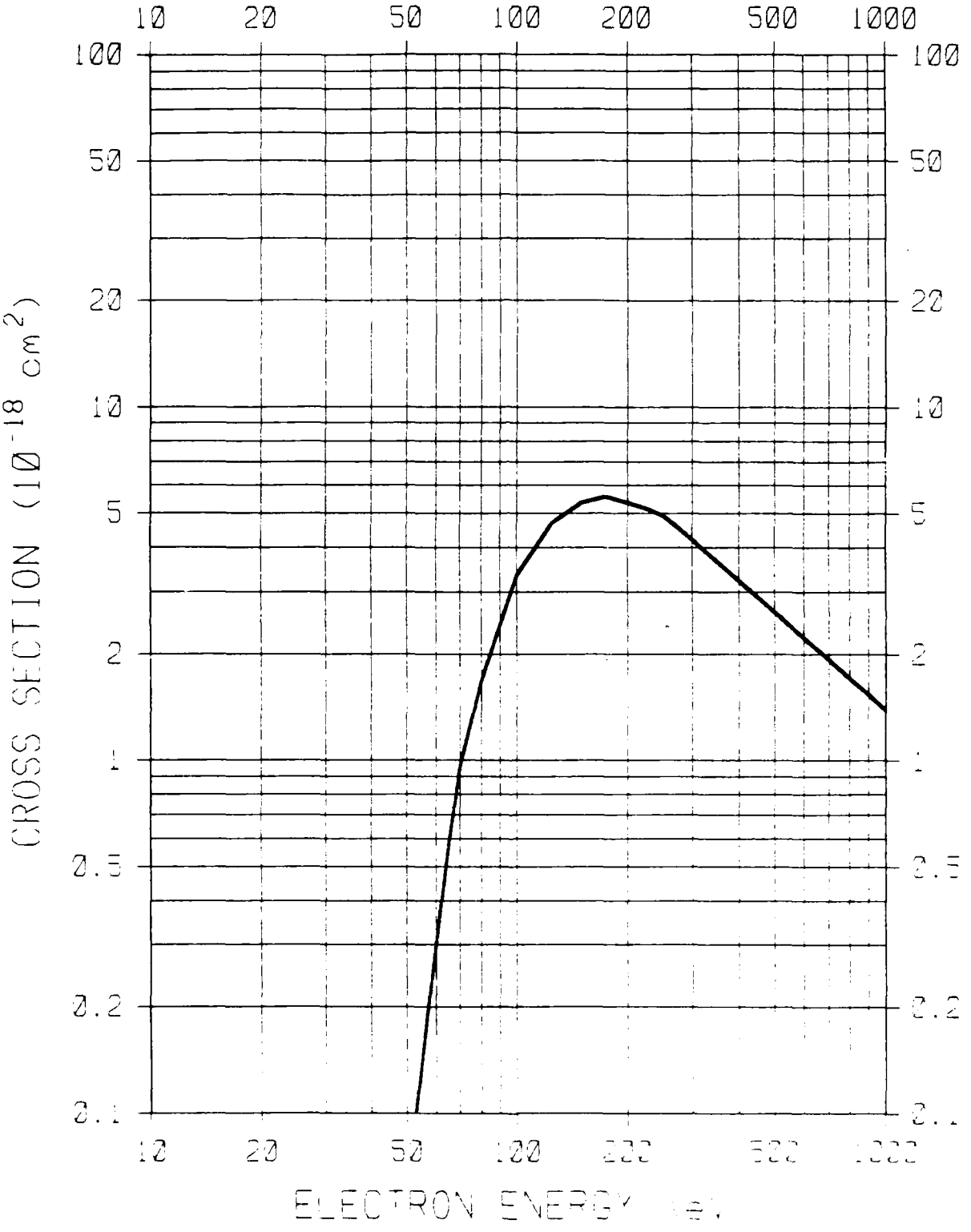

Figure 24. $O(^3P) \longrightarrow O^{2+}$ **ionization cross section.**

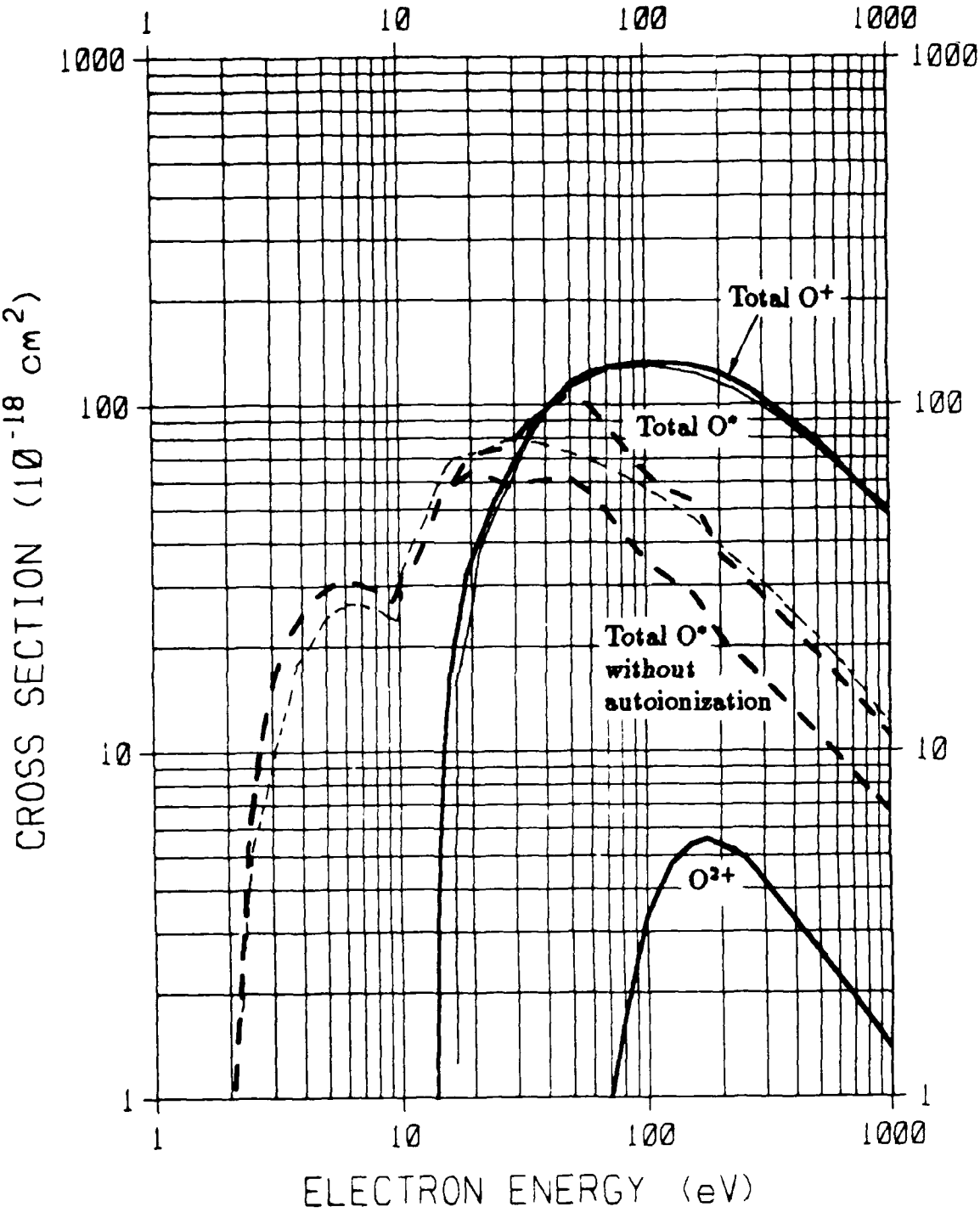

Figure 25. Total $O(^3P) \longrightarrow O^*$ excitation cross sections, with and without autoionization, and total $O(^3P) \longrightarrow O^+$ and $O(^3P) \longrightarrow O^{2+}$ ionization cross sections. The light solid and dashed lines are from Slinker and Ali (1986); the heavy solid and dashed lines are values recommended in this report.

Table 1. Excited and ionized states of atomic oxygen included in this report.

Final state	Threshold (eV)	Final state	Threshold (eV)
$O(^1D)$	1.96	$O(4d'\ ^1SPDFG^o)$	16.07
$O(^1S)$	4.18	$O(ns'\ ^3D^o)$	16.46*
		$O(ns'\ ^1D^o)$	16.47*
$O(2p^5\ ^3P^o)$	15.65	$O(np'\ ^3PDF)$	16.54*
		$O(np'\ ^1PDF)$	16.54*
$O(3s\ ^5S^o)$	9.14	$O(nd'\ ^3SPD^o)$	16.65*
$O(3s\ ^3S^o)$	9.51	$O(nd'\ ^3FG^o)$	16.65*
$O(3p\ ^5P)$	10.73	$O(nd'\ ^1SPDFG^o)$	16.66*
$O(3p\ ^3P)$	10.98		
$O(3d\ ^5D^o)$	12.07	$O(3s''\ ^3P^o)$	14.11
$O(3d\ ^3D^o)$	12.08	$O(3s''\ ^1P^o)$	14.36
$O(4s\ ^5S^o)$	11.83	$O(3p''\ ^3SPD)$	15.77
$O(4s\ ^3S^o)$	11.92	$O(3p''\ ^1SPD)$	15.99
$O(4p\ ^5P)$	12.28	$O(3d''\ ^3P^o, ^3D^o)$	17.09
$O(4p\ ^3P)$	12.35	$O(3d''\ ^3F^o)$	17.09
$O(4d\ ^5D^o)$	12.74	$O(3d''\ ^1PDF^o)$	17.09
$O(4d\ ^3D^o)$	12.75	$O(4s''\ ^3P^o)$	16.81
$O(ns\ ^5S^o)$	13.13*	$O(4s''\ ^1P^o)$	16.90
$O(ns\ ^3S^o)$	13.15*	$O(4p''\ ^3SPD)$	17.24
$O(np\ ^5P)$	13.22*	$O(4p''\ ^1SPD)$	17.25
$O(np\ ^3P)$	13.24*	$O(4d''\ ^3PD^o)$	17.77
$O(nd\ ^5D^o)$	13.33*	$O(4d''\ ^3F^o)$	17.77
$O(nd\ ^3D^o)$	13.33*	$O(4d''\ ^1PDF^o)$	17.77
		$O(ns''\ ^3P^o)$	18.15*
$O(3s'\ ^3D^o)$	12.53	$O(ns''\ ^1P^o)$	18.16*
$O(3s'\ ^1D^o)$	12.72	$O(np''\ ^3SPD)$	18.22*
$O(3p'\ ^3PDF)$	14.06	$O(np''\ ^1SPD)$	18.22*
$O(3p'\ ^1PDF)$	14.20	$O(nd''\ ^3PD^o)$	18.35*
$O(3d'\ ^3S^o, ^3P^o, ^3D^o)$	15.36	$O(nd''\ ^3F^o)$	18.35*
$O(3d'\ ^3FG^o)$	15.39	$O(nd''\ ^1PDF^o)$	18.35*
$O(3d'\ ^1SPDFG^o)$	15.40		
$O(4s'\ ^3D^o)$	15.17	$O^+(^4S^o)$	13.61
$O(4s'\ ^1D^o)$	15.22	$O^+(^2D^o)$	16.93
$O(4p'\ ^3PDF)$	15.59	$O^+(^2P^o)$	18.63
$O(4p'\ ^1PDF)$	15.58	$O^+(^4P^o)$	28.49
$O(4d'\ ^3SPD^o)$	16.08		
$O(4d'\ ^3FG^o)$	16.07	O^{2+}	48.77

* Average energy of $n = 5$ and ∞ (ionization limit) states

Table 2. Quantum defects for Rydberg excitations. Adapted from Jackman *et al.* (1977).

Rydberg state	δ
$ns\ ^5S^o$	1.24
$ns\ ^3S^o$	1.16
$np\ ^5P$	0.81
$np\ ^3P$	0.69
$nd\ ^5D^o$	0.01
$nd\ ^3D^o$	0.01
$ns'\ ^3D^o$	1.21
$ns'\ ^1D^o$	1.18
$np'\ ^3P, ^3D, ^3F$	0.84
$np'\ ^1P, ^1D, ^1F$	0.83
$nd'\ ^3S^o, ^3P^o, ^3D^o, ^3F^o, ^3G^o$	0.04
$nd'\ ^1S^o, ^1P^o, ^1D^o, ^1F^o, ^1G^o$	0.04
$ns''\ ^3P^o$	1.25
$ns''\ ^1P^o$	1.19
$np''\ ^3S, ^3P, ^3D$	0.86
$np''\ ^1S, ^1P, ^1D$	0.85
$nd''\ ^3P^o, ^3D^o, ^3F^o$	0.05
$nd''\ ^1P^o, ^1D^o, ^1F^o$	0.05

Table 3. O($^3P \longrightarrow 2p^4\ ^1D$, $2p^4\ ^1S$, $2p^5\ ^3P^o$) excitation cross sections.

Electron energy (eV)	σ (10^{-18} cm^2)		
	$2p^4\ ^1D$	$2p^4\ ^1S$	$2p^5\ ^3P^o$
2.1	0.82	-	-
2.4	5.41	-	-
2.7	10.7	-	-
3	15.4	-	-
4	24.9	-	-
4.4	26.7	0.54	-
4.8	27.7	1.30	-
5	28.0	1.60	-
6	28.3	2.57	-
7	27.4	3.02	-
8	26.0	3.22	-
9	24.4	3.28	-
10	22.8	3.27	-
12	19.8	3.15	-
14	17.1	2.97	-
16	14.8	2.79	0.17
18	12.9	2.61	1.27
20	11.2	2.44	2.09
25	8.07	2.09	4.11
30	5.90	1.80	6.82
40	3.34	1.37	12.7
45	2.58	1.21	13.6
50	2.02	1.07	14.1
55	1.61	0.95	13.7
70	0.87	0.69	11.5
100	0.33	0.38	7.45
150	0.11	0.16	4.49
200	0.05	0.08	3.14
>200	$4.0 \times 10^5 E^{-3}$		$(-914 + 291\ \ln E)/E$
	$6.4 \times 10^5 E^{-3}$		

Table 4. $O(^3P \longrightarrow 3s\ ^5S^o, 3s\ ^3S^o)$ excitation cross sections.

Electron energy (eV)	σ (10^{-18} cm^2)	
	$3s\ ^5S^o$	$3s\ ^3S^o$
9.9	0.35	3.42
10.1	0.54	4.41
10.5	1.06	5.48
11	1.37	6.28
12	1.78	7.71
14	2.33	9.87
16	2.85	10.5
18	3.19	11.0
20	3.08	11.1
22	2.78	10.8
25	2.29	10.4
28	1.77	9.30
30	1.51	8.69
35	0.91	8.37
40	0.61	8.10
45	0.43	7.95
50	0.31	7.81
55	0.23	7.62
60	0.18	7.45
70	0.11	7.16
100	0.04	6.30
150	0.011	5.27
200	0.005	4.37
>200	$3.88 \times 10^4 E^{-3}$	$(-869 + 329 \ln E)/E$

Table 5. O($^3P \longrightarrow 3p\ ^5P$, $3p\ ^3P$, $3d\ ^5D^o$, $3d\ ^3D^o$) excitation cross sections.

Electron energy (eV)	σ (10^{-18} cm^2)			
	$3p\ ^5P$	$3p\ ^3P$	$3d\ ^5D^o$	$3d\ ^3D^o$
11.1	0.22	0.15	-	-
11.3	0.71	0.47	-	-
11.5	1.00	1.42	-	-
12	1.31	2.72	-	-
14	2.31	5.22	0.041	0.62
16	2.35	6.63	0.087	1.22
18	2.23	7.52	0.109	1.59
20	2.10	7.70	0.116	1.94
22	1.86	7.13	0.113	2.26
24	1.61	6.26	0.105	2.45
26	1.18	5.32	0.096	2.64
28	0.88	4.58	0.087	2.85
30	0.67	4.00	0.078	3.06
35	0.42	3.41	0.059	3.31
40	0.28	3.13	0.045	3.44
45	0.20	2.95	0.035	3.50
50	0.14	2.80	0.027	3.53
55	0.11	2.54	0.022	3.39
60	0.08	2.32	0.017	3.22
70	0.05	1.91	0.012	2.78
100	0.018	1.10	0.005	1.69
150	0.005	0.73	0.0015	1.42
200	0.002	0.55	0.0006	1.21
>200	$1.81 \times 10^4 E^{-3}$	$110E^{-1}$	$4.8 \times 10^3 E^{-3}$	$(-298 + 102 \ln E)/E$

Table 6. O($^3P \longrightarrow 4s\ ^5S^o$, $4s\ ^3S^o$) excitation cross sections.

Electron energy (eV)	σ (10^{-18} cm^2)	
	$4s\ ^5S^o$	$4s\ ^3S^o$
11.9	0.01	-
12	0.02	0.04
12.1	0.03	0.19
12.5	0.11	1.20
13	0.34	1.54
14	0.46	1.68
16	0.57	1.79
18	0.64	1.86
20	0.62	1.89
25	0.46	1.77
28	0.35	1.58
30	0.30	1.48
35	0.18	1.42
40	0.12	1.38
45	0.09	1.35
50	0.06	1.33
55	0.05	1.30
60	0.04	1.27
70	0.02	1.22
100	0.01	1.07
150	0.002	0.90
200	0.0009	0.74
>200	$7.5 \times 10^3 E^{-3}$	$(-148 + 56\ \ln E)/E$

Table 7. $O(^3P \longrightarrow 4p\ ^5P,\ 4p\ ^3P,\ 4d\ ^5D^o,\ 4d\ ^3D^o)$ excitation cross sections.

Electron energy (eV)	σ (10^{-18} cm^2)			
	$4p\ ^5P$	$4p\ ^3P$	$4d\ ^5D^o$	$4d\ ^3D^o$
12.5	0.48	0.02	-	-
12.7	0.52	0.07	-	-
12.9	0.56	0.20	0.00019	-
13	0.59	0.36	0.0005	-
13.5	0.62	0.84	0.0034	0.01
14	0.65	1.57	0.008	0.02
15	0.67	1.83	0.018	0.03
16	0.66	1.99	0.026	0.06
17	0.64	2.14	0.033	0.11
18	0.62	2.26	0.038	0.14
20	0.59	2.31	0.043	0.22
22	0.52	2.14	0.043	0.34
25	0.38	1.74	0.040	0.62
28	0.25	1.37	0.035	1.03
30	0.19	1.20	0.032	1.29
35	0.12	1.02	0.025	1.78
40	0.08	0.94	0.019	2.00
45	0.06	0.89	0.015	2.12
50	0.04	0.84	0.012	2.17
55	0.03	0.76	0.009	2.12
60	0.02	0.70	0.008	2.03
70	0.01	0.57	0.005	1.50
100	0.01	0.33	0.002	0.72
150	0.0015	0.22	0.0007	0.69
200	0.0006	0.17	0.0003	0.64
>200	$5.1 \times 10^3 E^{-3}$	$33E^{-1}$	$2.4 \times 10^3 E^{-3}$	$(-306 + 82 \ln E)/E$

Table 8. $O(^3P \longrightarrow \Sigma(n \geq 5)\ ns\ ^5S^o,\ \Sigma(n \geq 5)\ ns\ ^3S^o)$ excitation cross sections.

Electron energy (eV)	σ (10^{-18} cm^2)	
	$\Sigma(n \geq 5)\ ns\ ^5S^o$	$\Sigma(n \geq 5)\ ns\ ^3S^o$
13.4	0.10	0.04
13.6	0.31	0.14
13.8	0.36	0.45
14	0.40	1.04
15	0.46	1.49
16	0.51	1.61
17	0.55	1.67
18	0.57	1.73
19	0.57	1.74
20	0.56	1.76
22	0.50	1.71
25	0.41	1.64
28	0.32	1.47
30	0.27	1.37
35	0.16	1.32
40	0.11	1.28
45	0.08	1.26
50	0.06	1.23
55	0.04	1.20
60	0.03	1.18
70	0.02	1.13
100	0.01	1.00
150	0.002	0.83
200	0.0009	0.69
>200	$7.5 \times 10^3 E^{-3}$	$(-137 + 52\ \ln E)/E$

Table 9. $O(^3P \longrightarrow \Sigma(n \geq 5)\ np\ ^5P,\ \Sigma(n \geq 5)\ np\ ^3P,\ \Sigma(n \geq 5)\ nd\ ^5D^o,\ \Sigma(n \geq 5)\ nd\ ^3D^o)$ excitation cross sections.

Electron energy (eV)	σ (10^{-18} cm^2)			
	$\Sigma(n \geq 5)\ np\ ^5P$	$\Sigma(n \geq 5)\ np\ ^3P$	$\Sigma(n \geq 5)\ nd\ ^5D^o$	$\Sigma(n \geq 5)\ nd\ ^3D^o$
13.4	0.07	0.04	-	-
13.6	0.25	0.18	0.0007	-
13.8	0.40	0.82	0.0019	0.01
14	0.62	1.48	0.0036	0.02
15	0.69	2.13	0.016	0.04
16	0.70	2.32	0.029	0.08
17	0.71	2.50	0.041	0.16
18	0.69	2.63	0.050	0.21
19	0.67	2.66	0.056	0.26
20	0.65	2.70	0.060	0.33
22	0.58	2.49	0.063	0.52
25	0.43	2.03	0.060	0.92
28	0.27	1.60	0.054	1.54
30	0.21	1.40	0.049	1.94
35	0.13	1.19	0.039	2.67
40	0.09	1.10	0.030	3.00
45	0.06	1.03	0.023	3.17
50	0.04	0.98	0.019	3.26
55	0.03	0.89	0.015	3.18
60	0.03	0.81	0.012	3.05
70	0.02	0.67	0.008	2.25
100	0.01	0.38	0.003	1.08
150	0.0017	0.26	0.0011	1.04
200	0.0007	0.195	0.00047	0.95
>200	$5.6 \times 10^3 E^{-3}$	$39E^{-1}$	$3.76 \times 10^3 E^{-3}$	$(-461 + 123 \ln E)/E$

Table 10. O($^3P \longrightarrow 3s'\ ^3D^o$, $3s'\ ^1D^o$, $3p'\ ^3PDF$, $3p'\ ^1PDF$) excitation cross sections.

Electron energy (eV)	σ (10^{-18} cm^2)			
	$3s'\ ^3D^o$	$3s'\ ^1D^o$	$3p'\ ^3PDF$	$3p'\ ^1PDF$
13	0.05	0.006	-	-
13.5	0.24	0.037	-	-
14	1.08	0.080	-	-
14.5	2.47	0.135	-	0.024
15	3.56	0.187	-	0.057
16	5.10	0.28	0.144	0.099
17	5.52	0.35	0.399	0.120
18	5.61	0.40	0.586	0.130
19	5.50	0.43	0.722	0.132
20	5.41	0.45	0.822	0.130
22	5.09	0.46	0.945	0.120
25	4.88	0.42	1.019	0.099
28	4.95	0.37	1.026	0.081
30	5.07	0.34	1.013	0.070
35	5.64	0.26	0.953	0.050
40	5.85	0.20	0.882	0.036
45	5.98	0.154	0.813	0.027
50	5.87	0.122	0.751	0.021
55	5.58	0.097	0.695	0.016
60	5.33	0.079	0.646	0.013
70	4.93	0.053	0.564	0.008
100	4.48	0.021	0.406	0.003
150	4.00	0.007	0.274	0.001
200	2.67	0.003	0.207	0.0004
>200	$(-1145 + 317\ \ln E)/E$		$41.4E^{-1}$	
		$2.4 \times 10^4 E^{-3}$		$3.3 \times 10^3 E^{-3}$

Table 11. O($^3P \longrightarrow 3d'\ ^3S^o$, $3d'\ ^3P^o$, $3d'\ ^3D^o$, $3d'\ ^3FG^o$, $3d'\ ^1SPDFG^o$) excitation cross sections.

Electron energy (eV)	σ (10^{-18} cm^2)				
	$3d'\ ^3S^o$	$3d'\ ^3P^o$	$3d'\ ^3D^o$	$3d'\ ^3FG^o$	$3d'\ ^1SPDFG^o$
15.8	0.01	0.01	0.01	0.052	0.0012
16	0.02	0.02	0.02	0.075	0.003
17	0.04	0.04	0.04	0.171	0.014
18	0.08	0.10	0.07	0.24	0.027
19	0.14	0.16	0.11	0.29	0.040
20	0.21	0.25	0.17	0.33	0.050
22	0.34	0.41	0.27	0.37	0.064
25	0.65	0.78	0.52	0.40	0.072
28	1.15	1.36	0.92	0.40	0.070
30	1.57	1.86	1.26	0.395	0.067
35	3.02	3.58	2.42	0.37	0.056
40	4.10	4.86	3.28	0.34	0.045
45	4.98	5.90	3.98	0.32	0.036
50	5.57	6.60	4.46	0.29	0.029
55	5.62	6.65	4.49	0.27	0.024
60	5.34	6.33	4.27	0.25	0.020
70	4.68	5.54	3.74	0.22	0.0135
100	3.42	4.06	2.74	0.157	0.0055
150	3.57	4.23	2.86	0.106	0.0018
200	1.87	2.22	1.50	0.080	0.0008
>200	$(229 + 27.5 \ln E)/E$		$(183 + 22.0 \ln E)/E$		$6.4 \times 10^3 E^{-3}$
		$(271 + 32.6 \ln E)/E$		$16.0E^{-1}$	

Table 12. O($^3P \longrightarrow 4s'\ ^3D^o$, $4s'\ ^1D^o$, $4p'\ ^3PDF$, $4p'\ ^1PDF$) excitation cross sections.

Electron energy (eV)	σ (10^{-18} cm^2)			
	$4s'\ ^3D^o$	$4s'\ ^1D^o$	$4p'\ ^3PDF$	$4p'\ ^1PDF$
15.5	0.02	0.0008	-	-
16	0.09	0.0051	0.042	0.0082
16.5	0.33	0.012	0.086	0.016
17	0.52	0.020	0.124	0.022
18	0.95	0.036	0.184	0.029
19	1.17	0.051	0.228	0.034
20	1.23	0.063	0.260	0.035
22	1.22	0.079	0.300	0.035
25	1.15	0.086	0.324	0.031
28	1.13	0.084	0.326	0.026
30	1.12	0.079	0.322	0.023
35	1.24	0.066	0.303	0.017
40	1.29	0.053	0.281	0.012
45	1.32	0.042	0.259	0.0091
50	1.29	0.034	0.239	0.0070
55	1.23	0.028	0.221	0.0055
60	1.17	0.023	0.206	0.0043
70	1.08	0.016	0.180	0.0029
100	0.99	0.0063	0.129	0.0010
150	0.88	0.0021	0.087	0.00034
200	0.59	0.0009	0.066	0.00015
>200	$(-253 + 70\ \ln E)/E$		$13.2E^{-1}$	
		$7.5 \times 10^3 E^{-3}$		$1.2 \times 10^3 E^{-3}$

Table 13. O($^3P \longrightarrow 4d'\ ^3SPD^o$, $4d'\ ^3FG^o$, $4d'\ ^1SPDFG^o$) excitation cross sections.

Electron energy (eV)	σ (10^{-18} cm^2)		
	$4d'\ ^3SPD^o$	$4d'\ ^3FG^o$	$4d'\ ^1SPDFG^o$
16.2	-	0.008	-
16.4	0.01	0.018	-
16.8	0.02	0.035	0.001
17	0.03	0.043	0.002
18	0.10	0.075	0.007
19	0.16	0.099	0.012
20	0.25	0.117	0.017
21	0.32	0.130	0.020
22	0.41	0.139	0.023
25	0.78	0.154	0.028
28	1.36	0.157	0.028
30	1.86	0.156	0.027
35	3.58	0.148	0.023
40	4.86	0.137	0.019
45	5.90	0.127	0.015
50	6.60	0.117	0.012
55	6.65	0.109	0.010
60	6.33	0.101	0.008
70	5.54	0.089	0.006
100	4.06	0.064	0.002
150	4.23	0.043	0.001
200	2.22	0.032	0.0004
>200	$(272 + 32.4 \ln E)/E$	$6.4E^{-1}$	$3.3 \times 10^3 E^{-3}$

Table 14. O($^3P \longrightarrow \Sigma(n \geq 5)\ ns'\ ^3D^o$, $\Sigma(n \geq 5)\ ns'\ ^1D^o$, $\Sigma(n \geq 5)\ np'\ ^3PDF$, $\Sigma(n \geq 5)\ np'\ ^1PDF$) excitation cross sections.

Electron energy (eV)	σ (10^{-18} cm^2)			
	$\Sigma(n \geq 5)\ ns'\ ^3D^o$	$\Sigma(n \geq 5)\ ns'\ ^1D^o$	$\Sigma(n \geq 5)\ np'\ ^3PDF$	$\Sigma(n \geq 5)\ np'\ ^1PDF$
16.6	0.01	-	0.010	0.002
16.8	0.02	0.001	0.030	0.006
17	0.04	0.002	0.050	0.009
18	0.51	0.013	0.130	0.023
19	0.73	0.026	0.190	0.031
20	1.04	0.039	0.235	0.035
21	1.11	0.050	0.268	0.037
22	1.10	0.058	0.293	0.037
25	1.06	0.073	0.332	0.035
28	1.02	0.075	0.343	0.030
30	1.01	0.074	0.342	0.027
35	1.11	0.064	0.327	0.020
40	1.17	0.053	0.305	0.015
45	1.20	0.043	0.283	0.011
50	1.17	0.035	0.262	0.009
55	1.12	0.029	0.244	0.007
60	1.07	0.024	0.227	0.005
70	0.99	0.017	0.199	0.004
100	0.90	0.007	0.143	0.0014
150	0.80	0.002	0.097	0.0004
200	0.53	0.001	0.073	0.00018
>200	$(-228 + 63\ \ln E)/E$	$7 \times 10^3 E^{-3}$	$14.6E^{-1}$	$1.4 \times 10^3 E^{-3}$

Table 15. O($^3P \longrightarrow \Sigma(n \geq 5)\ nd'\ ^3SPD^o$, $\Sigma(n \geq 5)\ nd'\ ^3FG^o$, $\Sigma(n \geq 5)\ nd'\ ^1SPDFG^o$) excitation cross sections.

Electron energy (eV)	σ (10^{-18} cm^2)		
	$\Sigma(n \geq 5)\ nd'\ ^3SPD^o$	$\Sigma(n \geq 5)\ nd'\ ^3FG^o$	$\Sigma(n \geq 5)\ nd'\ ^1SPDFG^o$
16.8	0.01	0.012	-
17	0.02	0.025	0.001
18	0.15	0.080	0.005
19	0.24	0.122	0.012
20	0.38	0.152	0.019
21	0.48	0.175	0.026
22	0.61	0.192	0.031
23	0.76	0.205	0.034
25	1.16	0.220	0.039
28	2.04	0.228	0.041
30	2.79	0.227	0.040
35	5.37	0.218	0.035
40	7.29	0.204	0.029
45	8.85	0.189	0.024
50	9.90	0.175	0.019
55	9.98	0.163	0.016
60	9.49	0.152	0.013
70	8.32	0.133	0.009
100	6.09	0.096	0.004
150	6.35	0.065	0.0009
200	3.33	0.049	0.0004
>200	$(409 + 48.5 \ln E)/E$	$9.8E^{-1}$	$3.1 \times 10^3 E^{-3}$

Table 16. $O(^3P \longrightarrow 3s''\ ^3P^o,\ 3s''\ ^1P^o)$ excitation cross sections.

Electron energy (eV)	σ (10^{-18} cm^2)	
	$3s''\ ^3P^o$	$3s''\ ^1P^o$
14.2	0.08	-
14.4	0.09	-
14.6	0.10	0.003
14.8	0.11	0.009
15	0.13	0.018
16	0.25	0.082
17	0.47	0.156
18	0.78	0.222
19	1.08	0.275
20	1.48	0.315
22	2.46	0.358
25	3.99	0.366
28	5.88	0.341
30	6.77	0.318
35	8.48	0.256
40	9.64	0.203
45	10.41	0.160
50	10.92	0.128
55	10.74	0.103
60	10.57	0.084
70	9.93	0.058
100	7.40	0.023
150	5.24	0.008
200	4.67	0.003
>200	$(-1170 + 397 \ln E)/E$	$2.4 \times 10^4 E^{-3}$

Table 17. O($^3P \longrightarrow 3p''\ ^3SPD,\ 3p''\ ^1SPD$) excitation cross sections.

Electron energy (eV)	σ (10^{-18} cm^2)	
	$3p''\ ^3SPD$	$3p''\ ^1SPD$
15.8	0.092	0.016
16	0.155	0.028
17	0.416	0.070
18	0.608	0.095
19	0.747	0.108
20	0.849	0.113
21	0.923	0.114
22	0.976	0.112
23	1.012	0.108
25	1.051	0.099
28	1.058	0.083
30	1.044	0.073
35	0.982	0.053
40	0.909	0.039
45	0.838	0.029
50	0.773	0.022
55	0.716	0.018
60	0.665	0.014
70	0.581	0.009
100	0.418	0.003
150	0.282	0.001
200	0.213	0.0004
>200	$42.6E^{-1}$	$3.4 \times 10^3 E^{-3}$

Table 18. $O(^3P \longrightarrow 3d''\ ^3P^o,\ 3d''\ ^3D^o,\ 3d''\ ^3F^o,\ 3d''\ ^1PDF^o)$ excitation cross sections.

Electron energy (eV)	σ (10^{-18} cm^2)			
	$3d''\ ^3P^o$	$3d''\ ^3D^o$	$3d''\ ^3F^o$	$3d''\ ^1PDF^o$
18	0.74	0.56	0.095	0.005
19	0.99	0.74	0.162	0.015
20	1.14	0.85	0.212	0.025
21	1.24	0.93	0.249	0.035
22	1.30	0.98	0.277	0.043
23	1.35	1.01	0.298	0.049
24	1.38	1.04	0.313	0.054
25	1.40	1.05	0.324	0.057
26	1.42	1.06	0.332	0.059
27	1.42	1.07	0.336	0.061
28	1.43	1.07	0.339	0.061
30	1.42	1.07	0.340	0.060
35	1.38	1.04	0.328	0.053
40	1.33	1.00	0.307	0.045
45	1.27	0.95	0.286	0.037
50	1.21	0.91	0.265	0.030
55	1.15	0.87	0.247	0.025
60	1.10	0.83	0.230	0.020
70	1.01	0.76	0.201	0.014
100	0.82	0.61	0.145	0.006
150	0.63	0.47	0.099	0.002
200	0.51	0.39	0.074	0.001
>200	$(-59 + 30.5\ \ln E)/E$		$14.8E^{-1}$	
		$(-44 + 23\ \ln E)/E$		$8 \times 10^3 E^{-3}$

Table 19. O($^3P \longrightarrow 4s''\ ^3P^o$, $4s''\ ^1P^o$, $4p''\ ^3SPD$, $4p''\ ^1SPD$) excitation cross sections.

Electron energy (eV)	σ (10^{-18} cm^2)			
	$4s''\ ^3P^o$	$4s''\ ^1P^o$	$4p''\ ^3SPD$	$4p''\ ^1SPD$
17	0.02	-	-	-
18	0.17	0.008	0.065	0.012
19	0.24	0.020	0.122	0.020
20	0.33	0.032	0.164	0.026
21	0.45	0.043	0.196	0.028
22	0.54	0.052	0.220	0.030
23	0.65	0.059	0.238	0.030
24	0.76	0.065	0.251	0.030
25	0.88	0.068	0.261	0.029
26	1.03	0.071	0.268	0.028
28	1.29	0.072	0.275	0.025
30	1.49	0.071	0.276	0.023
35	1.86	0.062	0.267	0.017
40	2.12	0.052	0.251	0.013
45	2.29	0.043	0.234	0.010
50	2.40	0.035	0.217	0.008
55	2.36	0.029	0.202	0.006
60	2.32	0.024	0.188	0.005
70	2.19	0.017	0.165	0.003
100	1.63	0.007	0.119	0.001
150	1.15	0.002	0.081	0.0003
200	1.03	0.001	0.061	0.00013
>200	$(-255 + 87\ \ln E)/E$	$8 \times 10^3 E^{-3}$	$12.2E^{-1}$	$1 \times 10^3 E^{-3}$

Table 20. O($^3P \longrightarrow 4d''\ ^3PD^o$, $4d''\ ^3F^o$, $4d''\ ^1PDF^o$) excitation cross sections.

Electron energy (eV)	σ (10^{-18} cm^2)		
	$4d''\ ^3PD^o$	$4d''\ ^3F^o$	$4d''\ ^1PDF^o$
18	0.27	0.014	-
18.2	0.36	0.020	0.001
18.6	0.47	0.033	0.002
19	0.55	0.044	0.003
20	0.69	0.067	0.007
21	0.78	0.084	0.010
22	0.84	0.098	0.014
23	0.88	0.108	0.017
24	0.91	0.115	0.019
25	0.93	0.121	0.021
28	0.96	0.129	0.023
30	0.96	0.131	0.023
35	0.94	0.128	0.021
40	0.91	0.121	0.018
45	0.87	0.113	0.015
50	0.83	0.105	0.012
55	0.79	0.098	0.010
60	0.76	0.091	0.009
70	0.70	0.080	0.006
100	0.57	0.058	0.003
150	0.43	0.039	0.001
200	0.36	0.030	0.0004
>200	$(-44 + 22 \ln E)/E$	$6E^{-1}$	$3.4 \times 10^3 E^{-3}$

Table 21. O($^3P \longrightarrow \Sigma(n \geq 5)\ ns''\ ^3P^o$, $\Sigma(n \geq 5)\ ns''\ ^1P^o$, $\Sigma(n \geq 5)\ np''\ ^3SPD$, $\Sigma(n \geq 5)\ np''\ ^1SPD$) excitation cross sections.

Electron energy (eV)	σ (10^{-18} cm^2)			
	$\Sigma(n \geq 5)\ ns''\ ^3P^o$	$\Sigma(n \geq 5)\ ns''\ ^1P^o$	$\Sigma(n \geq 5)\ np''\ ^3SPD$	$\Sigma(n \geq 5)\ np''\ ^1SPD$
18.6	0.02	0.002	0.04	0.007
18.8	0.03	0.003	0.05	0.010
19	0.05	0.004	0.07	0.012
20	0.29	0.013	0.12	0.021
21	0.40	0.023	0.17	0.026
22	0.48	0.033	0.20	0.029
23	0.58	0.041	0.22	0.031
24	0.68	0.048	0.24	0.031
25	0.79	0.053	0.26	0.031
28	1.16	0.062	0.28	0.028
30	1.34	0.063	0.29	0.026
35	1.67	0.059	0.28	0.020
40	1.90	0.051	0.27	0.015
45	2.05	0.042	0.25	0.012
50	2.15	0.035	0.24	0.009
55	2.12	0.029	0.22	0.007
60	2.08	0.024	0.21	0.006
70	1.96	0.017	0.18	0.004
100	1.46	0.007	0.13	0.001
150	1.03	0.002	0.09	0.0003
200	0.92	0.001	0.07	0.00013
>200	$(-229 + 78\ \ln E)/E$	$8 \times 10^3 E^{-3}$	$13E^{-1}$	$1 \times 10^3 E^{-3}$

Table 22. O($^3P \longrightarrow \Sigma(n \geq 5)\ nd''\ ^3PD^o$, $\Sigma(n \geq 5)\ nd''\ ^3F^o$, $\Sigma(n \geq 5)\ nd''\ ^1PDF^o$) excitation cross sections.

Electron energy (eV)	σ (10^{-18} cm^2)		
	$\Sigma(n \geq 5)\ nd''\ ^3PD^o$	$\Sigma(n \geq 5)\ nd''\ ^3F^o$	$\Sigma(n \geq 5)\ nd''\ ^1PDF^o$
18.6	0.39	0.019	-
18.8	0.51	0.029	-
19	0.61	0.038	0.001
20	0.89	0.077	0.006
21	1.06	0.106	0.011
22	1.17	0.129	0.017
23	1.24	0.146	0.021
24	1.30	0.159	0.025
25	1.34	0.169	0.028
28	1.39	0.186	0.033
30	1.40	0.190	0.034
35	1.38	0.188	0.032
40	1.34	0.179	0.028
45	1.28	0.168	0.023
50	1.23	0.157	0.019
55	1.18	0.146	0.016
60	1.13	0.137	0.013
70	1.04	0.120	0.010
100	0.84	0.087	0.004
150	0.65	0.059	0.001
200	0.53	0.045	0.0004
>200	$(-63 + 32 \ln E)/E$	$9E^{-1}$	$3.4 \times 10^3 E^{-3}$

Table 23. $O(^3P) \longrightarrow O^+(^4S^o, {}^2D^o, {}^2P^o, {}^4P)$ ionization cross sections.

Electron energy (eV)	σ (10^{-18} cm^2)				
	$^4S^o$	$^2D^o$	$^2P^o$	^4P	Total
14	2.6	-	-	-	2.6
16	16.3	-	-	-	16.3
18	23.0	2.2	-	-	26.5
20	27.6	7.0	1.4	-	36.0
25	36.1	12.8	4.2	-	53.0
30	44.8	16.3	6.6	1.0	68.8
35	52.7	18.5	8.0	2.5	82.3
40	60.8	20.6	9.4	5.7	96.5
50	68.5	23.8	11.5	11.5	115.3
60	70.1	25.8	13.3	15.1	124.3
70	68.0	28.2	15.0	17.0	128.2
80	66.1	30.6	16.2	18.1	131.0
90	63.0	32.3	17.9	18.8	132.0
100	61.6	34.0	18.9	19.1	133.0
150	55.0	36.2	20.4	19.5	131.0
200	48.4	36.0	20.4	19.2	124.0
300	38.4	30.3	18.5	17.0	104.2
400	32.3	26.0	15.8	15.3	89.3
500	28.2	23.0	13.9	14.0	79.2
600	24.7	20.3	12.1	12.4	69.4
700	22.1	18.2	10.8	11.1	62.2
800	20.1	16.6	9.7	10.1	56.5
900	18.4	15.3	8.9	9.3	51.9
1000	17.1	14.2	8.2	8.7	48.1
	Fraction of total				
>1000	0.36	0.30	0.17	0.18	$(-43,100 + 13,200 \ln E)/E$

Table 24. $O(^3P) \longrightarrow O^{2+}$ ionization cross section.
From Zipf (1985).

Electron energy (eV)	σ (10^{-18} cm^2)
60	0.296
65	0.563
70	0.963
80	1.68
90	2.42
100	3.34
125	4.72
150	5.38
175	5.59
200	5.37
225	5.17
250	4.93
275	4.57
300	4.22
400	3.24
500	2.64
600	2.23
700	1.94
800	1.71
900	1.54
1000	1.39
>1000	$(660 + 106 \ln E)/E$

Table 25. Total $O(^3P) \longrightarrow O^*$ excitation cross sections, with and without autoionization, and total inelastic cross sections.

Electron energy (eV)	σ (10^{-18} cm^2)		
	Excitation with autoionization	Excitation without autoionization	Inelastic
3	15.4	15.4	15.4
4	24.9	24.9	24.9
6	30.9	30.9	30.9
8	29.2	29.2	29.2
10	30.3	30.3	30.3
12	36.4	36.4	36.4
14	49.3	49.3	51.8
16	57.4	57.1	73.3
18	65.5	61.8	88.1
20	71.7	64.2	100
25	74.2	60.9	114
30	79.1	58.0	127
35	91.6	60.5	143
40	99.1	61.4	158
50	107.0	61.5	177
60	99.4	56.0	181
70	88.0	49.2	178
80	78.0	43.3	176
90	69.7	38.8	173
100	64.0	35.5	172
150	54.0	28.9	165
200	37.0	21.2	151
300	27.8	16.1	125
400	22.5	13.1	106
500	19.0	11.2	93.0
600	16.6	9.8	81.4
700	14.7	8.7	72.8
800	13.3	7.9	66.0
900	12.1	7.2	60.6
1000	11.1	6.6	56.1

Table 26. Autoionization factors for the autoionizing excited states.

State	A.F.
O($2p^5\ ^3P^0$)	0.51
O($3d'\ ^3S^0$)	0.50
O($3d'\ ^3P^0$)	0.65
O($3d'\ ^3D^0$)	0.50
O($4s'\ ^3D^0$)	1.00
O($4d'\ ^3SPD^0$)	0.70
O($ns'\ ^3D^0$)	1.00
O($nd'\ ^3SPD^0$)	1.00
O($3s''\ ^3P^0$)	0.46
O($3d''\ ^3P^0$)	0.30
O($3d''\ ^3D^0$)	0.50
O($4s''\ ^3P^0$)	1.00
O($4d''\ ^3PD^0$)	0.75
O($ns''\ ^3P^0$)	1.00
O($nd''\ ^3PD^0$)	0.75

DISTRIBUTION LIST

DNA-TR-88-72

DEPARTMENT OF DEFENSE

ASSISTANT SEC OF DEF (C3I)
ATTN: DASD(I)

ASSISTANT TO THE SECRETARY OF DEFENSE
ATOMIC ENERGY
ATTN: EXECUTIVE ASSISTANT

DEFENSE ADVANCED RSCH PROJ AGENCY
ATTN: DR MANSFIELD

DEFENSE COMMUNICATIONS AGENCY
ATTN: J DIETZ

DEFENSE INTELLIGENCE AGENCY
ATTN: RTS-2B

DEFENSE NUCLEAR AGENCY
ATTN: OPNA
3 CYS ATTN: RAAE
ATTN: B PRASAD
ATTN: K SCHWARTZ
ATTN: L SCHROCK
ATTN: L WITTWER
4 CYS ATTN: TITL

DEFENSE NUCLEAR AGENCY
ATTN: TDNM-CF
ATTN: TDTT
ATTN: TDTT W SUMMA

DEFENSE TECHNICAL INFORMATION CENTER
2 CYS ATTN: DTIC/FDAB

JOINT STRAT TGT PLANNING STAFF
ATTN: JK
ATTN: JKCS
ATTN: JLWT
ATTN: JPEP
ATTN: JPTM

LAWRENCE LIVERMORE NATIONAL LABORATORY
ATTN: DNA-LL

NATIONAL SECURITY AGENCY
ATTN: C GOEDEKE

STRATEGIC DEFENSE INITIATIVE ORGANIZATION
ATTN: KE
ATTN: SLKT
ATTN: SN

UNDER SECRETARY OF DEFENSE
ATTN: DEFENSIVE SYSTEMS
ATTN: STRAT & THEATER NUC FOR

DEPARTMENT OF THE ARMY

HARRY DIAMOND LABORATORIES
ATTN: SLCIS-IM-TL

U S ARMY ATMOSPHERIC SCIENCES LAB
ATTN: DR F NILES
3 CYS ATTN: SLCAS-AE-E

U S ARMY BALLISTIC RESEARCH LAB
ATTN: SLCBR-SS-T

U S ARMY FOREIGN SCIENCE & TECH CTR
ATTN: DRXST-SD

U S ARMY MATERIEL COMMAND
ATTN: J BENDER

U S ARMY MISSILE COMMAND/AMSMI-RD-CS-R
ATTN: AMSMI-RD-CS-R

U S ARMY NUCLEAR & CHEMICAL AGENCY
ATTN: MONA-NU

U S ARMY NUCLEAR EFFECTS LABORATORY
ATTN: ATAA-PL

U S ARMY RESEARCH OFFICE
ATTN: R MACE

U S ARMY STRATEGIC DEFENSE CMD
ATTN: DASD-H-SAV

U S ARMY STRATEGIC DEFENSE COMMAND
ATTN: W DAVIES

U S ARMY WHITE SANDS MISSILE RANGE
ATTN: K CUMMINGS

USA ELECT WARFARE/SEC,SURV & TARGET ACQ CTR
ATTN: AMSEL-EW-SS

USA SURVIVABILITY MANAGMENT OFFICE
ATTN: J BRAND

DEPARTMENT OF THE NAVY

NAVAL AIR PROPULSION CENTER
ATTN: F HUSTED

NAVAL ELECTRONICS ENGRG ACTVY, PACIFIC
ATTN: D OBRYHIM

NAVAL INTELLIGENCE SUPPORT CTR
ATTN: NISC-50

NAVAL OCEAN SYSTEMS CENTER
ATTN: J FERGUSON

NAVAL POSTGRADUATE SCHOOL
ATTN: LIBRARY

NAVAL RESEARCH LABORATORY
ATTN: J BROWN
ATTN: TECH LIB
ATTN: J JOHNSON
ATTN: CODE 4183
ATTN: W ALI
ATTN: S OSSAKOW
ATTN: J DAVIS
ATTN: B RIPIN
ATTN: D STROBEL
ATTN: J HUBA
ATTN: P PALMADESSO

NAVAL SURFACE WARFARE CENTER
ATTN: CODE X211

NAVAL UNDERWATER SYSTEMS CENTER
ATTN: J KATAN

OFC OF THE DEPUTY CHIEF OF NAVAL OPS
ATTN: NOP 941D

OFFICE OF NAVAL RESEARCH
ATTN: A TUCKER

SPACE & NAVAL WARFARE SYSTEMS CMD
ATTN: PD 50TD
ATTN: B KRUGER
ATTN: G BRUNHART
ATTN: S KEARNEY

THEATER NUCLEAR WARFARE PROGRAM OFC
ATTN: PMS-42331F

DEPARTMENT OF THE AIR FORCE

AIR FORCE CTR FOR STUDIES & ANALYSIS
ATTN: AFCSA/SAMI
ATTN: AFCSA/SASC

AIR FORCE GEOPHYSICS LABORATORY
2 CYS ATTN: W SWIDER
ATTN: J BUCHAU
2 CYS ATTN: R HUFFMAN
ATTN: LS
2 CYS ATTN: R MURPHY
ATTN: R O'NIEL
ATTN: H GARDINER
2 CYS ATTN: R SHARMA
2 CYS ATTN: D PAULSON
ATTN: D SMITH
2 CYS ATTN: R NADILE
2 CYS ATTN: K CHAMPION

AIR FORCE OFFICE OF SCIENTIFIC RSCH
ATTN: AFOSR/NC

AIR FORCE SPACE DIVISION
ATTN: YA
ATTN: YG
2 CYS ATTN: YN

AIR FORCE TECHNICAL APPLICATIONS CTR
ATTN: TN
ATTN: TX

AIR FORCE WEAPONS LABORATORY
ATTN: SUL

AIR FORCE WRIGHT AERONAUTICAL LAB/AAAD
ATTN: W HUNT

AIR UNIVERSITY LIBRARY
ATTN: AUL-LSE

BALLISTIC MISSILE OFFICE
ATTN: PK

HILL AIR FORCE BASE
ATTN: TRW/H L DEPT

ROME AIR DEVELOPMENT CENTER, AFSC
ATTN: J SIMONS

SPACE DIVISION/AQ
ATTN: WE

SPACE DIVISION/CNCIV
ATTN: YN

SPACE DIVISION/YA
ATTN: YAR

SPACE DIVISION/YG
ATTN: P KELLY

STRATEGIC AIR COMMAND/INCR
ATTN: INCR

DEPARTMENT OF ENERGY

EG&G, INC
ATTN: D WRIGHT

LAWRENCE LIVERMORE NATIONAL LAB
ATTN: A GROSSMAN
ATTN: D WUEBBLES
ATTN: R HAGER
ATTN: G HAUGAN
ATTN: E WOODWARD
ATTN: H KRUGER

LOS ALAMOS NATIONAL LABORATORY
ATTN: D SAPPENFIELD
ATTN: D SIMONS
ATTN: G M SMITH
ATTN: J WOLCOTT
ATTN: M PONGRATZ
ATTN: M SANDFORD
ATTN: J ZINN
ATTN: REPORT LIBRARY
ATTN: R W WHITAKER
ATTN: REPORT LIBRARY
ATTN: T BIENIEWSKI
ATTN: T KUNKLE

SANDIA NATIONAL LABORATORIES
ATTN: R BACKSTROM
ATTN: D DAHLGREN
ATTN: L ANDERSON
ATTN: M KRAMM
ATTN: T P WRIGHT
ATTN: W D BROWN
ATTN: TECH LIB 3141

OTHER GOVERNMENT

CENTRAL INTELLIGENCE AGENCY
ATTN: OSWR/NED
ATTN: OSWR/SSD

DEPARTMENT OF COMMERCE
ATTN: J DEVOE

ATTN: M KRAUSS
ATTN: R LEVINE
ATTN: S ABRAMOWITZ

DEPARTMENT OF COMMERCE
ATTN: C RUSH
ATTN: E MORRISON
ATTN: J HOFFMEYER
ATTN: R GRUBB
ATTN: W UTLAUT

NASA
3 CYS ATTN: A AIKIN
ATTN: A TEMPKIN

NASA
ATTN: R WHITTEN

NASA
ATTN: J GRAY

NASA HEADQUARTERS
ATTN: 1 SCHARDT

NATIONAL OCEANIC & ATMOSPHERIC ADMIN
3 CYS ATTN: E FERGUSON
3 CYS ATTN: F FEHSENFELD

U S DEPARTMENT OF STATE
ATTN: PM/TMP

DEPARTMENT OF DEFENSE CONTRACTORS

AERODYNE RESEARCH, INC
ATTN: C KOLB

AEROJET ELECTRO-SYSTEMS CO
ATTN: J GRAHAM

AEROSPACE CORP
ATTN: C RICE
ATTN: G LIGHT
ATTN: J REINHEIMER
ATTN: J STRAUS
ATTN: N COHEN

ATMOSPHERIC AND ENVIRONMENTAL RESEARCH INC
ATTN: M KO

AUSTIN RESEARCH ASSOCIATES
ATTN: J THOMPSON

AVCO EVERETT RESEARCH LAB, INC
ATTN: C VON ROSENBERG JR

BERKELEY RSCH ASSOCIATES, INC
ATTN: C PRETTIE
ATTN: J WORKMAN
ATTN: S BRECHT

BOSTON COLLEGE, TRUSTEES OF
ATTN: E HEGBLOM
ATTN: W GRIEDER

CALIFORNIA RESEARCH & TECHNOLOGY, INC
ATTN: M ROSENBLATT

CALIFORNIA, UNIVERSITY AT RIVERSIDE
ATTN: J PITTS JR

CALSPAN CORP
ATTN: C TREANOR
ATTN: J GRACE
ATTN: M DUNN

CHARLES STARK DRAPER LAB, INC
ATTN: A TETEWSKI

CONCORD SCIENCES CORP
ATTN: E SUTTON

CORNELL UNIVERSITY
ATTN: D FARLEY JR
ATTN: M KELLY

ELECTROSPACE SYSTEMS, INC
ATTN: P PHILLIPS

EOS TECHNOLOGIES, INC
ATTN: B GABBARD
ATTN: W LELEVIER

GEO CENTERS, INC
ATTN: E MARRAM

GTE GOVERNMENT SYSTEMS CORPORATION
ATTN: W I THOMPSON

HARRIS CORPORATION
ATTN: E KNICK

HSS, INC
ATTN: D HANSEN
ATTN: M SHULER

INSTITUTE FOR DEFENSE ANALYSES
ATTN: E BAUER
ATTN: H WOLFHARD

J S LEE ASSOCIATES INC
ATTN: DR J LEE

JAMIESON SCIENCE & ENGINEERING
ATTN: J JAMIESON

JOHNS HOPKINS UNIVERSITY
ATTN: C MENG

KAMAN SCIENCES CORP
ATTN: D PERIO
ATTN: P TRACY

KAMAN SCIENCES CORP
ATTN: E CONRAD

KAMAN SCIENCES CORPORATION
ATTN: B GAMBILL
5 CYS ATTN: DASIAC
ATTN: R RUTHERFORD
ATTN: W MCNAMARA

KAMAN SCIENCES CORPORATION
ATTN: DASIAC

LOCKHEED MISSILES & SPACE CO, INC
ATTN: J CLADIS
ATTN: J HENLEY
ATTN: J KUMER
ATTN: M WALT
ATTN: R SEARS

M I T LINCOLN LAB
ATTN: D TOWLE

MAXIM TECHNOLOGIES, INC
ATTN: J SO

MCDONNELL DOUGLAS CORP
ATTN: T CRANOR

MCDONNELL DOUGLAS SPACE SYSTEMS COMPANY
ATTN: J GROSSMAN
ATTN: R HALPRIN

METATECH CORPORATION
ATTN: R SCHAEFER
ATTN: W RADASKY

METEOR COMMUNICATIONS CORP
ATTN: R LEADER

MISSION RESEARCH CORP
ATTN: B R MILNER
ATTN: C LAUER
ATTN: D ARCHER
ATTN: D KNEPP
ATTN: D SOWLE
ATTN: F FAJEN
ATTN: F GUIGLIANO
ATTN: G MCCARTOR
ATTN: K COSNER
ATTN: M FIRESTONE
ATTN: R BIGONI
ATTN: R BOGUSCH
ATTN: R DANA
ATTN: R HENDRICK
ATTN: R KILB
ATTN: S GUTSCHE
2 CYS ATTN: TECH LIBRARY

MISSION RESEARCH CORP
ATTN: R PETERKIN
ATTN: R STELLINGWERF

MITRE CORPORATION
ATTN: D RAMPTON
ATTN: M R DRESP

MITRE CORPORATION
ATTN: J WHEELER
ATTN: R C PESCI
ATTN: W FOSTER

NICHOLS RESEARCH CORP, INC
ATTN: J SMITH
ATTN: R BYRN

NORTHWEST RESEARCH ASSOC, INC
ATTN: E FREMOUW

PACIFIC-SIERRA RESEARCH CORP
ATTN: H BRODE

PHOTOMETRICS, INC
ATTN: I L KOFSKY

PHYSICAL RESEARCH INC
ATTN: W. SHIH

PHYSICAL RESEARCH INC
ATTN: H FITZ
ATTN: P LUNN

PHYSICAL RESEARCH, INC
ATTN: R DELIBERIS
ATTN: T STEPHENS

PHYSICAL RESEARCH, INC
ATTN: J DEVORE
ATTN: J THOMPSON
ATTN: W SCHLUETER

PHYSICAL SCIENCE LAB
ATTN: W BERNING

PHYSICAL SCIENCES, INC
ATTN: G CALEDONIA

PITTSBURGH, UNIV OF THE COMMONWEALTH
ATTN: M BIONDI

PRINCETON UNIVERSITY
ATTN: LIBRARIAN

R & D ASSOCIATES
2 CYS ATTN: F GILMORE
ATTN: M GANTSWEG
2 CYS ATTN: R LAHER

R & D ASSOCIATES
ATTN: J ROSENGREN

R & D ASSOCIATES
ATTN: G GANONG

RAND CORP
ATTN: C CRAIN
ATTN: E BEDROZIAN

RAND CORP
ATTN: B BENNETT

SCIENCE APPLICATIONS INTL CORP
ATTN: D HAMLIN
ATTN: D SACHS
ATTN: L LINSON

SCIENCE APPLICATIONS INTL CORP
ATTN: R LEADABRAND

SCIENCE APPLICATIONS INTL CORP
ATTN: E HYMAN
ATTN: J COCKAYNE

SCIENCE APPLICATIONS INTL CORP
ATTN: D TELAGE
ATTN: M CROSS

SPACE DATA CORP
ATTN: S FISHER

SRI INTERNATIONAL
ATTN: D MCDANIEL
ATTN: W CHESNUT
ATTN: W JAYE

SRS TECHNOLOGIES, INC
ATTN: R EVANS

STEWART RADIANCE LABORATORY
ATTN: R HUPPI

TELECOMMUNICATION SCIENCE ASSOCIATES
ATTN: R BUCKNER

TELECOMMUNICATION SCIENCE ASSOCIATES, INC
ATTN: D MIDDLESTEAD

TELEDYNE BROWN ENGINEERING
ATTN: J CATO
ATTN: J WOLFSBERGER, JR
ATTN: TECHNICAL LIBRARY
ATTN: N PASSINO

TOYON RESEARCH CORP
ATTN: J ISE

TRW INC
ATTN: DR D GRYBOS
ATTN: R PLEBUCH

TRW SPACE & DEFENSE SYSTEMS
ATTN: D M LAYTON

UTAH STATE UNIVERSITY
ATTN: C WYATT
ATTN: D BAKER
ATTN: K BAKER

VISIDYNE, INC
ATTN: J CARPENTER

WAYNE STATE UNIVERSITY
ATTN: R KUMMLER

WAYNE STATE UNIVERSITY
ATTN: W KAUPPILA

FOREIGN

OA 2
ATTN: B SJOHOLM

FOA 3
ATTN: T KARLSSON

DIRECTORY OF OTHER

GOVERNMENT PUBLICATIONS LIBRARY M
ATTN: J WINKLER

YALE UNIVERSITY
ATTN: ENGINEERING DEPARTMENT